DOE/CE/50390--9

Conceptual Design Report for a Direct Hydrogen Proton Exchange Membrane Fuel Cell for Transportation Application

RECEIVED
NOV 14 1995
OSTI

5 September 1995

Contract DE-AC02-94CE50390
Document Control Number 6004707
(DOE/CE/50390-9)

Prepared By:

Pentastar Electronics, Inc.
110 Wynn Drive
P. O. Box 1929
Huntsville, AL 35807-0929

Prepared For:

U.S Department of Energy
Chicago Operations Office
9800 South Cass Avenue
Argonne, IL 60439

TR95H081

MASTER

DISTRIBUTION OF THIS DOCUMENT IS UNLIMITED

TABLE OF CONTENTS

Page

EXECUTIVE SUMMARY 1

1.0 VEHICLE CONSIDERATIONS 1-1
  1.1 Vehicle Determination 1-1
  1.2 Powertrain Size and Operational Requirements 1-23

2.0 VEHICLE PERFORMANCE REQUIREMENTS 2-1
  2.1 Driving Cycles 2-1
  2.2 Vehicle Configuration 2-4
  2.3 Vehicle Simulation 2-4
  2.4 Baseline Performance 2-17
  2.5 Conclusions 2-19

3.0 PEM FUEL CELL SUBSYSTEM 3-1
  3.1 Vehicular PEM Fuel Cells 3-1
  3.2 PEM Fuel Cell Conceptual Design 3-2
  3.3 Fuel Cell Subsystem Conceptual Design 3-5
  3.4 Performance Characteristics 3-8
  3.5 Gas Management Subsystem Description 3-18

4.0 HYDROGEN STORAGE SUBSYSTEM REQUIREMENTS 4-1
  4.1 Hydrogen Storage On Board Vehicles 4-1
  4.2 Gaseous Hydrogen Storage System Concept 4-3
  4.3 Liquid Hydrogen Storage System Concept 4-15
  4.4 Dewar Size Estimates 4-17

5.0 LOAD LEVELING UNIT SUBSYSTEM 5-1
  5.1 Load Leveling Unit Concept 5-1
  5.2 LLU Subsystem Description 5-3
  5.3 DTC Considerations for LLU 5-24

6.0 POWER TRAIN REQUIREMENTS 6-1
  6.1 Motor Operating Characteristics 6-1

7.0 AUXILIARY SUBSYSTEM REQUIREMENTS 7-1
  7.1 Heating/Cooling Subsystem Design 7-1
  7.2 Regenerative Braking Subsystem 7-2
  7.3 Electrical Power Steering (EPS) Subsystem 7-2

TABLE OF CONTENTS (Continued)

Page

8.0 ACRONYM LIST AND DEFINITIONS 8-1

APPENDIX A. Chopper/Regulator Design A-1

APPENDIX B. Controller Design B-1

APPENDIX C. Gas Management Controller C-1

APPENDIX D. LLU Design To Cost Summary D-1

APPENDIX E. Simulation Modeling Data E-1

APPENDIX F. Hydrogen Storage Designs F-1

LIST OF ILLUSTRATIONS

Figure		Page
1	DPHV Vehicle Configuration	3
2	DPHV Electrical Configuration	6
1-1	Vehicle Parameters for Goal 3	1-1
1-2	Propulsion and Vehicle Improvements Needed for 80 MPG	1-2
1-3	Fuel Cell Pathway to 80 MPG	1-2
1-4	Subcompact Packaging Design	1-7
1-5	Minivan Packaging Design	1-9
1-6	Full-Size Pick-Up Truck Packaging Design	1-12
1-7	PNGV LH Mid-Size Sedan Packaging Design	1-13
1-8	PNGV LH Mid-Size Sedan Packaging Design	1-15
1-9	PNGV LH Mid-Size Sedan Packaging Design	1-17
1-10	PNGV LH Mid-Size Sedan Packaging Design	1-19
1-11	PNGV LH Mid-Size Sedan Packaging Design	1-21
1-12	System Efficiency	1-24
1-13	Precision Vehicle Control	1-25
1-14	Acceleration Histogram (EPA City Driving Cycle)	1-26
2-1	Alternative Acceleration Profiles	2-2
2-2	Baker Grade Velocity Profile	2-2
2-3	FUDS Velocity Profiles	2-3
2-4	LA92 Velocity Profiles	2-3
2-5	Hiway Velocity Profile	2-5
3-1	Basic Operation of the Vehicular PEM Fuel Cell	3-3
3-2	Optimal PEM Fuel Cell Subsystem Configuration	3-6
3-3	AlliedSignal Automotive PEM Fuel Cell Power Plant Concept	3-6
3-4	PEM Fuel Cell Subsystem Cooling Scheme	3-7
3-5	Overall Water Balance for the FCS Subsystem at 2 Atmospheres	3-10
3-6	Comparison of Model Prediction with Experimental Polarization Curve	3-10
3-7	Rated Power and off-Design Stack Voltages for 50 kW Fuel Cell Stack	3-11

LIST OF ILLUSTRATIONS (Continued)

Figure **Page**

3-8 Stack and Subsystem Efficiency for 50 kW FCS 3-11
3-9 Hydrogen Usage Rate (50-kW Stack) 3-15
3-10 Hydrogen Consumption per Unit Power (50 kW Fuel Cell Stack) 3-15
3-11 Effect of Turbocompressor Design on Subsystem Efficiency 3-16
3-12 Fuel Cell Subsystem Transient Response 20-50 kW Load Change (50 kW Stack) 3-17
3-13 Optimal PEM FCS Configuration 3-18
4-1 Gaseous Hydrogen Storage System Schematic 4-4
4-2 Hydrogen Density as a Function of Pressure and Temperature 4-6
4-3 Best-Fit Gaseous Hydrogen Installation Layout 4-7
4-4 Tank Refuel Adiabatic Temperature Response 4-9
4-5 Refuel Temperature Response with Heat Transfer 4-11
4-6 Hydrogen Tank Refueling Temperature Rise 4-12
4-7 Refueling Tank Temperature Rise Without Turbine 4-13
4-8 Potential Refueling Schemes for Pressurized Gas Storage Systems 4-14
4-9 Proposed Liquid Refueling Scheme 4-16
4-10 Liquid Hydrogen Installation Layout (1-Tank) 4-19
5-1 LLU Component Configuration 5-2
5-2 Vehicle Operational Effects on LLU Operation 5-4
5-3 DPHV Battery Configuration for Cell and Stack Monitoring 5-11
5-4 Typical Battery Temperature Sensing Circuitry 5-12
5-5 Bolder Spiral-Wound Battery Technology 5-13
5-6 Electrosource "Horizon" Battery Features 5-14
5-7 Chopper/Regulator Configuration 5-16
5-8 Current Control Circuit 5-17
5-9 Simplified Boost Current Circuit 5-18
5-10 Simplified Buck Current Circuit 5-19
5-11 MC68332 Block Diagram 5-22
7-1 HVAC Refrigerant Circuit Diagram 7-1
7-2 Regenerative Braking Subsystem Configuration 7-3
7-3 Electric Power Steering Subsystem 7-4

LIST OF TABLES

Table		Page
1	DPHV Vehicle Design Goals	5
2	DPHV Weight Allocation	6
1-1	Vehicular Performance Requirements	1-4
2-1	LH Sedan Test Vehicle Parameters	2-4
2-2	City/HIWAY Cycle System Response	2-8
2-3	DPHV Combined Mileage and Range Results	2-9
3-1	PEM FCS Design Goals	3-1
3-2	Mass and Volume Projections for 50 kW PEM Fuel Cell Stack	3-5
3-3	Peak Power and Off-Design Performance Data	3-12
3-4	Peak Power and Off-Design Performance Data	3-13
3-5	Peak Power and Off-Design Performance Data	3-14
4-1	Gaseous Hydrogen Storage System Design Goals	4-3
4-2	Liquid Hydrogen Storage System Design Goals	4-15
5-1	DPHV Mode Description	5-5
5-2	LLU Battery Requirements	5-10
5-3	Battery Technology Comparison Trade-Off Matrix	5-13
5-4	Chopper/Regulator Requirements	5-15
6-1	Westinghouse 3-Phase AC Induction Motor Design Characteristics	6-1
6-2	Westinghouse Motor Operating Characteristics	6-1
7-1	HVAC Subsystem Allocations	7-2
8-1	List of Acronyms	8-1

DISCLAIMER

This report was prepared as an account of work sponsored by an agency of the United States Government. Neither the United States Government nor any agency thereof, nor any of their employees, makes any warranty, express or implied, or assumes any legal liability or responsibility for the accuracy, completeness, or usefulness of any information, apparatus, product, or process disclosed, or represents that its use would not infringe privately owned rights. Reference herein to any specific commercial product, process, or service by trade name, trademark, manufacturer, or otherwise does not necessarily constitute or imply its endorsement, recommendation, or favoring by the United States Government or any agency thereof. The views and opinions of authors expressed herein do not necessarily state or reflect those of the United States Government or any agency thereof.

Executive Summary

This report presents the conceptual design for a Direct-Hydrogen-Fueled Proton Exchange Membrane (PEM) Fuel Cell System for transportation applications. The design is based on the initial selection of the Chrysler LH sedan as the target vehicle with a 50 kW (gross) PEM Fuel Cell Stack (FCS) as the primary power source, a battery-powered Load Leveling Unit (LLU) for surge power requirements, an on-board hydrogen storage subsystem containing high pressure gaseous storage, a Gas Management Subsystem (GMS) to manage the hydrogen and air supplies for the FCS, and electronic controllers to control the electrical system. The design process has been dedicated to the use of Design-to-Cost (DTC) principles.

The Direct Hydrogen-Powered PEM Fuel Cell Stack Hybrid Vehicle (DPHV) system is designed to operate on the Federal Urban Driving Schedule (FUDS) and Hiway Cycles. These cycles have been used to evaluate the vehicle performance with regard to range and hydrogen usage. The PEM FCS, the hydrogen storage and the gas management subsystems will be developed by AlliedSignal Aerospace Engineering. The lead acid batteries used to supply surge power will be selected as test data and availability dictate.

The major constraints for the DPHV vehicle are vehicle and battery weight, transparency of the power system and drive train to the user, equivalence of fuel and life cycle costs to conventional vehicles, and vehicle range. The energy and power requirements are derived by the capability of the DPHV system to achieve an acceleration from 0 to 60 MPH within 12 seconds, and the capability to achieve and maintain a speed of 55 MPH on a grade of seven percent.

The size of the vehicle was selected as a six passenger payload capability and the need for cargo storage for those passengers. The vehicle test weight (curbside weight plus test payload) is 3330 pounds, representing a design task 10 percent lower than that of the current Chrysler LH sedan.

The conceptual design for the DPHV vehicle is shown in Figure 1. This design shows the Hydrogen Storage Subsystem (HSS) being located beneath the trunk and separated by the rear suspension with three 5000 psia tanks being used to provide 12 pounds of usable hydrogen (lower pressure limit is fixed by the outlet Hydrogen Low Pressure Control Valve). A detailed description of the HSS is given in section 4. The FCS is located in the space currently containing the transmission for the conventional Internal Combustion Engine power train. The GMS hardware is mainly located in the front of the vehicle in the engine compartment. A detailed description of the FCS Subsystem and GMS is given in section 3.

Batteries have been chosen as the supplemental energy supply for the LLU Subsystem. Load Leveling Batteries which provide surge power support to supplement the FCS Subsystem are located under the vehicle front seats. The controller units (motor and power) are located under the hood in the engine compartment. A detailed description of the LLU, selection of the LLU energy source, and the power controller designs is given in section 5.

DIRECT HYDROGEN PEM FUEL CELL VEHICLE

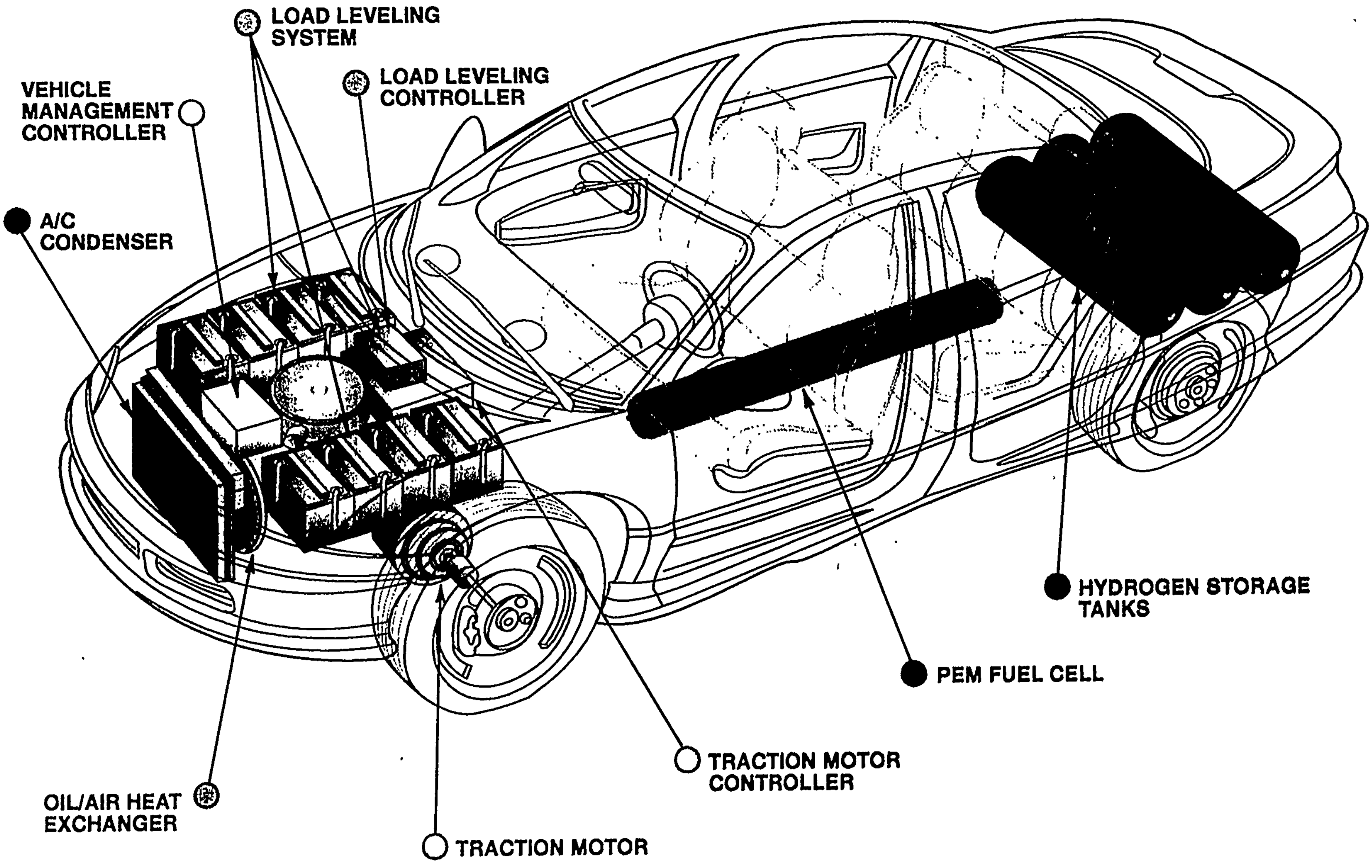
LOAD LEVELING SYSTEM
LOAD LEVELING CONTROLLER
VEHICLE MANAGEMENT CONTROLLER
A/C CONDENSER
HYDROGEN STORAGE TANKS
PEM FUEL CELL
TRACTION MOTOR CONTROLLER
OIL/AIR HEAT EXCHANGER
TRACTION MOTOR

Figure 1. DPHV Vehicle Configuration

The conceptual DPHV system is based on a 50 kW-rated PEM Fuel Cell Stack with a net, usable power of 40 kW. The PEM fuel cell will consist of five 10 kW modules. Although materials have been selected for the membrane, bipolar plates and the electrode assemblies for the prototype PEM fuel cell continue to be researched and developed as an ongoing cost sharing effort. The lead acid battery-powered LLU subsystem has a specific energy content greater than 30 Wh/kg and a specific power density less than 0.2 kW/kg. The motor tentatively selected for use as the power train drive source is the Westinghouse 3 phase AC motor. The DC input power bus to this motor's controller will have a nominal voltage of 320 VDC. A chopper/regulator circuit will control the output of the FCS to provide the primary power to the power train. The LLU subsystem will be connected directly to the DC power bus. Regenerative braking will be used to provide extended range of operation for the vehicle. The electrical configuration for the system is shown in Figure 2.

Preliminary simulation results for the DPHV system show that the peak power required to accelerate the vehicle to 60 MPH within 12 seconds requires values between 65 and 100 kW depending on the manner in which the peak speed is attained. The steady-state system power required to sustain the vehicle speed at 55 MPH on a seven percent grade is 40 kW.

Preliminary simulation of the FUDS and Hiway cycles indicates a hydrogen use (mileage) of 67.6 miles per gallon (gasoline equivalent) for no regenerative braking and 73.2 miles per gallon for regenerative braking. These values correspond to ranges of 321 and 348 miles, respectively. The use of the FCS Subsystem and the GMS will be optimized as the system design is finalized in order to achieve the goal of a 380 mile range. Table 1 provides the design goals for the DPHV system. These goals have been developed to conform to the Partnership for a New Generation of Vehicles (PNGV) goals wherever possible.

Table 1. DPHV Vehicle Design Goals

Parameter	Units	Value
Vehicle Test Weight	Pounds	3330
Wheel Radius	Feet	1.07
Frontal Area	Feet^2	23.5
Drag Coefficient (Cd)	***	0.250
Rolling Resistance Coefficient (Cr)	***	.0064
Vehicle Range	Miles	380
Time to Accelerate to 60 MPH	Seconds	12
Peak Power to Achieve Acceleration Goal	kW	76.3
Steady-State Power for Baker Grade Achievement	kW	40
FCS Peak Power (Deliverable)	kW	40
FCS Nominal Operating Temperature	°C	85
HSS Pressure	Pounds/Inch^2	5000
Hydrogen Storage Capacity	Pounds	12.6
LLU Power Source	***	Batteries
LLU Peak Power	kW	60
Nominal DC Battery Voltage	VDC	320
LLU Energy Density	Wh/kg	41
Chopper/Regulator Input Voltage	VDC	200-400
Chopper/Regulat or Output Voltage	VDC	240-320

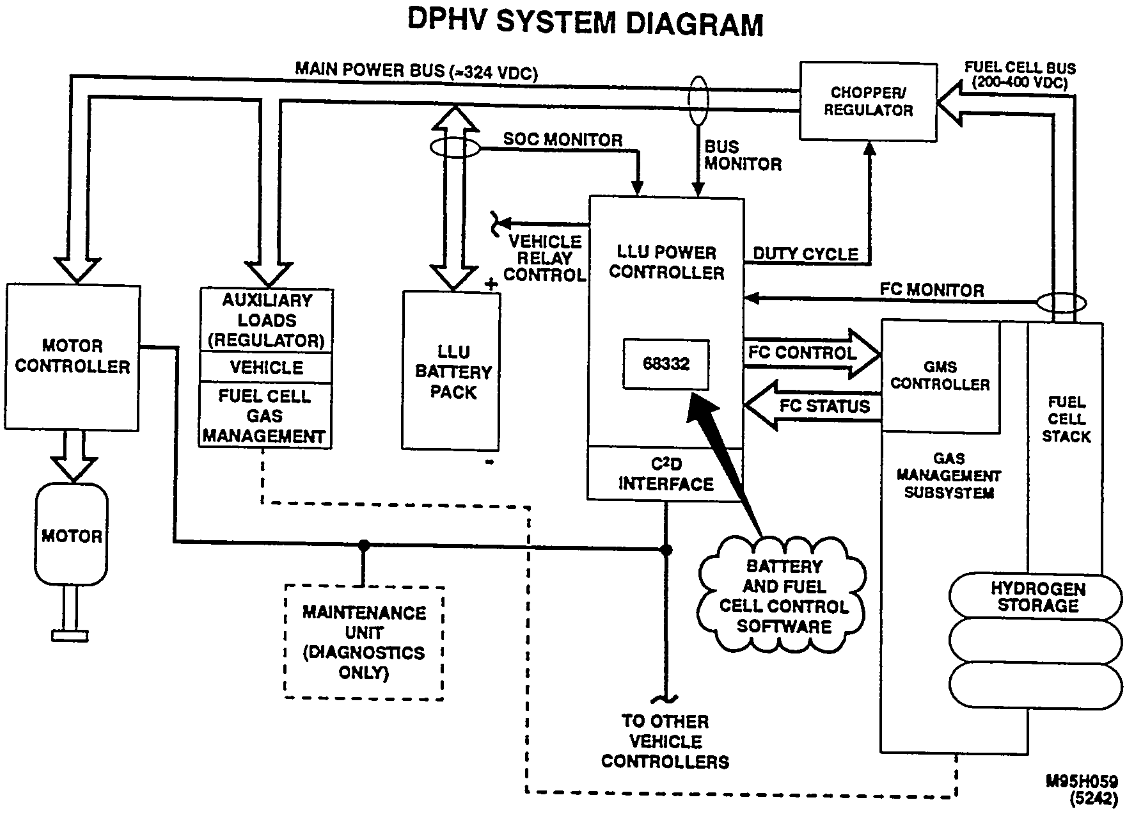
DPHV SYSTEM DIAGRAM
MAIN POWER BUS (~324 VDC)
CHOPPER/ REGULATOR
FUEL CELL BUS (200-400 VDC)
SOC MONITOR
BUS MONITOR
VEHICLE RELAY CONTROL
+
LLU POWER CONTROLLER
DUTY CYCLE
FC MONITOR
MOTOR CONTROLLER
AUXILIARY LOADS (REGULATOR)
VEHICLE
FUEL CELL GAS MANAGEMENT
LLU BATTERY PACK
-
68332
FC CONTROL
FC STATUS
GMS CONTROLLER
FUEL CELL STACK
C²D INTERFACE
GAS MANAGEMENT SUBSYSTEM
MOTOR
BATTERY AND FUEL CELL CONTROL SOFTWARE
HYDROGEN STORAGE
MAINTENANCE UNIT (DIAGNOSTICS ONLY)
TO OTHER VEHICLE CONTROLLERS
M95H059 (5242)

Figure 2. DPHV Electrical Configuration

Table 2 provides the weight allocation which has been assigned to the DPHV system. Column 2 of this table provides the system design goals while column 3 provides the current weight of the subsystem defined in column 1.

Table 2. DPHV Weight Allocation

Subsystem	Design Goal (lbs)	Current Weight (lbs)
Chassis/Body	2290	2550
Fuel Cell Stack	110	110
Hydrogen Storage	230	230
Gas Management	55	55
Load Leveling	205	314
Power Train	290	290
Total Weight	**3180**	**3549**

SECTION 1
VEHICLE CONSIDERATIONS

1.1 Vehicle Determination

1.1.1 Introduction

As part of this design study, four vehicle classes (subcompact sedan, midsize sedan [LH], minivan and full-size pickup truck) were considered before one was chosen. An assumption was made in this study that all of the vehicles, except the LH, had 1995 model specifications. The LH, by virtue of being chosen for the Partnership for a New Generation of Vehicles (PNGV), was considered in terms of both a 1995 model, for prototype (mule) purposes, and in terms of an 80 mpg PNGV LH vehicle. The performance objectives of PNGV are shown in Figure 1-1.

- Six-passenger vehicle (similar to Taurus, Lumina, or Concorde).
- Current Taurus: 26.5 mpg, therefore mpg goal is about 80 mpg combined city/highway (unadjusted Federal test procedure).
- Performance of 0 to 60 MPH in 12 seconds.
- Operating metro-highway range of 380 miles on the 1994 Federal Drive Cycle. Operating life of 100,000 miles.
- Equivalent:
  - Performance, ride, handling, noise, vibration, etc.
  - Customer features: interior volume, luggage space, climate control, entertainment packages.

Figure 1-1. Vehicle Parameters for Goal 3

In order to arrive at an 80 mpg LH sedan, the improvements shown in Figure 1-2, path 1, were modified using 85 percent efficient energy storage, a motor/ controller efficiency of 85 percent, and fuel cell efficiency of 50 percent (figures are averaged over the combined city and highway driving cycles).

Based on Figure 1-3, it is assumed that the fuel economy improvement in using such a combination will be (67/27) or 2.5 times that of the conventional Internal Combustion Engine (ICE) version. For example, since an LH currently provides approximately 30 mpg (Environmental Protection Agency [EPA]-adjusted, or labeled), the fuel economy figure used in Table 1-1 is 75 mpg

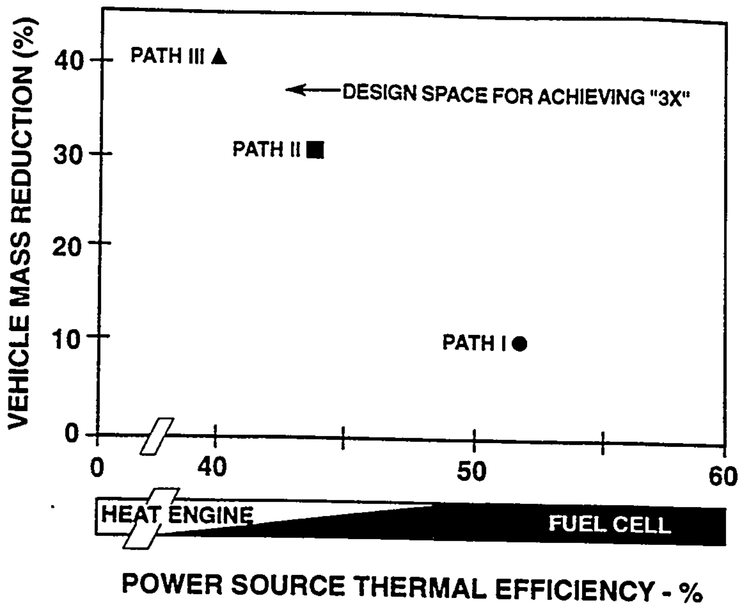

***EXAMPLE PATH I* ●**

51% THERMAL EFFICIENCY
10% MASS REDUCTION
50% REGENERATIVE BRAKING
90% EFFICIENT ENERGY STORAGE
76.5% EFFICIENT DRIVELINE
20% LOWER DRAG
20% LOWER ROLLING RESISTANCE
30% LOWER ACCESSORIES LOADS

***EXAMPLE PATH II* ■**

44% THERMAL EFFICIENCY
30% MASS REDUCTION
60% REGENERATIVE BRAKING
90% EFFICIENT ENERGY STORAGE
76.5% EFFICIENT DRIVELINE
20% LOWER DRAG
20% LOWER ROLLING RESISTANCE
30% LOWER ACCESSORIES LOADS

***EXAMPLE PATH III* ▲**

40% THERMAL EFFICIENCY
40% MASS REDUCTION
70% REGENERATIVE BRAKING
90% EFFICIENT ENERGY STORAGE
76.5% EFFICIENT DRIVELINE
20% LOWER DRAG
20% LOWER ROLLING RESISTANCE
30% LOWER ACCESSORIES LOADS

M95H036
(5240)

Figure 1-2. Propulsion and Vehicle Improvements Needed for 80 MPG (Adapted from PNGV)

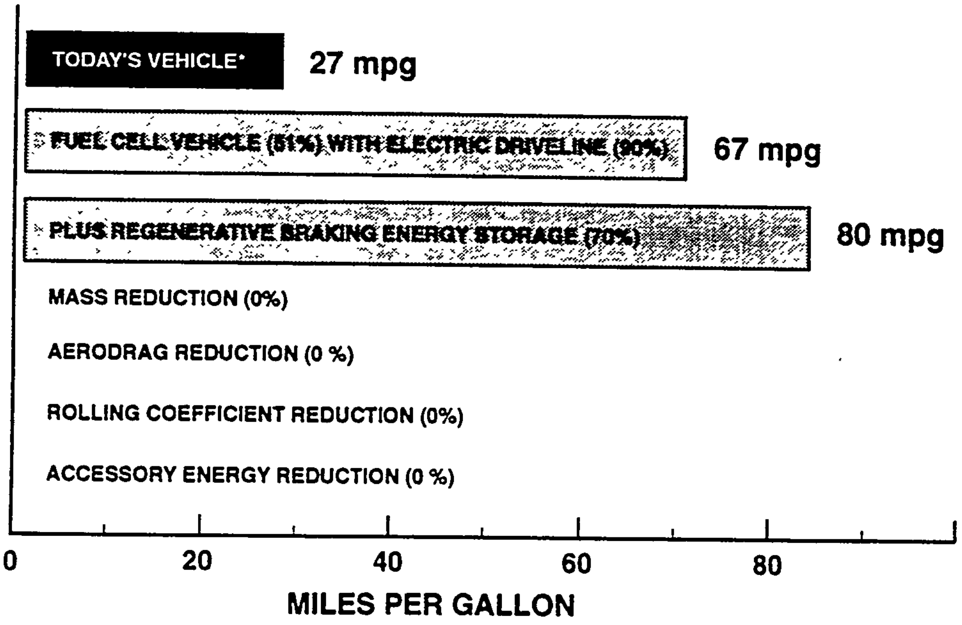

** TODAY'S VEHICLE (BASELINE): ENGINE (23%), DRIVETRAIN (70%)*

M95H033
(5237)

Figure 1-3. Fuel Cell Pathway to 80 MPG (Adapted from PNGV)

(30 x 2.5). As mentioned before, the sole exception to this 2.5X rule is the PNGV vehicle which is meant to provide 3X.

1.1.2 Vehicle Selection Process

The four factors discussed below were considered in making the vehicle selection.

- **Vehicle Power Requirements** – The following equation was used to determine steady-state power requirements:

  $$P = 0{*}5{*}p{*}C_d{*}A{*}v^3 \; + \; m{*}g{*}C_r{*}\cos(\;){*}v \; + \; m{*}g{*}\sin(\;){*}v$$

  where

  p = density of air at 300° K = 1.293 kg/m^3

  = angle of grade; v = vehicle velocity, in m/s

  g = acceleration due to gravity, in m/s^2

  C_d = drag coefficient; C_r = rolling resistance coefficient

  P = Power.

  Table 1-1 explains the other symbols and shows the specifications used for each vehicle. In every case, an energy storage (or peak power) device is required to make up the extra power needed to provide a 12 second, 0-60 MPH, acceleration.

  Power from the fuel cell is also needed to operate the hotel loads (e.g Heating/Ventilation/Air Conditioning [HVAC], power steering, headlights, etc.). For example, the power steering and headlight functions must be capable of being operated when the fuel cell is providing peak continuous power and the combination consumes around 2 kW; operation of HVAC, potentially capable of an even bigger power drain, is not typically required under these performance test conditions. If the HVAC is operating then hill climbing capability will be compromised slightly. However, in all other situations normal performance can still be obtained even with the HVAC on.

- **Vehicle Range Requirements** – Each of the four vehicle classes currently has a different range based on available packaging space for the fuel tank and vehicle's fuel economy. However, it was decided that since the range of these vehicles is somewhat arbitrary a reasonable comparison can still be made if it is assumed that each vehicle needs to provide approximately 380 miles range. This is in accordance with the PNGV goals for the LH.

Table 1-1. Vehicular Performance Requirements

	1995 Subcompact Sedan	1995 Midsize Sedan (LH) for Prototype Use	PNGV Midsize Sedan	1995 Minivan (AS)	1995 Fullsize Pickup Truck (BR)
Aerodynamic Drag Coefficient[1], C_d	0.33	0.35	0.25	0.40	0.48
Frontal Area, A, m^2 (ft^2)	1.92 (20.6)	2.20 (23.5)	2.20 (23.5)	2.63 (28.3)	5.95[2] (64)
Rolling Resistance Coefficient[1], C_r	0.0070	0.0076	0.0064	0.0091	0.0148
Vehicle Performance Test Weight[1], m, kg (lb)	1250 (2745)	1770 (3892)	1510 (3330)	2030 (4475)	5580 (12500)
Fuel Cell Power[3], kW (HP)	40 (53)	50 (67)	40 (53)	60 (80)	130 (174)
Fuel Economy[4], EPA-Adjusted, or Label Figure, mpg Gasoline Equivalent	75	54	66 (80 mpg based on CAFE credit)	50	37
Range Requirement, Miles	380	380	380	380	380
Hydrogen Internal Storage Volume[5], liter (ft3, gallons)	225 (7.9, 60)	310 (10.9, 80)	260 (9.1, 70)	330 (11.8, 87)	450 (16, 118)

[1] 1995 vehicle curb weight+300 lb payload (exception: pickup truck, which is tested at 12500 lb GVW); PL modifications shown in Figure 1-2
[2] trailer included
[3] net power
[4] assuming 2.5 times ICE vehicle's fuel economy except the PNGV vehicle (3X)
[5] unadjusted for ambient temperature

MS95I111

Labeled fuel economy figures, rather than EPA-tested figures, are used in determining the fuel's energy storage requirements. For example, the LH sedans achieve approximately 26-27 mpg on the EPA combined City/Highway Cycle (hence 3X is 80 mpg) and yet the EPA-adjusted figure is 21-22 mpg. When combined with the gasoline tank volume (or hydrogen storage tank volume if gallons gasoline equivalent is used) this adjusted fuel economy figure provides an approximate indication of the vehicle's range.

However, in the case of compressed gas storage, the actual range given ambient refueling conditions will be approximately 3/4 times the nominal range which is that predicted from the energy content of the fuel tank and the fuel economy; this discrepancy between actual and nominal range is explained in Section 4. In other words, if conventional pressurized five minute refueling takes place, then the vehicle's range would be reduced to approximately 285 miles for all of the vehicles. Nominal ranges of 380 miles will be used in Section 1.1.3.

- **Vehicle Cost** – Cost is vitally important but the sensitivity to increased cost due to advanced technology is clearly different when comparing the demographics of subcompact owners versus luxury car owners. For this reason, new technology is often introduced into the high end of the market first before the effects of mass production allow the same technology (e.g. ABS, fuel injection, etc.) to flow down to the subcompact car segment.

- **Vehicle Mission** – Attention was given to how the implications of fuel cell and hydrogen storage cost, weight and volume (dictated by factors 1, 2 and 3) might affect the vehicle's mission and how it would interact with the demographics of the vehicle's customers to ensure that the product could reasonably be marketed.

  As an extreme example, minivan customers take safety and interior cabin space more seriously than do sports car owners while hauling capability is of paramount important to pickup truck owners. For cars, a certain threshold trunk space has to be met, but this is subjective since a small trunk might be acceptable in certain situations (e.g. convertibles).

1.1.3 Conclusion

- **Subcompact Sedan** – The subcompact car, by virtue of its low cost, is not designed to have the same utility or performance as other vehicles and so in this sense it is not so demanding an application. For example, it is the lightest and most fuel efficient vehicle in the fleet and therefore requires the smallest fuel cell system and the smallest volume of hydrogen storage given the assumption that all vehicles, except the midsize LH sedans, need to provide 350 miles range. However, this reduction in fuel tank volume does not compensate for the fact that much less packaging space is available compared with the other vehicles. A packaging study, shown in Figure 1-4, reveals that two tanks of approximately equal length, mounted down the tunnel, may be the optimum use of available space and results in 2.7 ft^3 of hydrogen storage which translates into a range of approximately only 120 miles or three times less than required. For purposes of clarity, only the tanks are shown and not the supporting hardware. Another consideration is that the initial cost of a fuel cell hybrid vehicle is very likely to be higher than for a conventional vehicle and the likely consumers for such a vehicle must be both willing and able to pay extra to make an environmental statement. This tends to rule out an economical subcompact car at this time.

- **Minivan** – With regard to minivans, recent surveys confirm that interior volume is their most important attribute so that any reduction caused by a need for hydrogen storage is a critical problem. Figure 1-5 shows the arrangement of the four tanks used in Chrysler's 120 mile range CNG-powered minivan. Since, for a given pressure and volume hydrogen stores approximately three-four times less energy than natural gas, the same four tanks storing hydrogen at 5,000 psia will provide the fuel cell-powered minivan with approximately the same nominal range which is one-third the range required. (For the same safety factor, 5,000 psia hydrogen requires slightly thicker tank walls than 3,000 psia natural gas so the range may be impaired even more.) More

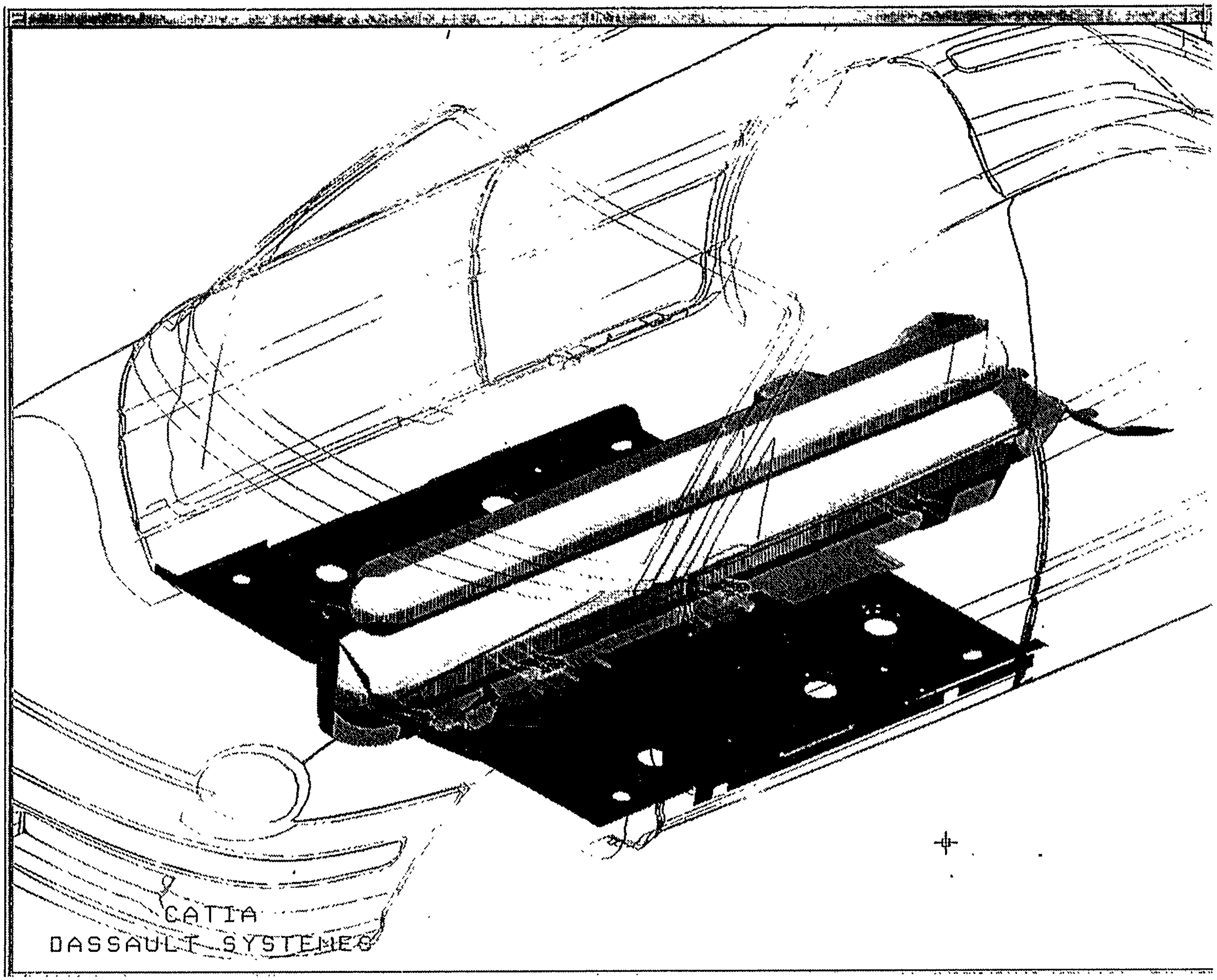
CATIA
DASSAULT SYSTEMES

Figure 1-4. Subcompact Packaging Design

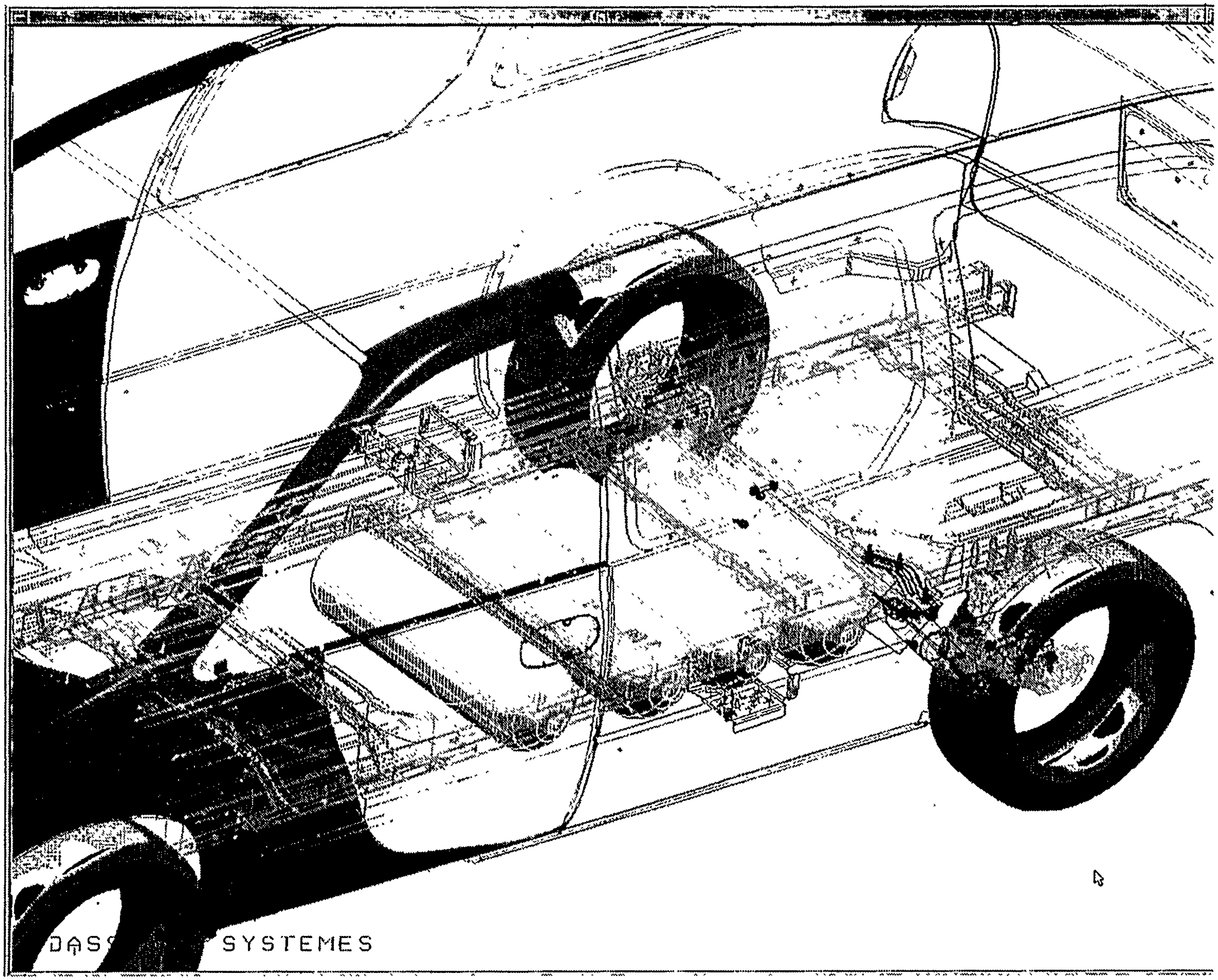
DASS SYSTEMES

Figure 1-5. Minivan Packaging Design

tanks can be added, of course, but the tank cost will be much too expensive and interior cabin space and payload will be compromised. Clearly, the need for 380 miles range imposes severe penalties for a hydrogen-powered minivan. Another factor which must be considered is safety which is particularly important in this category. The public's perception of hydrogen as a dangerous fuel may be more of an issue for this vehicle than for other vehicle segments. Finally, the need for a larger fuel cell and hydrogen storage tank will add more cost than for the midsize sedan and yet minivan customers may be even less willing to pay a premium.

- **Full-size Pickup Truck** – The pickup truck appears to be the least sensible choice for a hydrogen fuel cell powered vehicle because its specific mission requires high power requirements. Steady cruising at high speeds or up long grades create a special situation for a pickup truck since these vehicles are meant to be capable of carrying heavy payloads and towing trailers. The fuel cell power requirements will, therefore, be much higher than for other vehicles, even the minivan, and this will reduce payload capability and substantially increase vehicle cost. The volume occupied by the hydrogen storage tanks will also be higher than for the other vehicles because the vehicle is less fuel efficient and yet an equal or better range is demanded. Figure 1-6 shows a 3,000 psia CNG tank occupying part of the full-size pickup truck's bed and it is predicted that a 5,000 psia hydrogen fuel cell powered version might provide a range of up to 250 miles if the required fuel cell efficiency target is met.

- **Midsize Sedan** – The agreement between the automakers and the Federal Government PNGV is a major reason for the current interest in fuel cells for automotive applications. The midsize sedan may have been chosen as the Goal 3 (3X) vehicle because it represents the heart of a potential fuel cell vehicle market in that the demographics of vehicle ownership parallels closely the majority of the population that is both willing and able to adopt advanced technology. This has important consequences for the fuel cell and hydrogen storage tanks. From a technical challenge standpoint, the midsize sedan does not place the same burden on a powertrain as a truck and space is less critical than in a minivan so that the viability of both the fuel cell and the hydrogen storage is enhanced. Figures 1-7, 1-8, and 1-9 show a packaging study for a PNGV LH which will provide a nominal 380 mile range in an 80 mpg vehicle - more information concerning this design is contained in Section 4. A liquid hydrogen version was also studied, and is shown in Figure 1-10.

  Figure 1-11 illustrates the midsize sedan conceptual design with the three hydrogen storage tanks in the rear, the fuel cell stack in the tunnel and the ancillaries, motor/controller, and battery under the hood.

  In summary, the midsize sedan appears to represent the optimum vehicle in terms of fuel cell and hydrogen storage tank cost, weight and volume and customer acceptance.

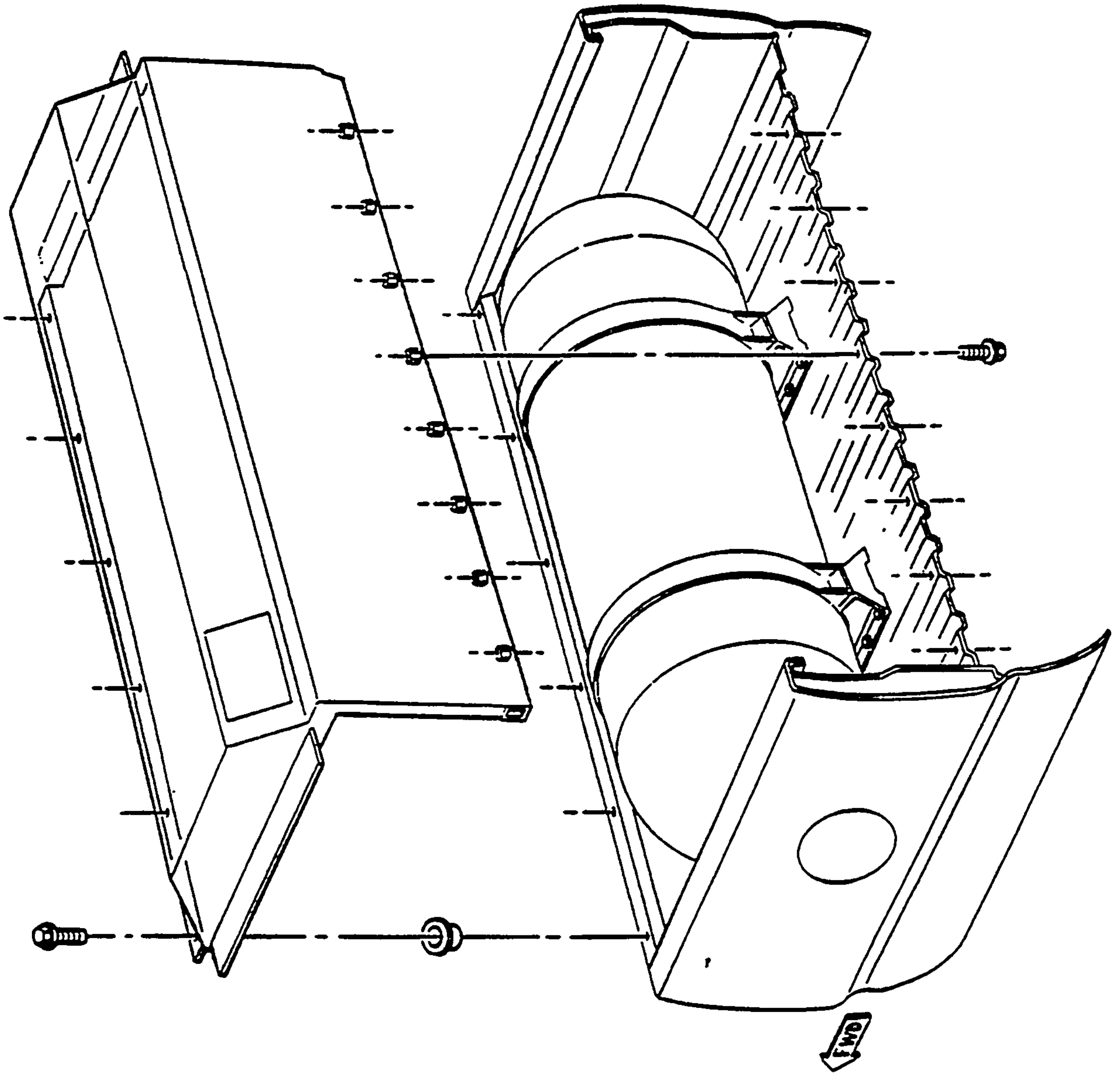

Figure 1-6. Full-size Pick-up Truck Packaging Design

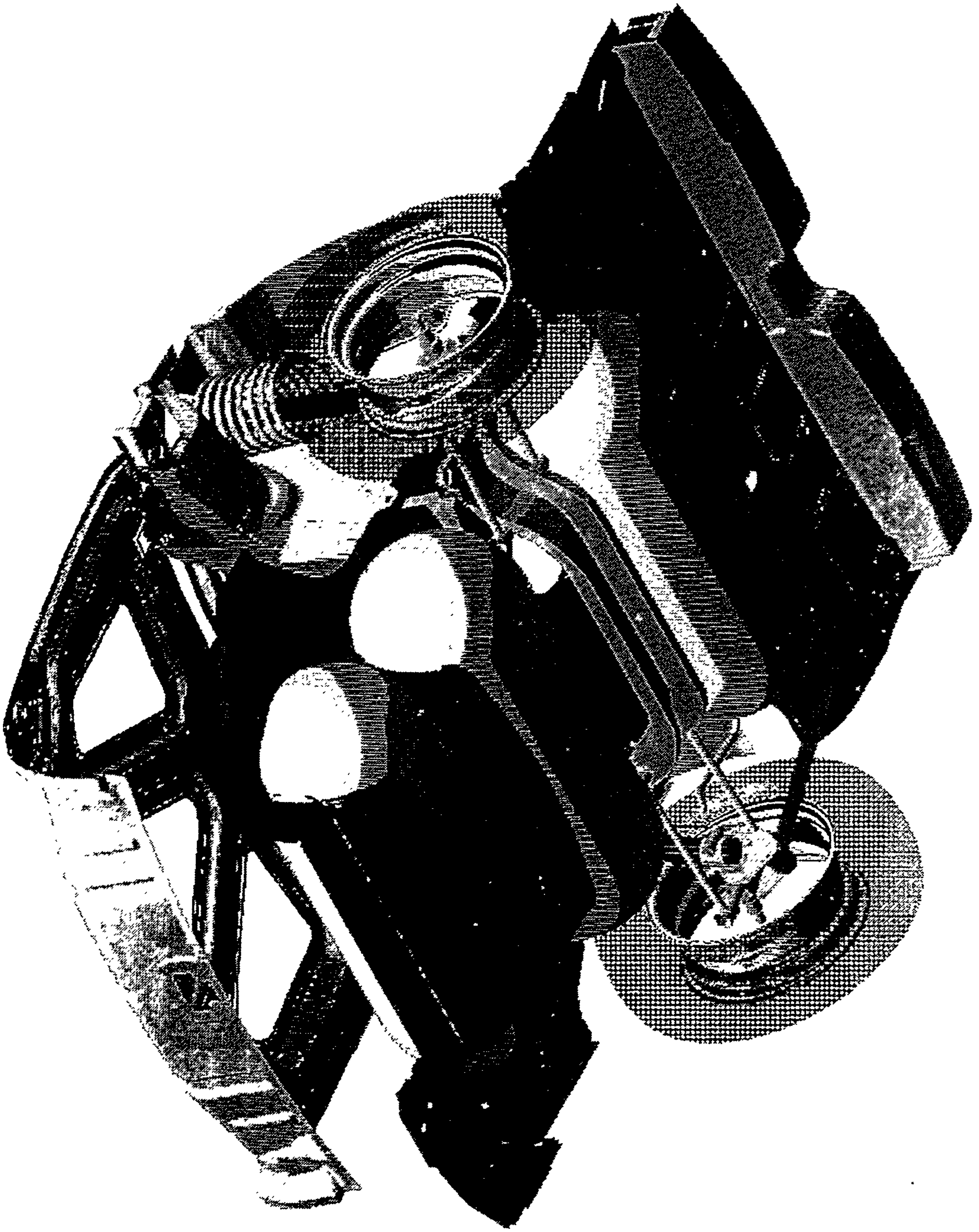

Figure 1-7. PNGV LH Mid-Size Sedan Packaging Design

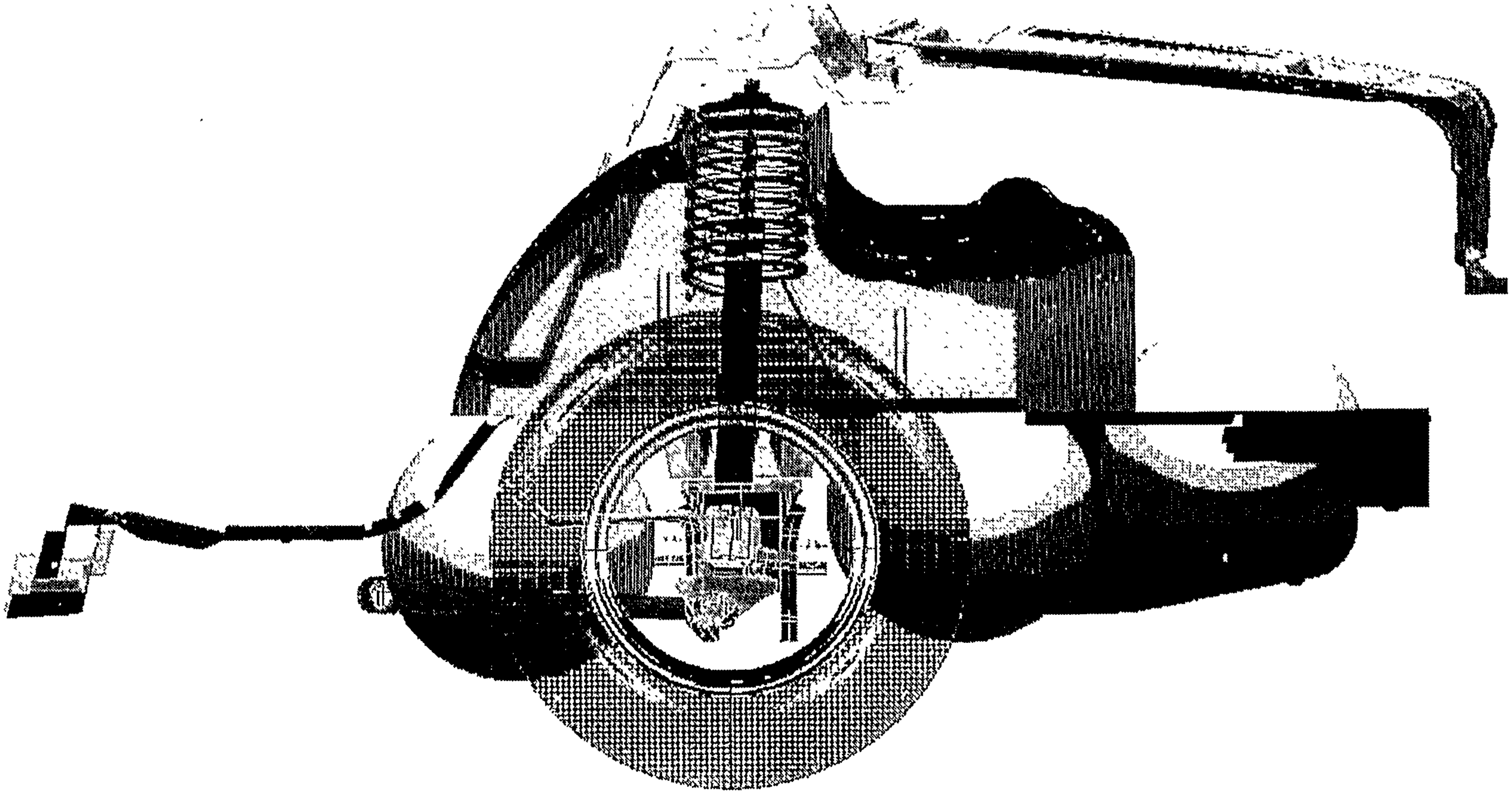

Figure 1-8. PNGV LH Mid-Size Sedan Packaging Design

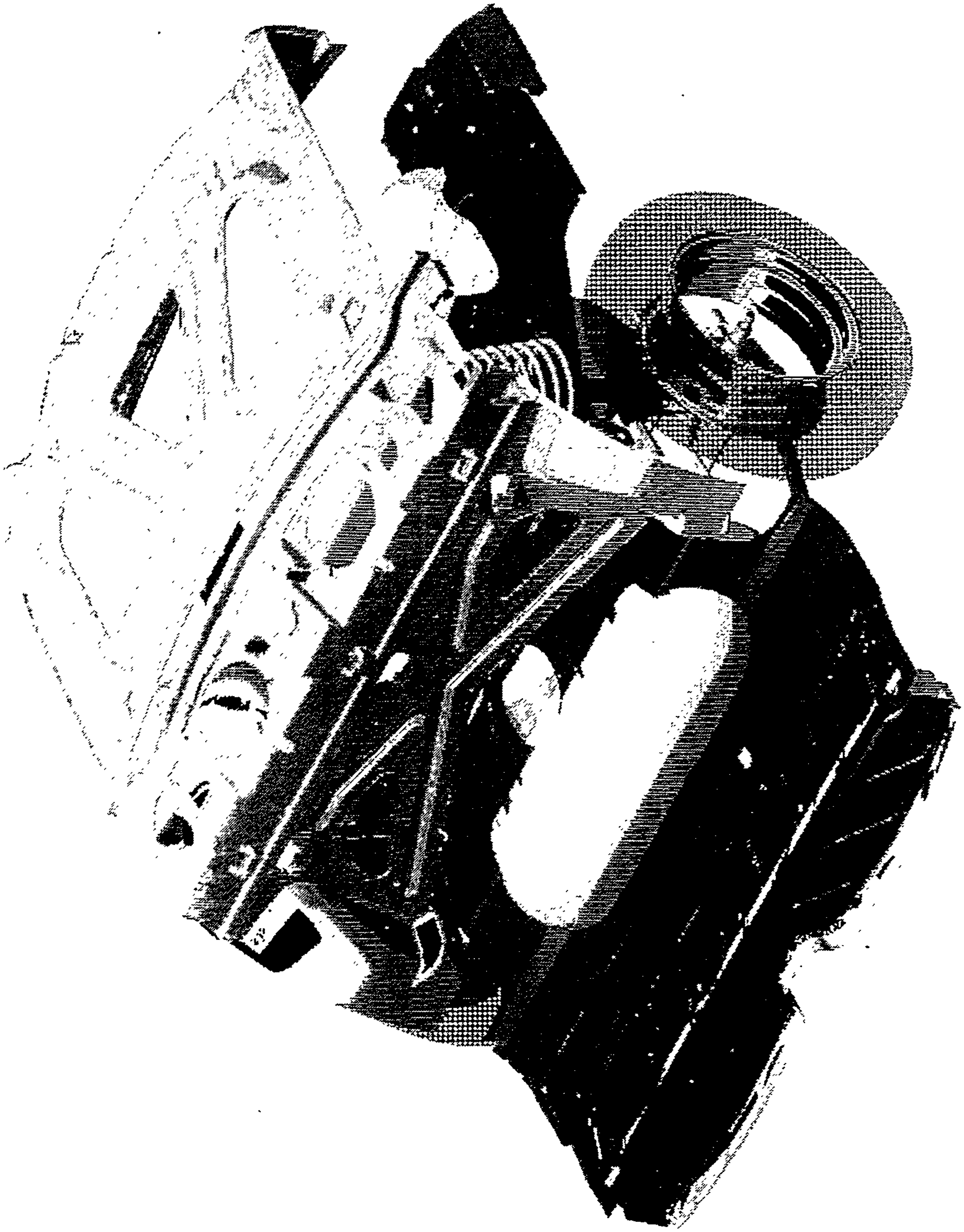

Figure 1-9. PNGV LH Mid-Size Sedan Packaging Design

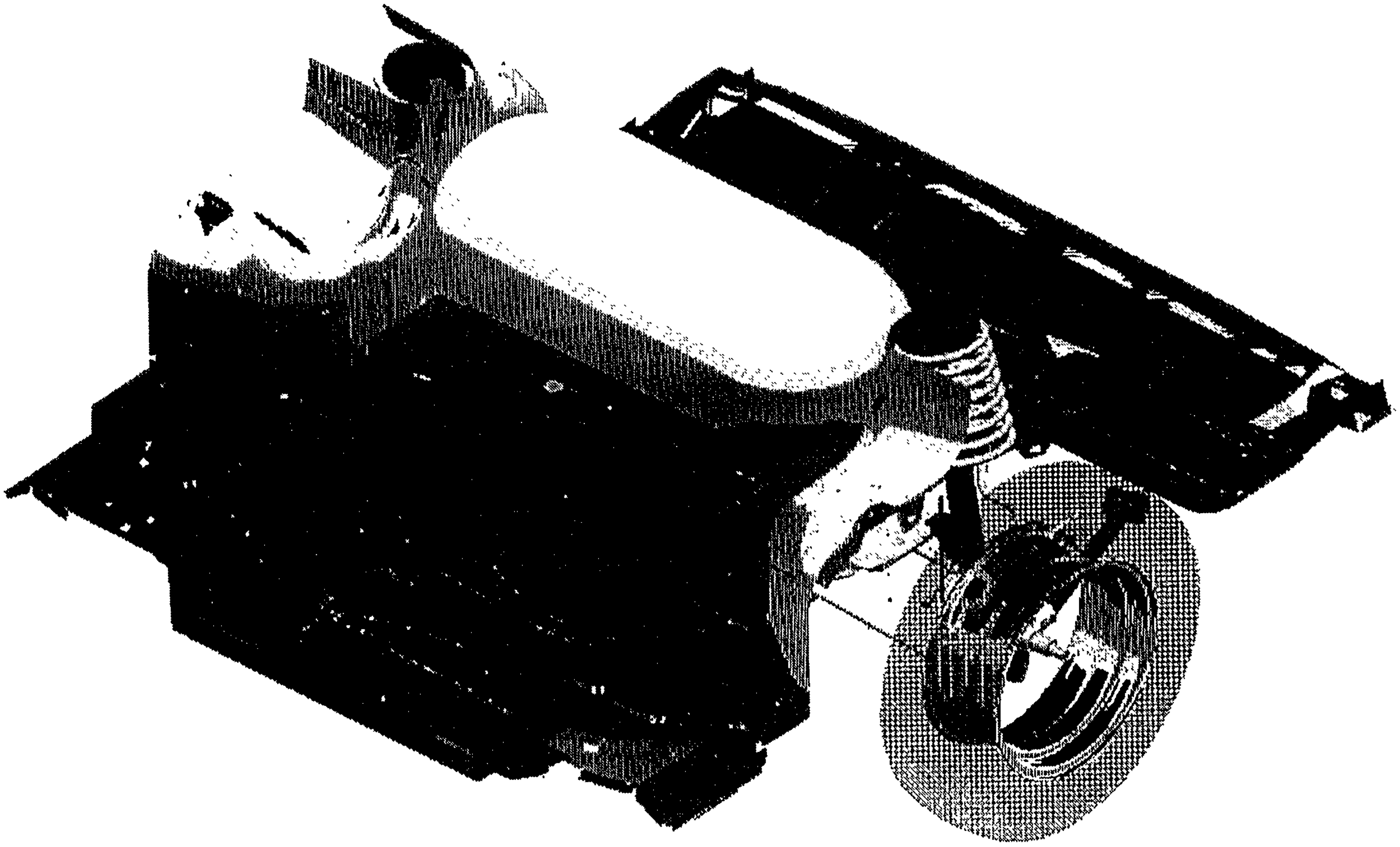

Figure 1-10. PNGV LH Mid-Size Sedan Packaging Design

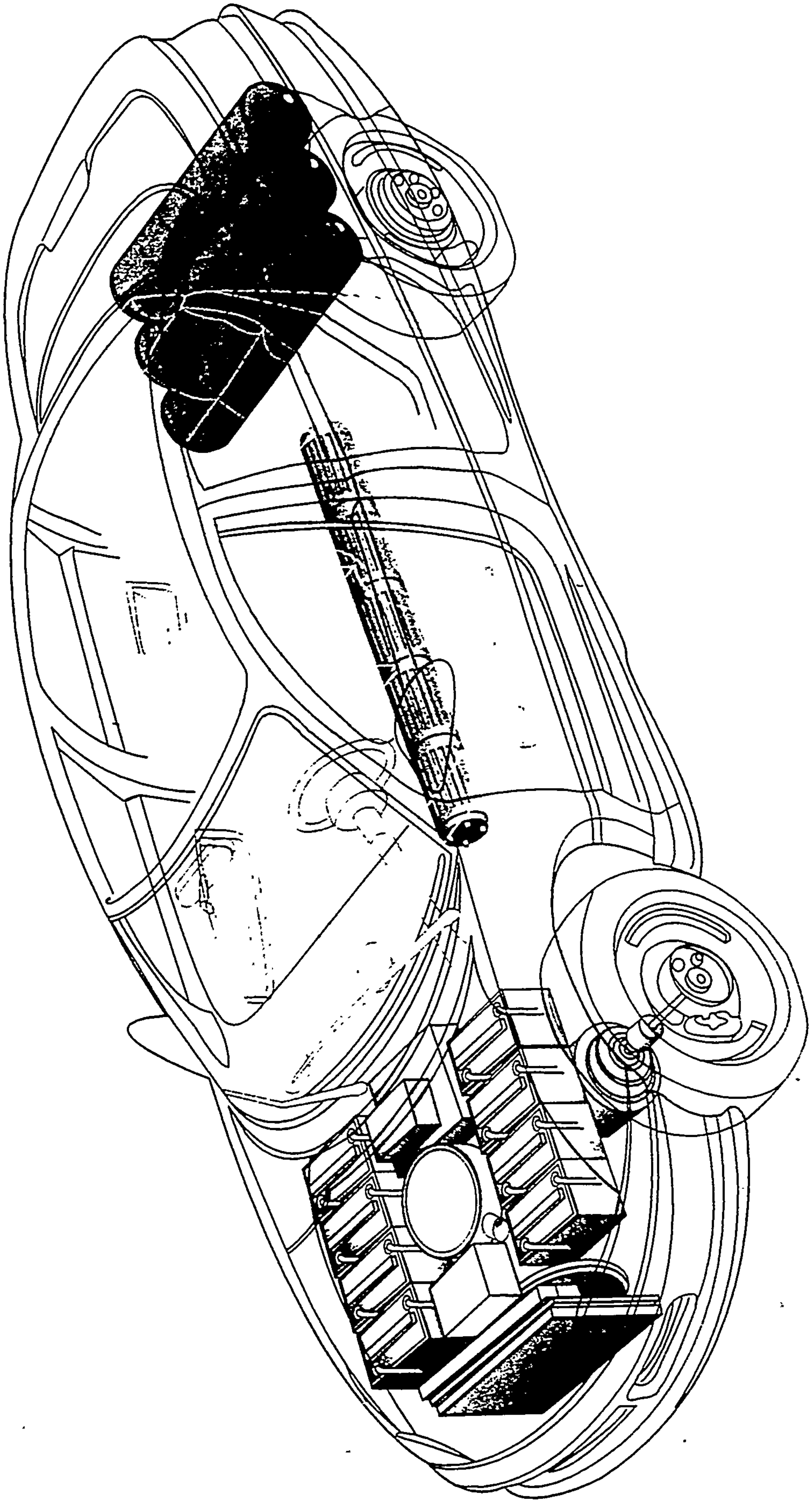

Figure 1-11. PNGV LH Mid-Size Sedan Packaging Design

1.2 Powertrain Size and Operational Requirements

1.2.1 Hybridization

Analyses to date have shown that hybridization is required for a fuel cell vehicle to meet cost, weight, efficiency, and performance goals. It is very important to consider more than just the fuel cell's polarization curve when trying to analyze the optimum system for maximizing vehicle fuel economy when designing systems for hybrid fuel cell vehicles; factors such as regenerative braking, fuel cell part load efficiency, and fuel cell shutdown capability must also be considered in the design process. Cost and weight are also factors to consider on a systems level since the level of improvement that can be made in competing technologies, such as batteries, is unknown. Tradeoff analyses are an ongoing process and will continue as new and better information becomes available.

Following is a discussion of the three major areas considered in the design of a hybrid system:

- **Regenerative Braking** – Since the vehicle mass of the fuel cell vehicle is relatively high (because it is assumed that the efficiency is so high that only a small mass reduction is necessary to meet 80 mpg PNGV goals) the effect of regenerative braking is marked. The dedicated fuel cell propulsion systems lacks regenerative braking, which can be the equivalent of 5-10 percent absolute efficiency, pointing out the difference between a 50 percent efficient fuel cell and a 40-45 percent efficient one. Such a difference is highly significant.

- **Fuel Cell Part Load Efficiency** – Most driving is done under very light load (for example, 10 kW corresponds to approximately 60 MPH cruising with a typical air conditioning load) and Figure 1-12 (taken from Figure 3-10) shows how the projected efficiency of a 40 kW fuel cell system's performance falls drastically below 4 kW (10 percent of rated load) due to the behavior of less-than-ideal air compressors. This leads to the conclusion that a 90 kW fuel cell system will probably operate less efficiently under 10 percent of rated load than a 40 kW fuel cell operating under the same driving conditions (i.e. between 10 and 25 percent rated load). When the vehicle demands 20-40 kW from the fuel cell system then the 90 kW version may be slightly more efficient than the 40 kW but the amount of time spent under these conditions is relatively small (steep hill climbing and fast cruising). Moreover, during periods of very light load (< 4 kW) the 40 kW fuel cell can recharge the battery. For example, if only 1-2 kW is required for propulsion or for hotel loads, the hybridized fuel cell can generate 5 kW and use the surplus power to regenerate the battery's charge. Despite the 60-65 percent turnaround efficiency of this approach it may still be more efficient than operating the fuel cell at 1-2 kW, as Figure 1-13 shows. The 90 kW fuel cell, on the other hand, has to provide the 1-2 kW since there will be no energy storage device. Improvements in air compressor technology and, to a lesser extent, the fuel cell stack may change this argument in the future.

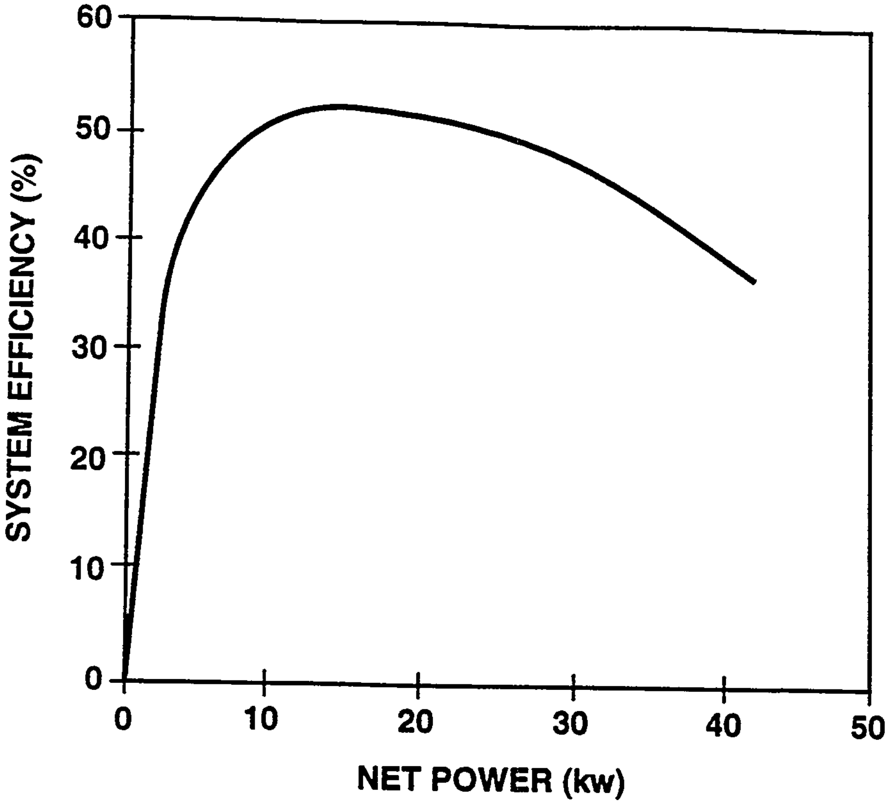

M95H035
(5237)

Figure 1-12. System Efficiency

- **Fuel Cell Shutoff Capability** – The ability to turn the fuel cell off while the vehicle is decelerating and idling may increase the efficiency of the fuel cell significantly during the EPA combined city/highway cycle, discussed in Section 2.1.

  Figure 1-14 shows that the vehicle does not require motive power for nearly 60 percent of the urban drive cycle. (The highway mode is not so critical in this respect but this cycle is also where the ICE is relatively competitive on an efficiency basis.)

  Another energy conversion device, the compression-ignition engine, has already demonstrated this idle-off capability in production versions and if fuel cells cannot meet the same requirement then the relative efficiency advantage of the fuel cell will be lowered to the point where it may not be competitive. A dedicated fuel cell will have to be kept on all the time since fast response is demanded while starting from a stoplight, for example. In this environment, a cooled-down fuel cell may be sluggish and, therefore, dangerous. However, if the fuel cell is hybridized the battery can cope with the fast takeoffs and allow the fuel cell the option of being turned off when the car is decelerating or idling.

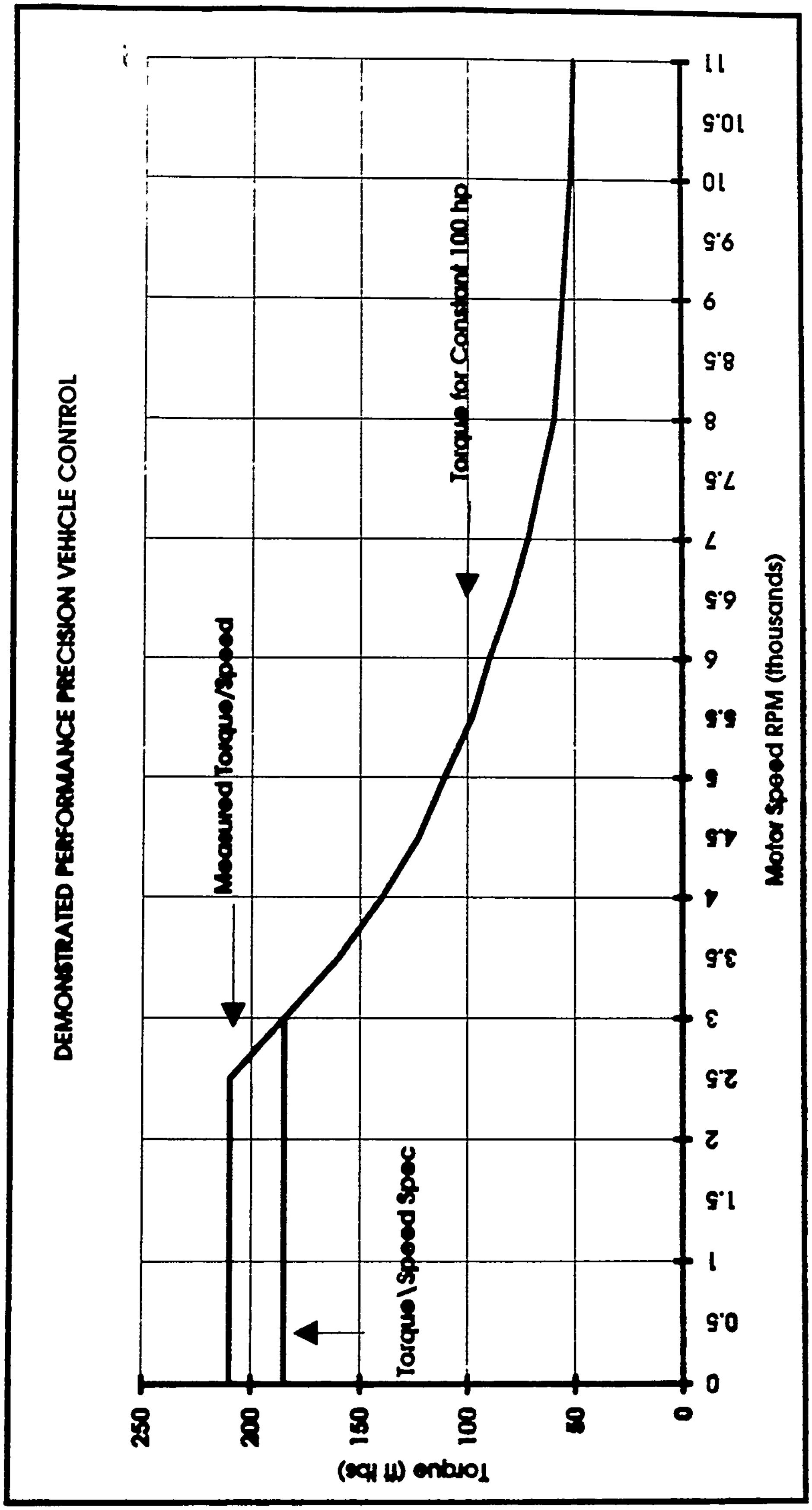

Figure 1-13. Precision Vehicle Control

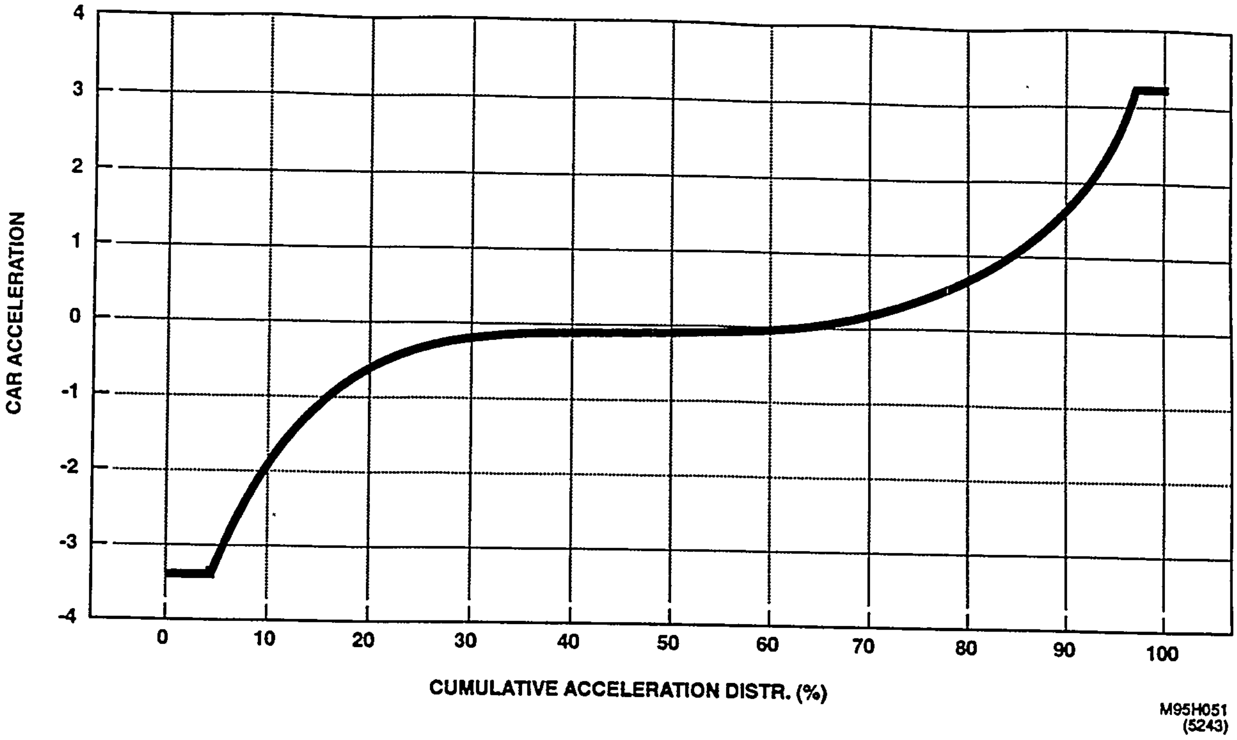

Figure 1-14. Acceleration Histogram (EPA City Driving Cycle)

The need for the powertrain to be operational at key-on is currently a restriction on fuel cells since they might not produce adequate power immediately and will not deliver power at all if the ambient temperature is sufficiently cold. If the fuel cell is not hybridized, the "solutions" to this dilemma may involve burning some hydrogen to heat the fuel cell but this would generate emissions. Alternatively, the fuel cell can be kept warm by feeding hydrogen transiently into it while the car is parked. The generated electricity, however, is wasted since there are no on-board batteries. Any approach will clearly reduce real-world fuel economy since hydrogen is consumed without the vehicle travelling anywhere. If the fuel cell is heated up by an external heating element, fuel must still be consumed somewhere to maintain the fuel cell in a state of operator readiness. Moreover, an external heating element will only work if an electrical supply is at hand so that airport parking may still be a problem. The EPA fuel economy tests do not consider these scenarios but they are important, nonetheless.

1.2.2 Fuel Cell Power Sizing

The following two factors were considered in the study to establish fuel cell power sizing.

- **Hill Climbing Capability** – The fuel cell is sized to give comparable hill-climbing performance with today's LH while the batteries take care of the supplemental power required for acceleration. The alternative approach of sizing the fuel cell for highway cruising and using enough batteries to allow the worst grades to be climbed was not used. The latter approach does allow a downsizing of the fuel cell as a favorable tradeoff for a larger battery in terms of weight, size, and cost and it will also create shallower discharges during startup and acceleration which might extend battery life.

However, it was not chosen because the control issues and drivability/ litigation concerns associated with ensuring that the vehicle never abruptly decelerates during hill climbing, due to the battery power failing, makes the latter approach more risky. Ensuring that the fuel cell will propel the vehicle up any grade so long as fuel is in the tank will also make the vehicle drive more like a conventional car.

- **Vehicle Selection** – A PNGV LH rather than a 1995 LH, was used since the fuel cell vehicle is being designed with PNGV in mind. This factor, as Table 1-1 shows, suggested that a 40 kW fuel cell system (all power figures quoted refer to net power, not gross) should be adequate to provide a PNGV LH with acceptable performance.

Since the fuel cell will consist of five 10 kW modules, the peak net power may actually be closer to 44 kW than 40 kW and thus will provide a useful margin of safety.

1.2.3 Electric Motor and Battery Sizing

The 1995 LH, fitted with the 3.3 liter 150 HP (112 kW) engine, obtains a 0-60 mph time in around 11.1 seconds so that if the PL is 10 percent lighter and more aerodynamic the total power requirements of a conventional LH should be at least 10 percent less, or 100 kW.

However, when determining the required balance between the 40 kW fuel cell system and the power required to accelerate the vehicle 0-60 mph in 12 seconds, it is very important to consider low-end torque since this also dictates how rapidly an acceleration can occur. Provided there is adequate cooling, certain electric motors (constant torque up to half speed followed by constant power as shown in Figure 1-13) can outperform a conventional mechanical drive system so that an electric powertrain conservatively might only need to deliver 75 kW to obtain a 0-60 MPH time comparable with a conventional 100 kW powertrain. Since the drive train is an average of 85 percent efficient during this period, the maximum power output from the electric powertrain has to be approximately 80 kW.

Since it must be assumed, under extreme cold conditions, that the fuel cell might be incapable of supplying power to the vehicle for the first several minutes, maintenance of the performance requirements under these conditions would dictate that the battery be sized for 80 kW. Thus, during typical driving conditions when the fuel cell is operational, the combined power of the battery and fuel cell would be greater than necessary.

In order to be able to accept regenerative braking at all times and yet be able to deliver pulse power for accelerations when required means that the battery State of Charge (SOC) should fluctuate within a narrow band (e.g. 60-90 percent SOC). This means that the battery may need to be sized for 3 kWh so that approximately 2 kWh, which should be sufficient for startup power and energy requirements, is usable. Worst case startup 0-60 MPH in 12 second accelerations require 0.5 kWh. Since further cruising at 60 MPH for two minutes consumes an additional 0.5 kWh, a usable energy storage of 2 kWh should be sufficient. Note that when the fuel cell can be kept viably in a state of near user readiness, by preventing it from freezing during very cold ambient conditions, less energy storage may be necessary since the cruising power requirements might be met by the fuel cell producing half its rated power after 15 seconds.

In the near term the batteries that can be used will have specific amp-hour capabilities such as 10 Ah, so that the difference between, say, a 6 kWh and a 3 kWh battery pack will be a marginal improvement in performance under extreme conditions. This will probably result in an unacceptable tradeoff in terms of doubling the cost, weight, and volume. When all performance requirements are balance against the cost, vehicle weight and system efficiency, the optimum specifications for a LLU should be a 60 kW, 3 kWh, and 320 VDC system.

1.2.4 Conclusion

Hybridization is imperative if the fuel-cell powered vehicle is going to meet cost, weight, and efficiency targets. It will also be essential if the vehicle's drivability and utility is to approximate that of a conventional vehicle in terms of startup and transient response. Table 1-1 provides the vehicle design requirements for each of the vehicles considered in the vehicle selection procedure.

Highly efficient, compact, and inexpensive insulation may be found to mitigate complications caused by cooling in the PEM FCS, but several other problems (e.g. regenerative braking, weight penalty, low power load inefficiency) still remain. There will have to be unforeseen major advances in fuel cells in order for the concept of a dedicated fuel cell to make sense for light-duty vehicle applications.

SECTION 2
VEHICLE PERFORMANCE REQUIREMENTS

This section provides a discussion of the analyses which have been performed to determine the response of the Direct Hydrogen Fueled Proton Exchange Membrane Fuel Cell System for a Hybrid Vehicle (DPHV) conceptual vehicle to various driving conditions and vehicle requirements.

2.1 Driving Cycles

The various driving cycles which determine the vehicle performance include the acceleration to 60 MPH within 12 seconds, the Baker Grade (vehicle attaining a speed of 55 MPH on a seven percent grade), the Federal Urban Driving Schedule (FUDS) and the HIWAY cycle. The impact of each of these driving cycles on vehicle performance is discussed below.

2.1.1 Acceleration Cycle

The definition of the 0 to 60 MPH acceleration within 12 seconds determines the peak power capability requirement for the DPHV system. The manner in which this acceleration is achieved should reflect the vehicle power train response capabilities. Thus the motor and motor controller must have performance characteristics which allow the achievement of the required acceleration with the minimum expenditure of power.

Figure 2-1 provides four different acceleration scenarios which have been analyzed for the DPHV system. The curve labelled as Accel1 corresponds to a two speed transmission acceleration, Accel corresponds to the 60 MPH cycle used in the first analysis using the SIMPLEV simulation code, and Accel2 corresponds to a constant acceleration cycle (7.33 ft/sec^2). The curve labelled as AccelL corresponds to the acceleration profile used for modelling the Partnership for a New Generation of Vehicles (PNGV) performance characteristics.

2.1.2 Baker Grade Cycle

The Baker Grade cycle provides a scenario in which the vehicle achieves a speed of 55 MPH on a seven percent grade. The vehicle speed and power versus time for this cycle is shown in Figure 2-2. It should be noted that 55 MPH speed is achieved for this cycle in 34 seconds. This is an arbitrary time allocation since the requirement does not specify the time in which the requirement must be met.

2.1.3 FUDS/LA92 Cycles

The FUDS cycle, shown in Figure 2-3, represents a nominal driving sequence in a city environment. This cycle has also been modified to represent driving conditions in a city with freeway access represented by the LA92 cycle, shown in Figure 2-4.

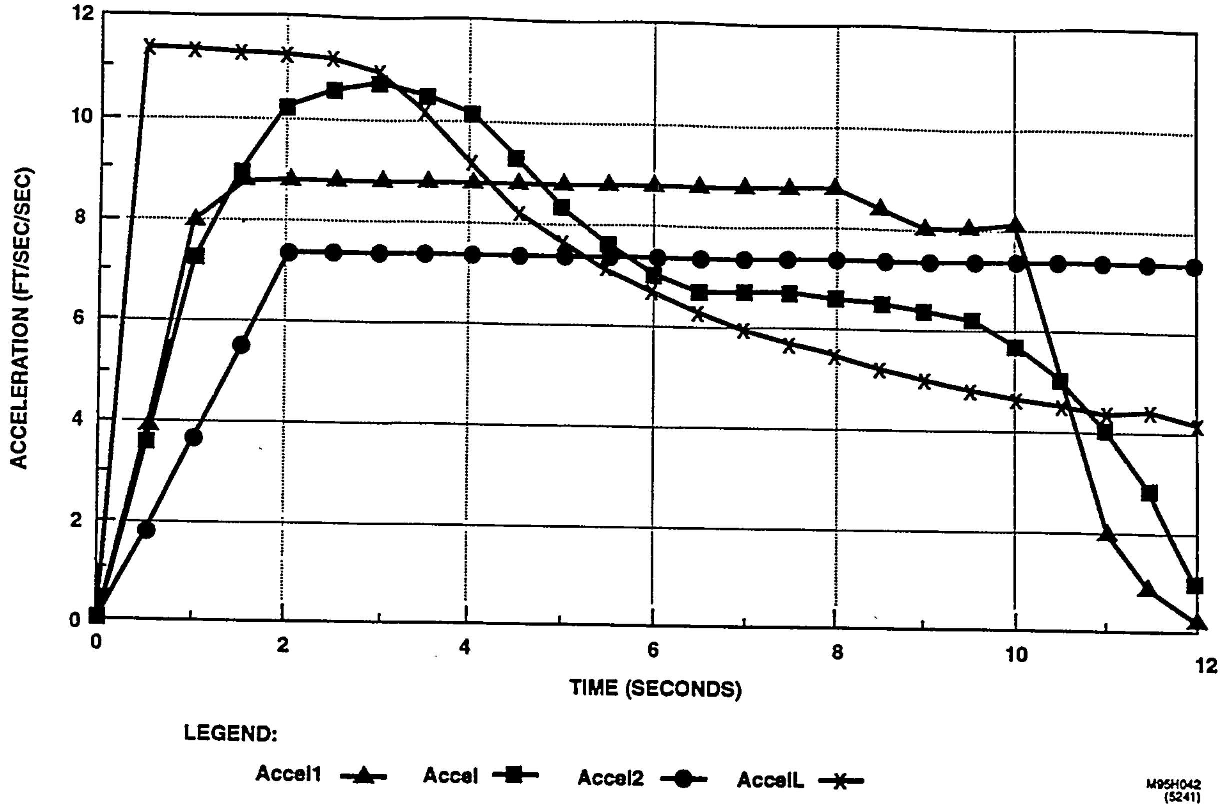

Figure 2-1. Alternative Acceleration Profiles

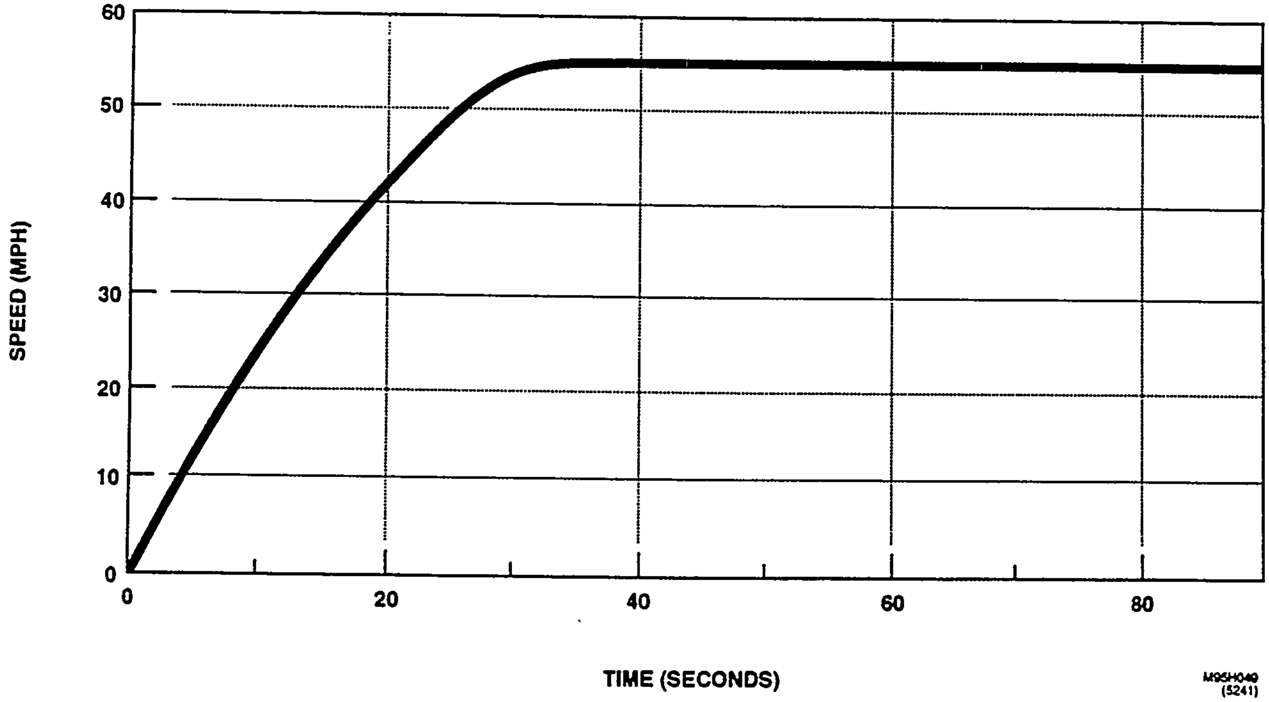

Figure 2-2. Baker Grade Velocity Profile

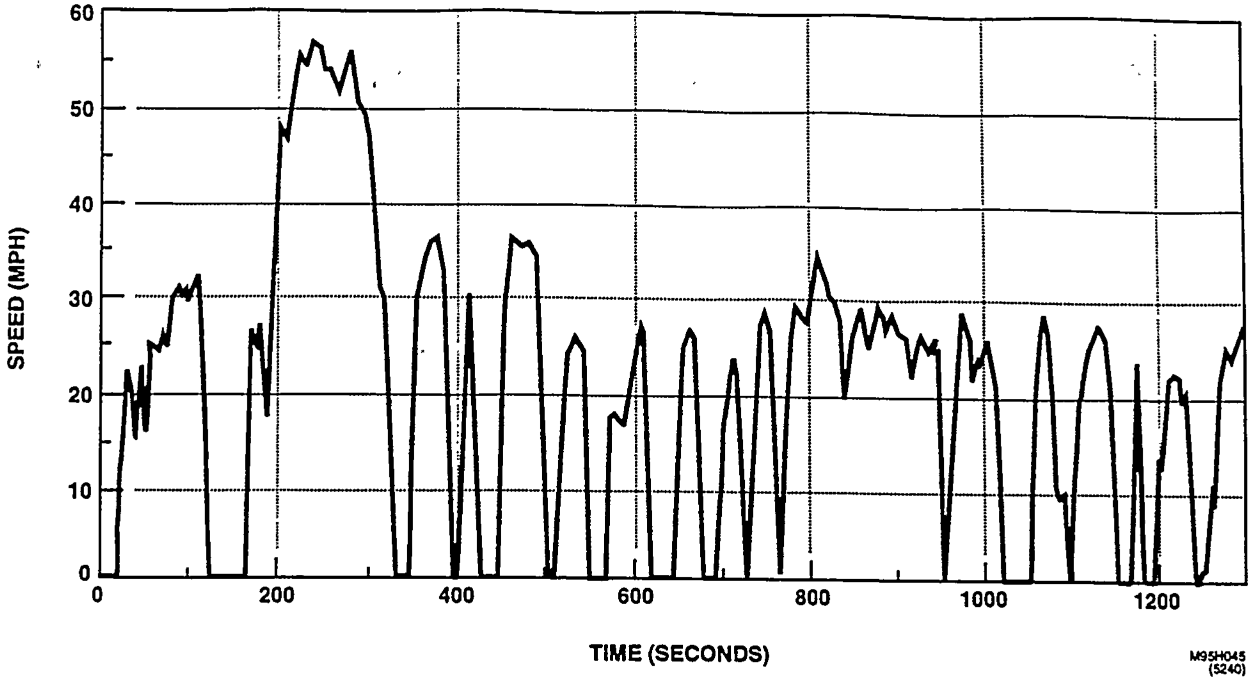

Figure 2-3. FUDS Velocity Profile

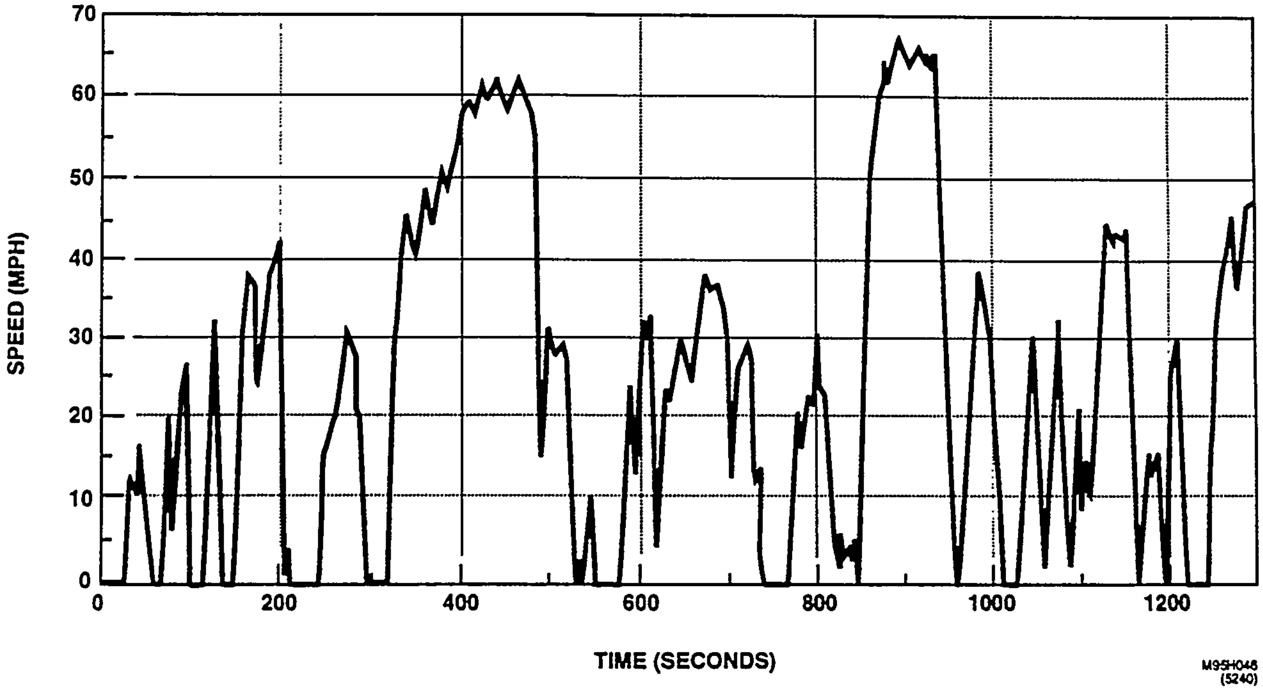

Figure 2-4. LA92 Velocity Profile

2.1.4 HIWAY Cycle

The HIWAY cycle represents a driving environment in which the vehicle travels on freeways with no impediments. This driving cycle requires much less stopping and starting than the FUDS or LA92 driving cycles. Figure 2-5 provides the velocity profile for the HIWAY cycle.

2.2 Vehicle Configuration

As noted in Section 1, the Chrysler LH Sedan has been selected as the target vehicle for the DPHV system. Figure 2 in the Executive Summary section shows the electrical configuration for the DPHV system. The basic system uses the Hydrogen-Powered Fuel Cell Stack (FCS) to provide for steady-state power with a battery-powered Load Leveling Unit (LLU) providing for surge power requirements.

2.2.1 Vehicle Physical Characteristics

Upon selection of the PL Sedan as the DPHV vehicle, Chrysler Liberty provided a set of vehicle characteristics, as shown in Table 2-1, to assist the analysis of system requirements. Additional vehicle definition has been provided by Liberty with the selection of the Westinghouse AC 3-phase motor and the identification of the transaxle member with a gear ratio of 9.34. The initial motor efficiency has been assumed to be 85 percent (less than the stretch goal of 90 percent for the PNGV program). The test weight for the vehicle is 10 percent less than the current Chrysler LH Sedan. The vehicle test weight includes a payload of 350 pounds.

Table 2-1. LH Sedan Test Vehicle Parameters

Parameter	Units	Value
Vehicle Test Weight	Pounds	3330
Wheel Radius	Feet	1.07
Frontal Area	Feet^2	23.5
Drag Coefficient (Cd)	***	0.250
Rolling Resistance Coefficient (Cr)	***	.0064

2.3 Vehicle Simulation

The simulation of the DPHV system has been performed using three different techniques. The first technique involved modeling the vehicle using the SIMPLEV simulation code. The second technique involved analysis of the vehicle via analytic techniques while the third method involved the application of the modified Chrysler TEVan simulation code. Each of these techniques are described on the following pages.

2.3.1 SIMPLEV, Version 3.1, Modeling

The SIMPLEV simulation code (Version 3.1) has been used to perform several parametric studies of the vehicle performance under each of the cycles noted in Section 2.1. A vehicle file

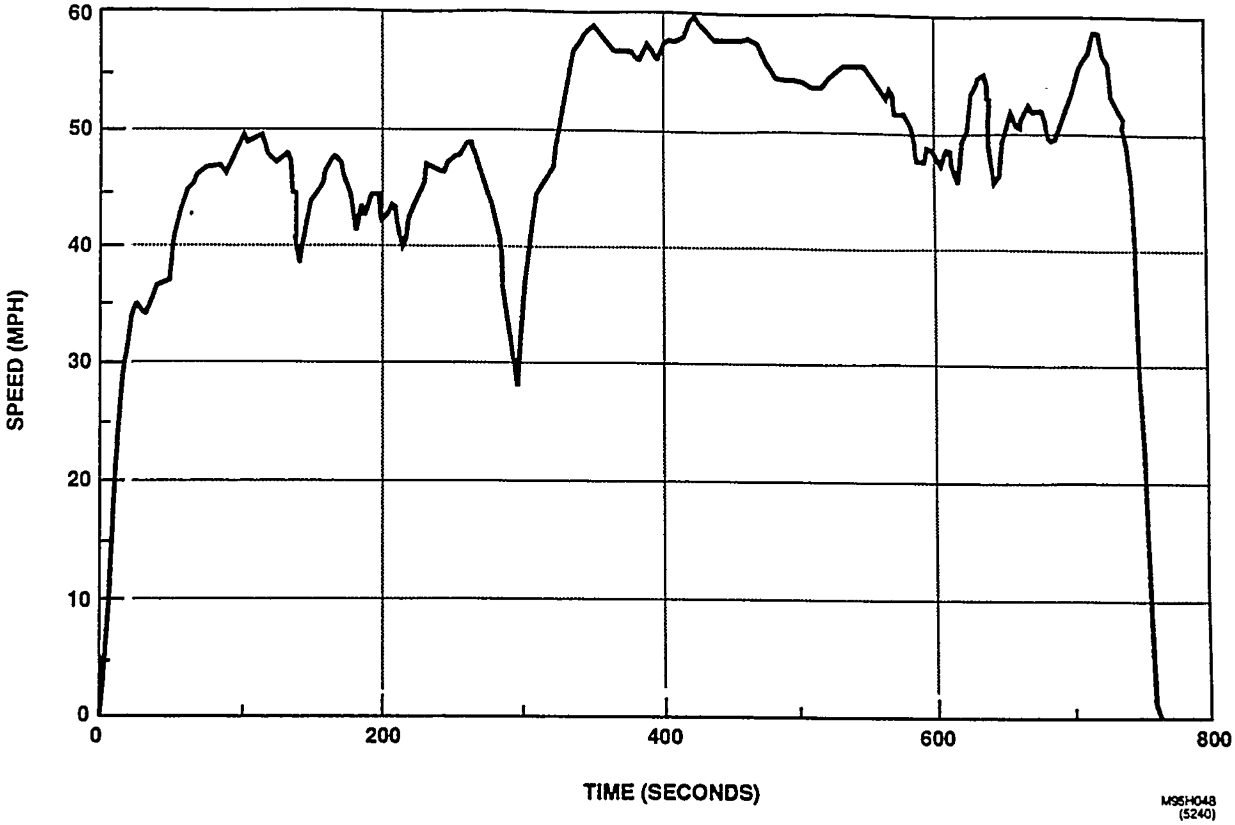

Figure 2-5. HIWAY Velocity Profile

used as input data for the code was created to reflect the vehicle characteristics shown in Table 2-1. The motor file corresponding to a 75 HP motor provided with the simulation package was also modified to reflect the Westinghouse motor as closely as possible.

System power was provided by batteries with an artificial energy content such that any acceleration or speed requirement could be achieved if the motor, transmission, and inverter controller were sufficient for the task. This was done by increasing the charge content of the batteries to 500 Ah and decreasing the output impedance of the battery modules such that the DC power bus will maintain a voltage of 300 VDC. This was done first to determine the vehicle requirements. Later the correct components were modified to determine component performance requirements to achieve the necessary vehicle performance.

2.3.2 Analytic Modeling

The power requirements for the system arise from the torque generated on the wheels of the vehicle and the angular velocity of the motor shaft. The torque may be calculated from the force which the wheels must generate against the highway to overcome the areal resistance and to achieve the dynamic vehicle performance. Equation 2-1 provides the force balancing equation (the rolling resistance force has not been included in this calculation).

Eq 2-1 $Fw = FArea + m*a$

where Fw is the force provided by the wheels, FArea represents the wind resistance force, m is the vehicle mass, and a is the dynamic acceleration of the vehicle.

The areal force is given by equation 2-2.

Eq 2-2 $FArea = K*p*A*v2$

where K is a constant, p is the density of air, A is the frontal area and v is the speed of the vehicle.

Since the speed for any time had been defined by the SIMPLEV acceleration cycle, the acceleration was derived from this known speed. As a result, the net force supplied by the wheels was obtained for each speed. The torque supplied to the wheels is then determined by multiplying the wheel force by the radius of the wheel. From this torque and the known transaxle ratio, the torque supplied by the motor is determined (the 85 percent efficiency is taken into account during this calculation).

Once the motor torque is determined, the input power to the motor may be obtained as shown in equation 2-3.

Eq 2-3 $P = *$

where P is instantaneous power to the motor, is the torque supplied by the motor, and is the angular speed of the motor.

2.3.3 CHYHV Modeling

At the same time that SIMPLEV, Version 3.1, modeling was being conducted, PEI instituted a program to upgrade the simulation code which was in existence at PEI. This program had been used for modeling the Chrysler TeVan and other hybrid vehicles and results from the simulation modeling had been verified by vehicle tests. The upgraded code was labelled, CHYHV, standing for the CHrYsler Hybrid Vehicle simulation code.

One immediate modification of the CHYHV code was to allow the simulation performance to be achieved with an input file defining the vehicle speed versus time (identical to the SIMPLEV cycle definition).

Two simulation runs were performed upon completion of the code modification. The first of these runs directed the vehicle to achieve 60 MPH in the least amount of time possible. The peak power requirement determined from this run was 115 kW. It was noted that the vehicle acceleration during this simulation was 7.33 feet/sec2 and that the peak power transfer was achieved during the latter stages of the acceleration phase. The second simulation run was performed using the same velocity cycle used in the SIMPLEV run. The result for this simulation run was a peak power transfer of 118 kW. These results compared favorably with those which had been obtained using SIMPLEV.

An analytical exercise was performed next using the SIMPLEV code in which an artificial acceleration cycle (called Accel1) was constructed. This acceleration cycle simulated that which would be expected if a two-speed transmission had been employed. The maximum acceleration was defined to occur within the early phase of the acceleration cycle and a second lower acceleration was sustained until the vehicle reached the 60 MPH speed.

2.3.4 Simulation Comparisons

In order to assess the validity of simulation modeling results, a test case was performed using SIMPLEV, CHYHV, and the analytical modeling tool. The test case involved the determination of the peak power and the steady state power requirements for the Baker Grade using the vehicle data provided in Table 2-1. Results for these simulation comparisons are shown in Appendix E, Table E-1. Inspection of this data shows that the agreement of results for all three methods is quite good.

2.4 Baseline Performance

Once the validity of the simulation modeling had been verified, the simulation of the DPHV system was analyzed using both the CHYHV and analytical model. The CHYHV code modifications included the ability to model the FCS performance using a look-up table for power, efficiency, current and stack voltage provided by AlliedSignal from test data on their 5-cell stacks. Results for each of the cycles described in Section 2.1 were obtained from these system simulations and are discussed below.

2.4.1 Acceleration Performance

The calculations were performed for each of the acceleration cycles shown in Figure 2-1. The results for the AccelL and the Accel2 acceleration profiles are shown in Appendix E, Table E-2. There are no regenerative braking effects occurring during this cycle. The acceleration curve for the AccelL cycle duplicates that which one would expect to occur for the Westinghouse motor performance in an acceleration phase. The consistency of results between the analytical calculation and those from the CHYHV simulation gives further confidence in the results which have been obtained.

In order to achieve the desired performance of the DPHV vehicle under less than optimal conditions, the higher peak power result determined from the Accel2 profile (rounded to the nearest decade) has been selected as the limiting peak power requirement for the system. Thus the system peak power requirement has been determined to be 100 kW.

2.4.2 Baker Grade Performance

The analysis for the Baker Grade cycle proceeded in the same manner as for the acceleration cycles. CHYHV was used to determine the vehicle peak and average power requirements. The cycle for determining the Baker Grade response requires approximately 34 seconds to achieve the speed of 55 MPH when on a seven percent grade. Results are shown in Appendix E, Table E-3.

The steady state power result validates the decision to specify the FCS power requirement at 40 kW. The LLU surge power only needs to be supplied during the acceleration phase of the cycle.

2.4.3 FUDS, LA92 Performance

The FUDS and the LA92 Driving Cycle simulations were performed with the CHYHV simulation code using the same vehicle configurations as the acceleration and Baker Grade cycles. Results of these simulations are shown in Appendix E, Table E-4.

After the system power requirements for the FUDS and LA92 cycles had been determined, the CHYHV simulation was performed with the FCS used as the steady state power source and the LLU used to provide surge power. This data will be discussed in Section 2.4.5.

2.4.4 HIWAY Performance

The HIWAY Cycle was performed with the CHYHV simulation code using the same vehicle configurations as the acceleration, Baker Grade, FUDS, and LA92 cycles. Results are shown in Appendix E, Table E-5.

2.4.5 Combined City/HIWAY Performance

Both FUDS and HIWAY cycles were simulated with the FCS providing steady state power and the LLU providing surge power requirements. These simulations were performed for the cases involving regenerative braking on and off. Results of these simulations are shown in Table 2-2. These results were obtained using the CHYHV simulation code.

Table 2-2. City/HIWAY Cycle System Response

Cycle	Regen Status	Peak Stack Power (kW)	Distance Covered (Mi)	Hydrogen Usage (Mi/gal gas equivalent)
FUDS	Off	13.53	9.59	55.8
FUDS	On	11.57	9.59	61.6
HIWAY	Off	11.66	10.26	91.2
HIWAY	On	1 1.61	10.26	94.7

The mileage for the vehicle is determined by the harmonic average of the mileage for the FUDS and HIWAY cycle as shown in equation 2-4. The range for the vehicle is based on the useable quantity of hydrogen contained within the hydrogen storage tanks, 12 pounds. Results for the combined mileage and the total range are shown in Table 2-3.

Eq 2-4 $$M = 1/(.55/Mf+.45/Mh)$$

where Mf represents the FUDS mileage, Mh the HIWAY mileage, and M the system mileage

Table 2-3. DPHV Combined Mileage and Range Results

Combined Mileage	**Total Range**	
Regen Status	**(mpg Gasoline Equivalent)**	**(Mi)**
On	73.1	348
Off	67.6	321

2.5 Conclusions

The DPHV system has been modeled using three different simulation techniques for those cycles which determine the system performance requirements. The peak power capability for the system is determined by the acceleration to 60 MPH within 12 seconds. For the LH Sedan this peak power requirement has been set at 100 kW. The steady state maximum power requirement for the system is set by the Baker Grade simulation and has been determined to be 40 kW. This value determines the peak power (net) requirement for the hydrogen-powered FCS. The simulation of the FUDS and HIWAY driving cycles determines the range of the vehicle. This simulation has determined that the system will be capable of achieving a 380 mile range with a 12 pound weight of useable hydrogen when a regenerative braking capability exists.

SECTION 3
PEM FUEL CELL SUBSYSTEM

3.1 Vehicular PEM Fuel Cells

3.1.1 Fuel Cells for Vehicular Power Production

The electrochemical engine, operating on a Proton Exchange Membrane (PEM) fuel cell stored hydrogen system, has the ability to provide clean and portable power in a safe and reliable manner. Electric vehicles offer a way of meeting zero-emission goals in vehicles powered by either batteries or hydrogen-powered fuel cells. Battery power systems based on current state-of-the-art technology are expensive, heavy, and allow only limited driving ranges. PEM fuel cells, enhanced by recent developments in membranes, electrodes, and bipolar plates, have exhibited the potential for low cost and for driving ranges comparable to those of current Internal Combustion Engine (ICE)-powered vehicles. The PEM fuel cell being developed at AlliedSignal is based on a low material and manufacturing cost approach that targets the automotive market.

3.1.2 Goals for Vehicular Fuel Cells

Using commercially available membranes, electrodes, and bipolar plates, PEM fuel cells are typically regarded as producing high power. Existing fuel cell stacks, however, are not commercially viable for automotive transportation applications based on their high cost, heavy weight, and large volume. The PEM fuel cell subsystem concept developed at AlliedSignal constitutes a viable power source for automotive transportation applications on both technical and economic bases.

Table 3-1. PEM FCS Design Goals

Topic	Goal
Cell Voltage (VDC) at Peak Power	0.5
Cell Current (Amperes/cm^2) at Peak Power	1.0
Specific Power Density (k W/kg)	1.1
Volumetric Power Density (kW/l)	1.0
Pt Loading (mg/cm^2)	0.25
FCS Target Cost ($/kW)	20
GMS Target Cost ($/kW)	10

Advanced lightweight, high-performance materials are used for key fuel cell stack components – membranes, electrodes, and bipolar plates. These materials are conducive to low-cost, high-speed manufacturing methods. Based on passenger vehicle weight and volume constraints, AlliedSignal has established specific and volumetric power density goals of 1.1 kW/kg and 1 kW/liter, respectively. The development of electrodes with Pt loading of less than 0.25 mg/cm^2/electrode is essential to achieving these power density goals at low cost. Target costs for the Subsystem are $20/kW for the fuel cell stack and $10/kW for the gas management assembly. These goals are in accordance with those set forth by the PNGV. Table 3-1 provides a summary view of the PEM FCS design goals.

3.1.3 Fuel Cell Stack Design to Cost

AlliedSignal has implemented a Design-To-Cost (DTC) plan for the direct-hydrogen-fueled PEM fuel cell development program to ensure that the system remains economically and technically viable for commercialization. The objective of the plan is to achieve established DTC target cost by treating cost equal in importance to technical and schedule requirements. The DTC approach analyzes what an item or part does relative to what it costs to perform the function. The Functional Analysis System Technique (FAST) is used to visually illustrate the relationship among the different subfunctions to accomplish the overall function. Costs are then allocated to each of these subfunctions and evaluated according to the contribution of each to the accomplishment of the overall function. Design For Manufacturing and Assembly (DFMA) and Integrated Product Development System (IPDS) principles are also applied to control cost. The cost reduction program for the fuel cell subsystem includes: use of existing vehicle parts, evaluation of alternative bipolar plate materials, evaluation of materials and alternative manufacturing processes for the Membrane and Electrode Assembly (MEA) and the canister, and simplification of the GMS.

3.2 PEM Fuel Cell Conceptual Design

3.2.1 Basic Operation of the PEM Fuel Cell

The basic characteristics of the PEM fuel cell are illustrated in Figure 3-1. Hydrogen gas is oxidized on the anode side to produce H+ ions, which migrate from anode to cathode where liquid water is produced in the reduction of oxygen gas. The overall cell reaction produces electricity and water as its only by-product. Waste heat is produced in the stack as the electrochemical reaction is not 100 percent efficient. Water condensation in the Fuel Cell Stack (FCS) also contributes to the generation of excess heat. With current state-of-the-art technology, adequate operating conditions of the PEM fuel cell for transportation applications were determined to be 2 atmospheres absolute pressure at a temperature of 80°C. In addition, the electrochemical reaction is enhanced by the humidification of the anode and cathode feed streams. As a result, conditioning of the gases entering the FCS is necessary and includes pressurizing the air stream to approximately 2 atmospheres (atm) and humidifying both the hydrogen and air streams to 85°C and 75°C, respectively.

3.2.2 Membranes

Achieving high power densities in the PEM fuel cell requires the membrane to hold the following properties: high proton conductivity, low ohmic resistance, chemical and electrochemical stability, low oxygen and hydrogen permeability, and high mechanical strength. Commercially available membranes were originally developed for use in the chlor-alkali industry, but have since found application as a fuel cell separator because of their ability to conduct protons. Because these membranes were not specifically designed for use in the PEM fuel cell, they have several

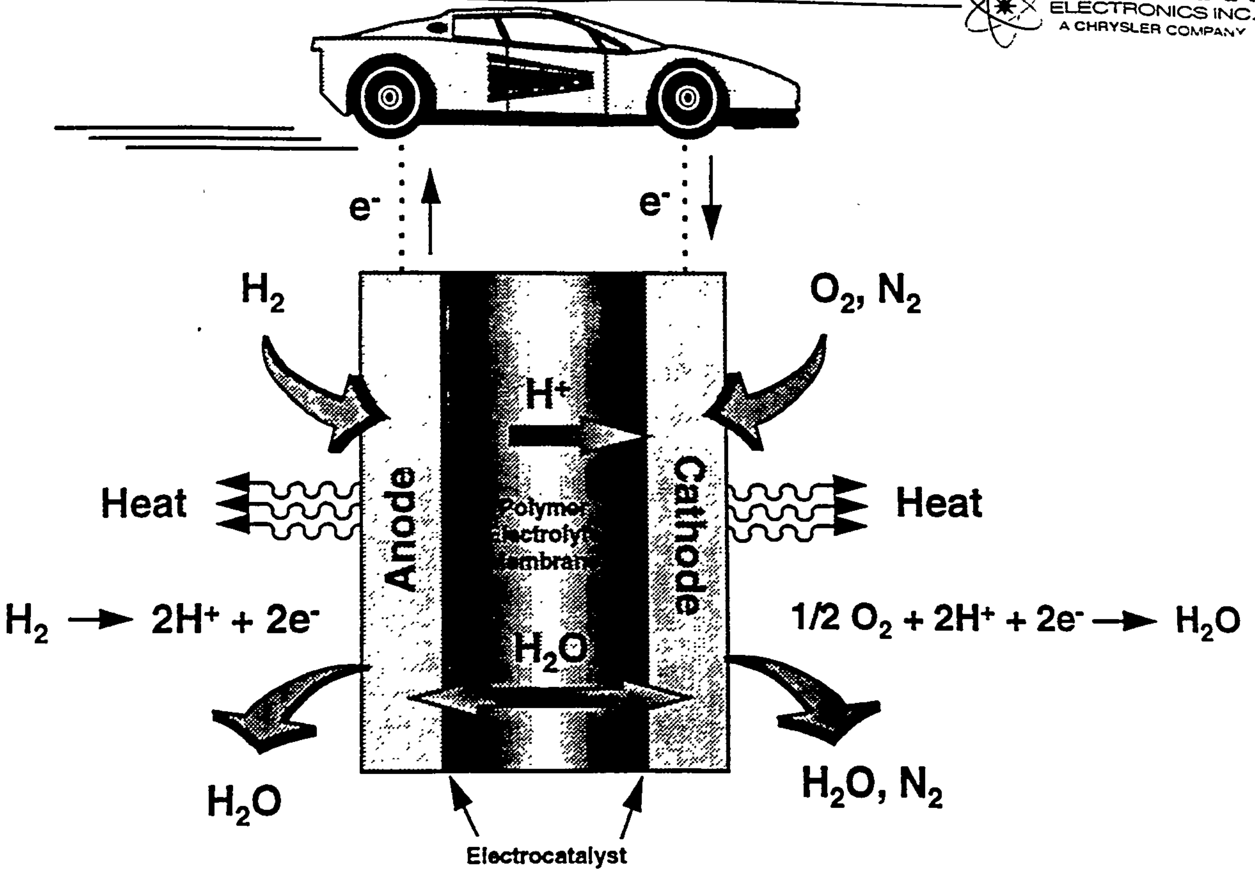
e^-
e^-
H_2
O_2, N_2
H^+
Heat
Anode
Polymer Electrolyte Membrane
Cathode
Heat
$H_2 \rightarrow 2H^+ + 2e^-$
$1/2\ O_2 + 2H^+ + 2e^- \rightarrow H_2O$
H_2O
H_2O
H_2O, N_2
Electrocatalyst

Figure 3-1. Basic Operation of the Vehicular PEM Fuel Cell

shortcomings which limit its potential. The high cost of the membranes, high dependence on water for proton conduction, and the relatively narrow operating temperature range, are just a few of the deficiencies affecting the technical and economic viability of the PEM fuel cell. Efforts at AlliedSignal are focusing on the development of a new generation of membranes specifically geared toward meeting the requirements of automotive applications.

3.2.3 Electrodes

Essential to developing low-cost, high power density FCSs is achieving low platinum loadings in the electrodes. Electrodes developed at AlliedSignal have achieved loadings as low as 0.35 $mg/cm^2/cell$, which is comparable to commercially available fuel cell electrodes. Further electrode development is minimizing the number of electrode constituents and improving electrode morphology, while still maintaining satisfactory fuel cell performance. In addition, inexpensive methods for fabricating MEAs are being explored. Working with AlliedSignal Automotive, an inexpensive manufacturing method was developed allowing large, active area MEAs of high quality to be produced in a manufacturing cell environment.

3.2.4 Bipolar Plates

Light weight, low volume, and low cost, as well as easy fabrication through mass production techniques, are important considerations in the development of innovative bipolar plate materials and flow field designs. Graphite has traditionally been the predominant bipolar plate material for PEM fuel cells because of its high conductivity, high strength, and immunity to corrosion. However, it is heavy (due to the required thickness) and expensive, and is not conducive to low-cost, high-speed manufacturing methods. Alternative materials, such as coated metals and conductive polymers, are thinner, lighter, inexpensive, and exhibit the requisite material properties. In addition, their physical structure greatly enhances the simple and inexpensive formation of flow fields. Development of thin, light-weight bipolar plates and compact FCS design packaging has allowed the AlliedSignal FCS to approach the 1.1 kW/kg and 1.0 kW/liter design goals.

3.2.5 Fuel Cell Stack Design

The PEM fuel cell system developed at AlliedSignal employs a modular concept. A set of identical modules connected in series provide the necessary power to the vehicle. Parallel arrangement of modules is also possible; however, the resulting fuel cell system weight, volume, and cost would be higher than if connected in a series arrangement. Voltage requirements of the electric motor govern the operating voltage of the fuel cell system, which is dependent on the total number of cells in the system. The available power for the vehicle is governed by the active area of each cell. As a result of this interaction between voltage and active area, the size and number of modules used depends on the power and voltage requirements of the vehicle. Additional constraints, such as the allowable installation envelope on the vehicle and the cost of each module, also influence the modular design.

Using projected cost targets for the fuel cell components, a study of the trade-offs between fuel cell material costs and stack voltage was conducted. The study focused on the power requirements of the Chrysler LH sedan (40 kw usable power for the vehicle). Five 10-kw modules are envisioned for this vehicle; the additional 10 kw are used to power the fuel cell gas management ancillaries and allow for up to 50 mv of degradation per cell in fuel cell performance. The results of the study indicate that a negligible cost difference exists between a fuel cell module designed to a large active area and a low voltage, and that designed to a small active area with a large voltage. In order to package the fuel cell modules in the tunnel of the Chrysler LH sedan, the outer diameter of the stack modules has to be less than 20.5 cm (8 inches). Table 3-2 shows the design goals for a 50 kW stack.

Table 3-2. Mass and Volume Projections for 50 kW PEM Fuel Cell Stack

Stack Voltage (VDC)	Number of Cells	Active Area, cm2	Module Weight, kg	Module lenght, cm	Module Diam., cm
200	400	248	7.76	21.2	22.9
220	440	225	7.92	23 .2	22.0
240	480	207	8.10	25.2	21.2
260	520	191	8.26	27.2	20.5
280	560	177	8.42	29.3	19.9
300	600	165	8.58	31.2	19. 3
320	640	155	8.72	33.1	18.8

3.3 Fuel Cell Subsystem Conceptual Design

The complete PEM fuel cell electrochemical engine incorporates gas management and controller assemblies. Overall fuel cell performance is dependent upon proper conditioning of the reactant gases and strict control of the operating conditions. In addition, adequate processing of the fuel cell product streams is required in order to recover products, unused reactants, and energy of the streams. Rigorous steady-state and dynamic models of the PEM fuel cell subsystem were developed to determine the required components and evaluate alternative configurations and operating points. A trade study of several designs resulted in a subsystem concept which minimizes the overall number of components and optimizes heat and water management at the system level. A flow diagram of the optimal subsystem configuration is shown in Figure 3-2. The subsystem integrates the PEM FCS and Gas Management System (GMS) auxiliaries which include a turbocompressor assembly for pressurization and energy recovery, a closed coolant loop for stack heat removal, and subsystem controls for heat and water management as well as power control. A mock-up of the AlliedSignal Automotive PEM fuel cell power plant concept was fabricated to highlight overall subsystem design requirements (Figure 3-3).

3.3.1 Turbomachinery

Rigorous steady-state modeling of the PEM fuel cell subsystem indicates that adequate performance for automotive transportation applications is achieved at approximately 2 atm absolute pressure. A significant fraction of the compression work is supplied through expansion of the exhaust stream from the cathode. A study was conducted on the various types of air compressors that could be used to supply air to the fuel cell stack. Several types of air moving devices were compared in terms of their advantages and disadvantages as applied to the PEM fuel cell. The study concluded that an electric motor-driven, high-speed dynamic compressor with bootstrap expansion turbine running on air bearings would be the smallest and lightest solution. In volume production, this compressor offers the lowest unit cost. The main disadvantage of dynamic compressor concepts is their limited flow range at constant pressure ratios, which severely penalizes fuel cell subsystem efficiencies at the very low power levels. Alternative configurations which would offer a wider operating flow range are also under consideration.

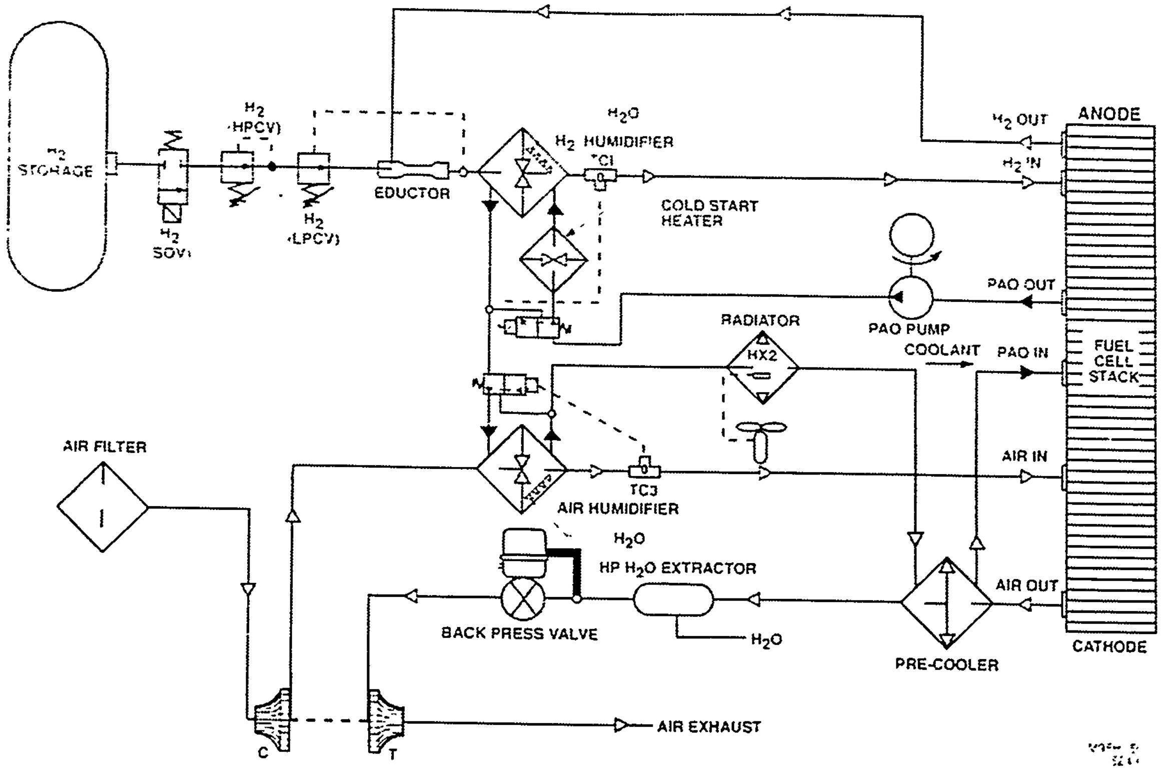
H2 STORAGE
H2 SOV
H2 (HPCV)
H2 (LPCV)
EDUCTOR
H2O
H2 HUMIDIFIER
TC1
COLD START HEATER
H2 OUT
H2 IN
ANODE
PAO OUT
PAO PUMP
RADIATOR
HX2
COOLANT
PAO IN
FUEL CELL STACK
AIR FILTER
TC3
AIR HUMIDIFIER
AIR IN
H2O
HP H2O EXTRACTOR
AIR OUT
BACK PRESS VALVE
H2O
PRE-COOLER
CATHODE
C
T
AIR EXHAUST

Figure 3-2. Optimal PEM Fuel Cell Subsystem Configuration

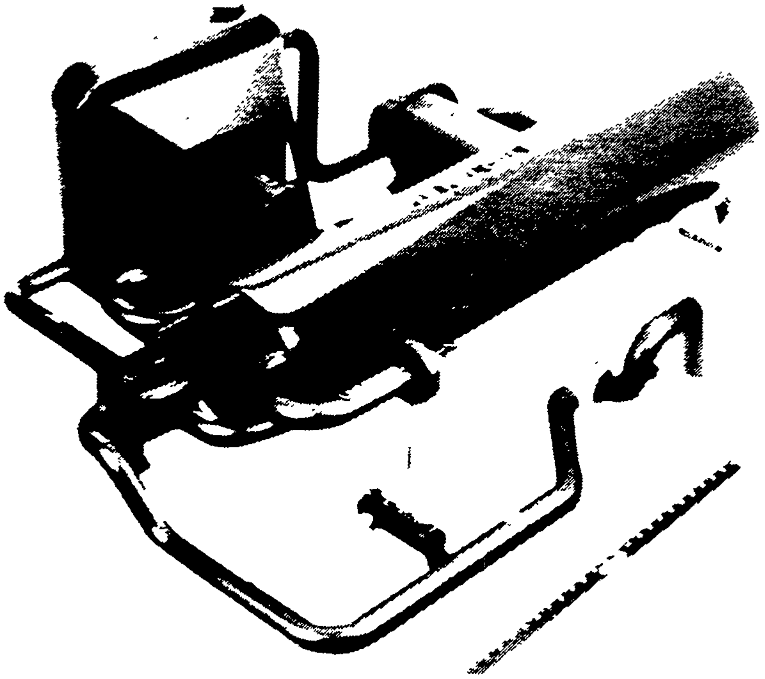

Figure 3-3. AlliedSignal Automotive PEM Fuel Cell Power Plant Concept

3.3.2 Heat and Water Management

Due to thermodynamic inefficiencies, a significant amount of waste heat is generated in the FCS. Heat removal in the fuel cell subsystem is achieved through the closed coolant loop highlighted in Figure 3-4. Requisite coolant properties are: high dielectric strength and specific heat, good thermal conductivity, and low corrosiveness. Coolant exiting the fuel cell stack at 90°C initially passes through a hydrogen heater/humidifier, where dry hydrogen is heated to 85°C and brought to 100 percent relative humidity using an ultrasonic atomizer. The coolant then passes through the air heater/humidifier, where dry air is saturated to 75°C. Additional heat removal from the coolant stream is achieved with a radiator. When the FCS is operating at its rated power, all of the coolant passes through the radiator since maximum heat rejection is required to dissipate the heat generated in the FCS. A three-way valve is used to partly bypass the radiator at off-peak power levels. An electric heater is used for cold start-up of the FCS.

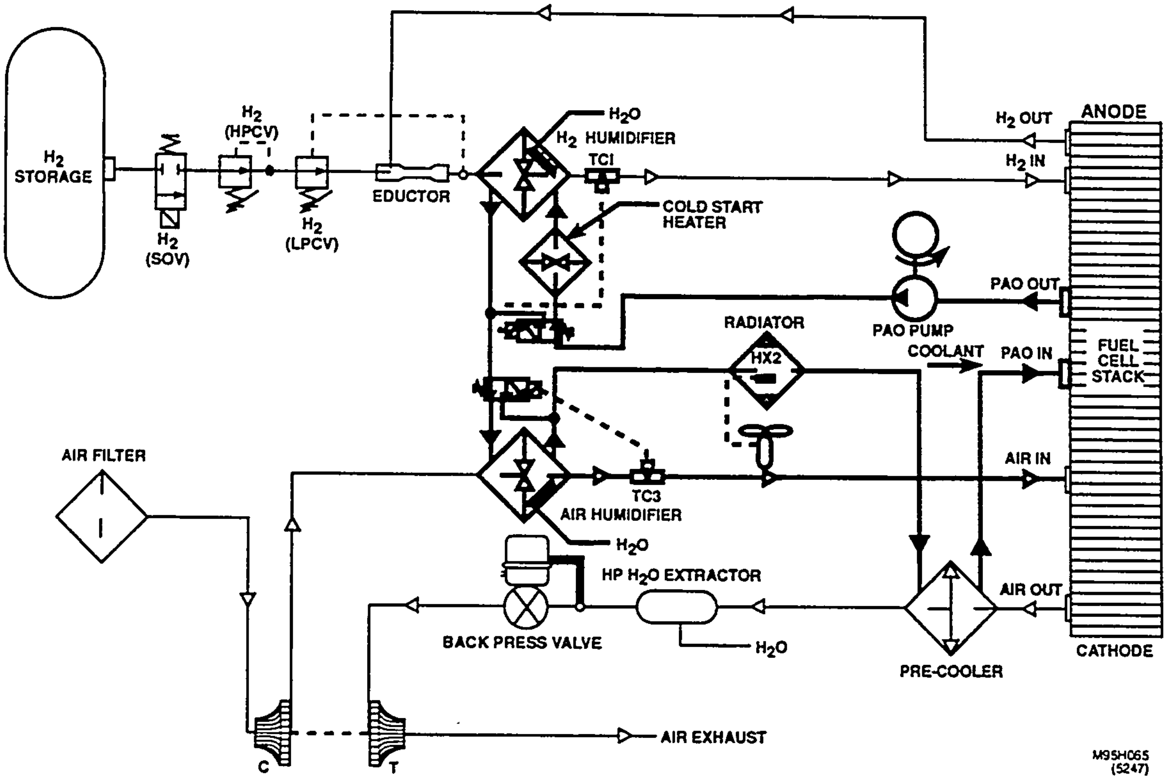
H_2 STORAGE
H_2 (SOV)
H_2 (HPCV)
H_2 (LPCV)
EDUCTOR
H_2O
H_2 HUMIDIFIER
TCI
COLD START HEATER
H_2 OUT
ANODE
H_2 IN
PAO OUT
PAO PUMP
RADIATOR
HX2
COOLANT
PAO IN
FUEL CELL STACK
AIR FILTER
AIR IN
TC3
AIR HUMIDIFIER
H_2O
HP H_2O EXTRACTOR
AIR OUT
BACK PRESS VALVE
H_2O
CATHODE
PRE-COOLER
C
T
AIR EXHAUST
M95H065
(5247)

Figure 3-4. PEM Fuel Cell Subsystem Cooling Scheme

Water condensed in the FCS is used in the humidification of the hydrogen and air streams entering the FCS. Cold turbine exhaust (Figure 3-4) passes through a pre-cooler to condense water from the cathode exhaust gas stream. The water is removed in a high pressure water extractor and used in the humidification process. The super-saturated anode exhaust stream is recirculated back to the hydrogen heater/humidifier inlet using a jet-pump eductor. Achievement of water balance in the fuel cell subsystem depends mostly on the operating pressure and air flow rate.

Efforts are currently focused on reducing both the energy and water requirements of the humidification process. Innovative humidification methods are being considered as viable substitutes for external gas humidification. In addition, technological advances in membrane properties, electrode morphology, and MEA fabrication will allow for lower operating pressures, therefore eliminating the need for a turbocompressor.

3.4 Performance Characteristics

Mathematical modeling of the fuel cell subsystem has been performed on several levels. The FCS performance model is an empirical model which uses the Tafel approximation to predict stack performance as a function of pressure, temperature, and gas mole fractions. A FCS design model was developed to predict the size, weight, and cost of the FCS for various geometries, component materials, power levels, and voltages.

At the subsystem level, an ASPEN Plus steady-state model provided preliminary estimates of subsystem performance, which was used in the development of a rigorous Fortran steady-state subsystem model. The Fortran model incorporates rigorous designs of the components shown in Figure 3-2 and uses the FCS performance model as a subroutine. It predicts overall subsystem performance (subsystem efficiency, parasitic power loads, flow rates, pressures, and temperatures of all streams). In addition, a dynamic model was developed to identify subsystem transients and to develop a procedure for start-up sequencing, idling, power load changes, and shutdown.

Water management at the fuel cell subsystem level constitutes a major issue in determining adequate operating conditions. Air stoichiometry and operating pressure need to be properly balanced in order to achieve water balance. Overall water balance in the FCS Subsystem is governed by the amount of water produced in the FCS and the requirements of the hydrogen and air humidifiers. Higher air flowrates and adequate humidification of both hydrogen and air feed streams enhance PEM fuel cell performance. In addition, power requirements for the GMS are minimized at lower operating pressures. However, water requirements for the humidification process increase at lower pressures and higher air flowrates. As a result, achievement of a water balance for the FCS Subsystem sets a lower limit on the operating pressure and an upper limit on the air stoichiometry. Adequate fuel cell performance for automotive applications is achieved at 80°C cell temperature and approximately 2 atm absolute pressure. As a result, air stoichiometries lower than 2.0 are required to achieve water balance (i.e. less than two times the required stoichiometric oxygen rate at a current density of 1 A/cm2). Figure 3-5 shows a representative water balance for the two atmosphere case at varying power levels. As shown in this figure, more water is collected from the stack than that which is required to humidify the inlet gases.

Figure 3-6 compares the polarization curve predicted by the fuel cell performance model with experimental data at 80 C and 2 atm. The experimental data was obtained on a Nafion_112 membrane using AlliedSignal electrodes with a platinum loading of 0.4 mg Pt/cm2/electrode. Further subsystem modeling is based on this polarization data. The rigorous Fortran model was exercised to characterize steady-state subsystem performance at the rated power level and at part-load conditions. Results are based on the performance map of an existing AlliedSignal turbocompressor, chosen for its relatively wide flow range at 2 atm. Flow and pressure control at part-load conditions is achieved by throttling the turbine inlet to regulate air flow (Figure 3-2).

The analysis covered rated power levels ranging between 30 kw and 100 kw, at stack voltages of 200-320 VDC. As shown in Figure 3-7, the operating voltage of the FCS has to be lower than 240 VDC at the 50 kW power level in order to avoid exceeding the 400 VDC level at off-peak power levels. Additional stack sizing constraints indicate that the optimal stack voltage is 240 VDC at the rated power level. Tables 3-3, 3-4, and 3-5 show peak power and off-design performance characteristics of the fuel cell subsystem at gross rated power levels of 30 kW, 50 kW, and 90 kW, respectively. Net power refers to the power generated by the FCS less the parasitic load of the gas management assembly. Subsystem efficiencies listed in these tables are based on the lower heating value of hydrogen fuel.

Figure 3-8 shows FCS and subsystem efficiencies as a function of net power output for a 50 kW stack (5 modules). The fuel cell subsystem delivers 46.7 kW to the vehicle with a 37.2 percent efficiency (40 percent stack efficiency) at the rated power level. As vehicle power requirements diminish, air flow rate through the turbocompressor is lowered by throttling the turbine inlet until surge level is reached. At that point, the bypass valve opens and a constant air flow is maintained through the turbocompressor, which has an adverse effect on overall subsystem efficiency. FCS efficiency increases from 40 percent at peak power to 66 percent at very low power levels. However, due to the limited flow range of the turbocompressor, overall subsystem efficiency peaks at 52 percent (20 kW net power). The corresponding hydrogen usage rate is shown in Figure 3-9 in terms of mass flow rate and in Figure 3-10 in terms of the net electrical output of the spent hydrogen fuel. At the lower power levels, a more significant fraction of hydrogen reacting in the FCS goes toward powering the turbocompressor, which results in higher hydrogen consumption rates per unit of net power delivered to the vehicle. The results highlighted in Figure 3-10 indicate that power levels below 5-7 percent of the rated power need to be avoided. This could be achieved by producing more power than required by the vehicle at the lower power requirements and using the excess power to recharge the battery. An alternative solution would be to reduce the operating pressure of the FCS at the lower power levels in order to minimize the energy requirements of the turbocompressor. Significant improvements in fuel cell subsystem efficiency could also be achieved through innovative turbocompressor design. Potential gains in efficiency

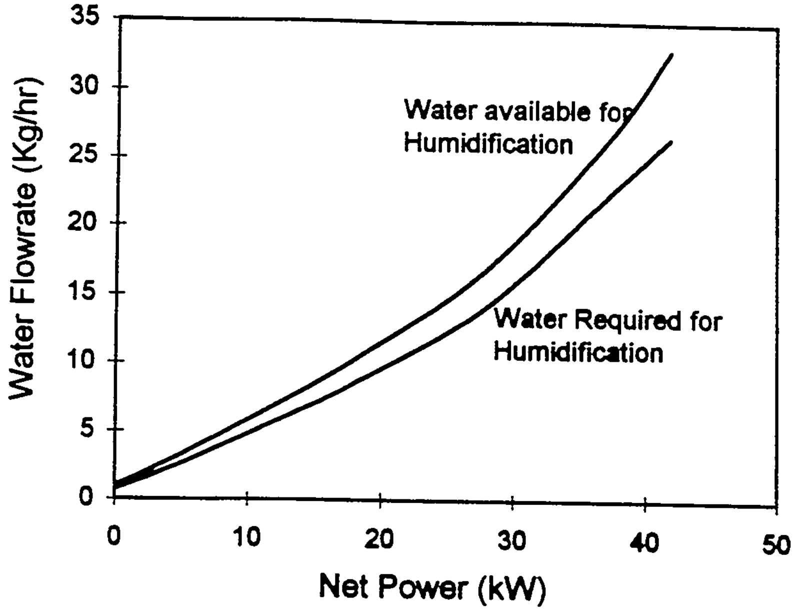

Figure 3-5. Overall Water Balance for the FCS Subsystem at 2 Atmospheres

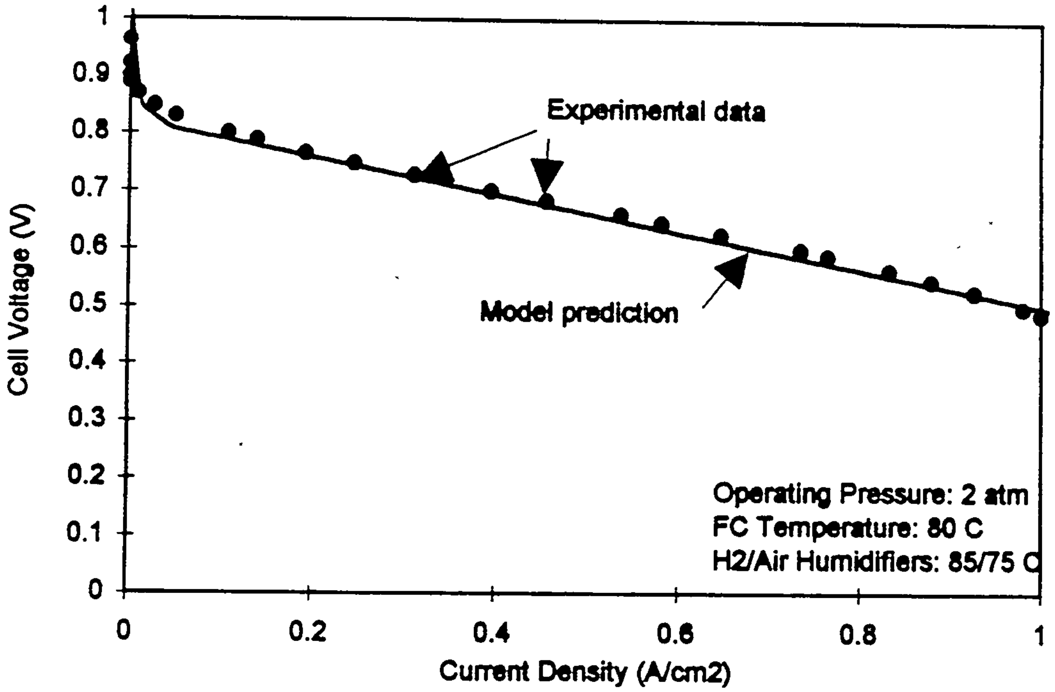

Figure 3-6. Comparison of Model Prediction with Experimental Polarization Curve

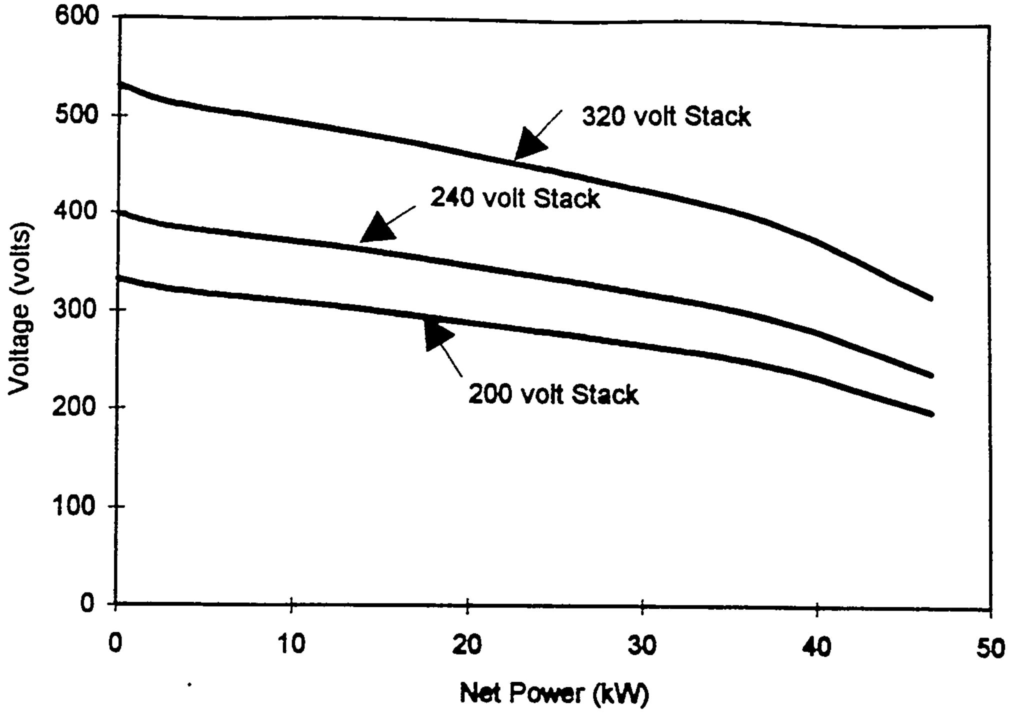

Figure 3-7. Rated Power and Off-Design Stack Voltages for 50 kW Fuel Cell Stack

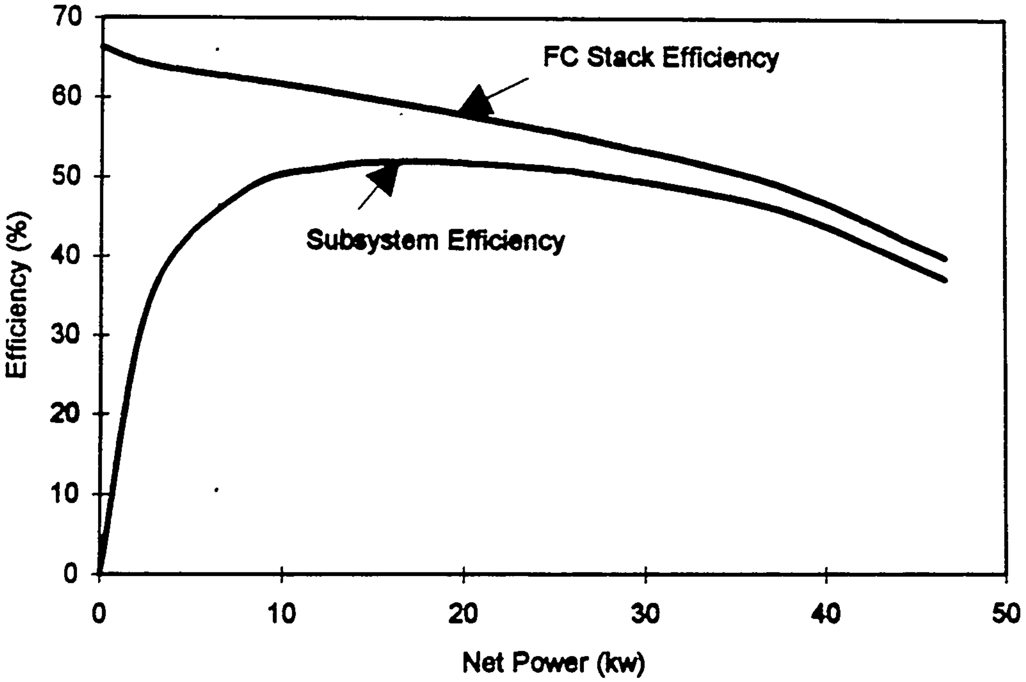

Figure 3-8. Stack and Subsystem Efficiency for 50 kW FCS

Table 3-3. Peak Power and Off-Design Performance Data
30 kW PEM FCS
480 Cells, 124 cm^2/Cell, 28.9 kg, 17.2 cm Diameter, 125.8 cm Length (total)

Gross Power, kW	30.06	25.01	20.01	15.00	10.02	5.00	2.00
Net Power, kW	27.90	23.48	18.60	13.60	8.62	3.60	0.60
Stack Efficiency, %	39.9	47.8	52.7	56.7	60.0	63.05	65.10
Subsystem Efficiency, %	37.0	44.9	49.0	51.4	51.7	45.4	19.6
Stack Voltage, VDC	240 .0	287.6	317.3	341.0	361.2	379.3	391.8
Fuel Cell Voltage, VDC	0.50	0.60	0.66	0.71	0.75	0.79	0.82
Stack Current, Amperes	125 .3	87.0	63.1	44.0	27.7	13.2	5.1
Current Density, Amps/cm^2	1.01	0.70	0.51	0.35	0.22	0.11	0.04
Fuel Cell Temperature, °C	80	80	80	80	80	80	80
Anode/Cathode Pressure, atm.	2/2	2/2	2/2	2/2	2/2	2/2	2/2
Hydrogen Usage Rate, kg/hour	2.27	1.57	1.14	0.80	0.50	0.24	0.09
Hydrogen Stoichiometry	1.5	1.5	1.5	1.5	1.5	1.5	1.5
Air Flowrate, kg/hour	120.3	84.3	66.3	66.0	66.0	66.0	66.0
Air Stoichiometry	1.5	1.5	1.7	2.4	3.8	8.4	20.9
Parasitic Power, kW	2.16	1.53	1.41	1.40	1.40	1.40	1.40
Excess System Water, kg/hour	4.4	2.7	1.8	1.3	0.8	0.4	0.2

Table 3-4. Peak Power and Off-Design Performance Data
50 kW PEM FCS
480 Cells, 206.5 cm²/Cell, 40.5 kg, 21.2 cm Diameter, 126.1 cm Length (total)

Gross Power, kW	50.06	40.02	30.02	25.02	20.02	15.00	10.01	5.01	2.32
Net Power, kW	46.65	37.57	27.68	22.69	17.69	12.68	7.69	2. 69	0.00
Stack Efficiency, %	39.9	48.9	54.4	56.7	58.7	60.7	62.4	64.1	66.3
Subsystem Efficiency, %	37.2	45.9	50.2	51.4	51.9	51. 3	48.0	34.4	0.00
Stack Voltage, VDC	240.0	294.1	327.2	340.9	353.4	365.0	375.8	386.0	398.5
Fuel Cell Voltage, VDC	0.50	0.61	0.68	0.71	0.74	0.76	0.78	0.80	0.83
Stack Current, Amperes	208.5	136.1	91.7	73.4	56.6	41.1	26.6	13.0	5.8
Current Density, Amps/cm2	1.01	0.66	0.44	0.36	0.27	0.20	0.13	0.06	0.03
Fuel Cell Temperature, °C	80	80	80	80	80	80	80	80	80
Anode/Cathode Pressure, atm.	2/2	2/2	2/2	2/2	2/2	2/2	2/2	2/2	2/2
Hydrogen Usage Rate, kg/hour	3.77	2.46	1.66	1.33	1.03	0.74	0.48	0.23	0.11
Hydrogen Stoichiometry	1.5	1.5	1.5	1.5	1.5	1.5	1.5	1.5	1.5
Air Flowrate, kg/hour	198.0	130.4	111.8	111.5	111.5	111.5	111.5	111.5	111.5
Air Stoichiometry	1.5	1.5	2.0	2.5	3.2	4.4	6.8	13.9	31.0
Parasitic Power, kW	3.40	2.45	2.34	2.33	2.33	2.32	2.32	2.32	2.32
Excess System Water, kg/hour	6.9	4.0	2.6	2.1	1.7	1.3	0.9	0.5	0.3

Table 3-5. Peak Power and Off-Design Performance Data
90 kW PEM FCS
480 Cells, 371.6 cm2/Cell, 61.3 kg, 27.4 cm Diameter, 126.1 cm Length (total)

Gross Power, kW	90.09	80.06	70.04	55.02	35.05	20.06	10.01	5.01	4.20
Net Power, kW	83.80	75.24	65.63	50.80	30.84	15.86	5.81	0.81	0.00
Stack Efficiency, %	39.9	45.7	49.6	54.1	58.9	62.0	64.0	65.7	66.1
Subsystem Efficiency, %	37.1	42.9	46.4	50.0	51.9	49.1	37.1	10.6	0.00
Stack Voltage, VDC	240.0	274.9	298.3	325.6	354.7	373.4	384.9	395.2	398.4
Fuel Cell Voltage, VDC	0.50	0.57	0.62	0.68	0.74	0.78	0.80	0.82	0.83
Stack Current, Amperes	375.4	291.2	234.8	169.0	98.8	53.7	28.0	12.7	10.6
Current Density, Amps/cm2	1.01	0.78	0.63	0.45	0.27	0.14	0.07	0.03	0.02
Fuel Cell Temperature, °C	80	80	80	80	80	80	80	80	80
Anode/Cathode Pressure, atm.	2/2	2/2	2/2	2/2	2/2	2/2	2/2	2/2	2/2
Hydrogen Usage Rate, kg/hour	6.79	5.27	4.25	3.06	1.79	1.30	0.97	0.47	0.19
Hydrogen Stoichiometry	1.5	1.5	1.5	1.5	1.5	1.5	1.5	1.5	1.5
Air Flowrate, kg/hour	354.0	275.6	222.5	198.8	198.3	198.0	198.0	198.0	198.0
Air Stoichiometry	1.5	1.5	1.5	1.9	3.2	6.0	12.3	25.3	30.4
Parasitic Power, kW	6.29	4.82	4.41	4.22	4.21	4.20	4.20	4.20	4.20
Excess System Water, kg/hour	10.1	7.7	6.1	4.5	2.8	1.7	0.9	0.5	0.4

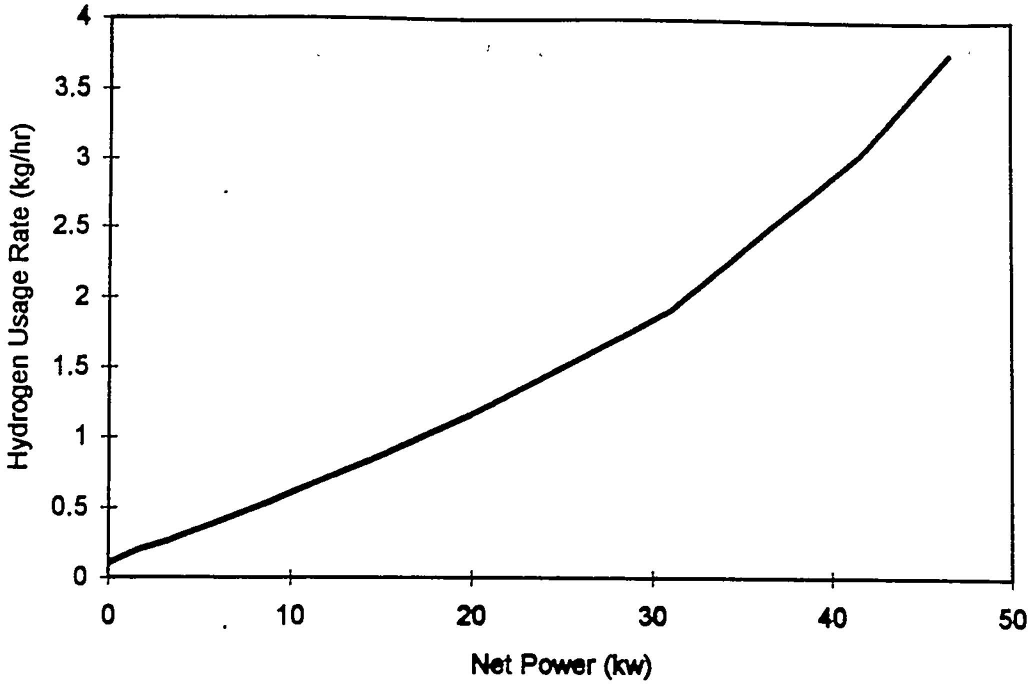

Figure 3-9. Hydrogen Usage Rate (50 kW Stack)

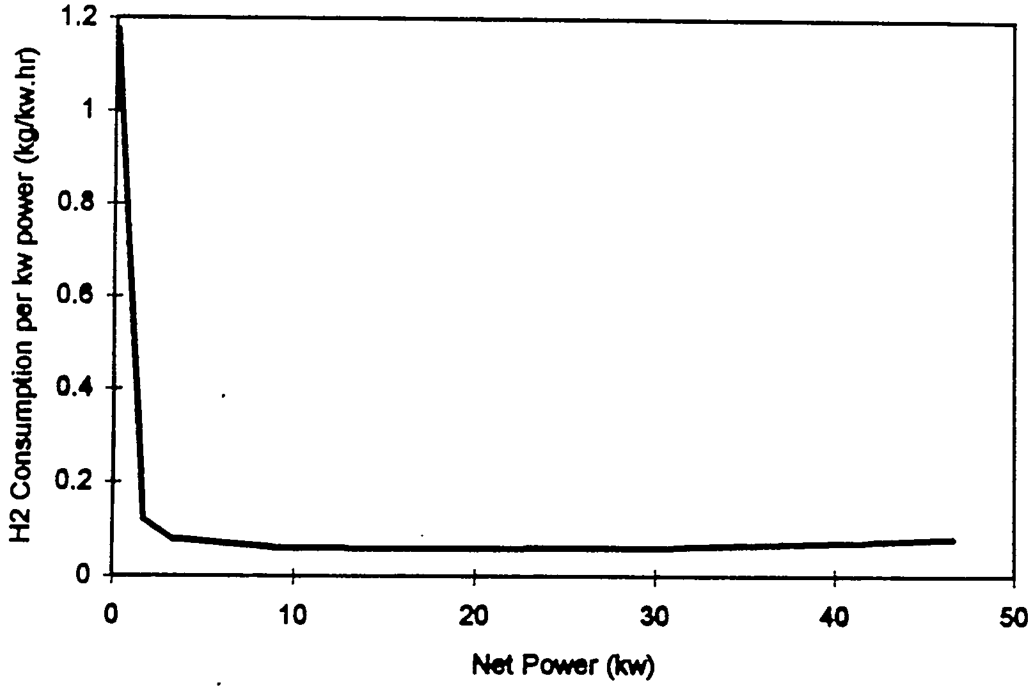

Figure 3-10. Hydrogen Consumption per Unit Power (50 kW Fuel Cell Stack)

are highlighted in Figure 3-11, which compares subsystem efficiency using existing turbomachinery with that assuming ideal turbocompressor performance (i.e. infinitely wide flow range).

Preliminary analysis of the dynamic behavior of the fuel cell subsystem identified fuel cell temperature as the main transient. As a result, the modeling effort focused on evaluating various temperature control schemes, assuming instantaneous variations in pressures and flow rates. An adequate Proportional-Integral (PI) control algorithm was developed to maintain the temperature of the fuel cell during power load changes. Figure 3-12 shows the effect of a disturbance caused by a load change from 20 kW to 50 kW, for a 50 kW stack. As the power required by the vehicle increases, gas flow rates are adjusted instantaneously, along with the coolant flow rate, to accommodate the increase in power and heat output of the stack. The fuel cell temperature increases to approximately 87°C, but is rapidly restored to 80°C.

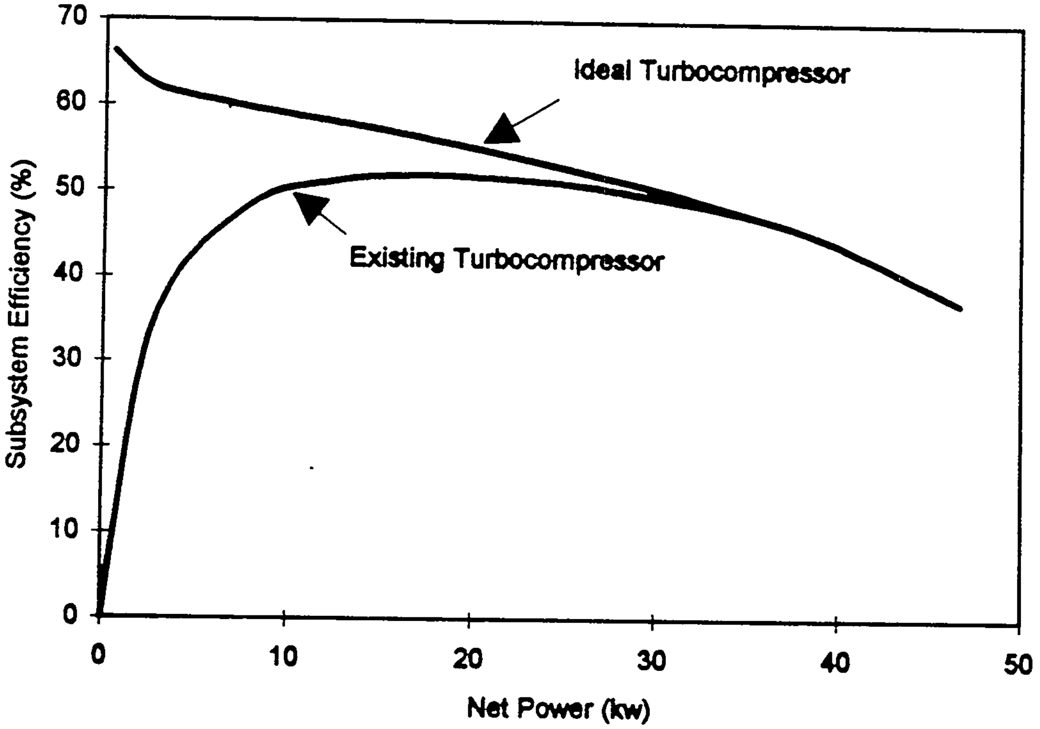

Figure 3-11. Effect of Turbocompressor Design on Subsystem Efficiency

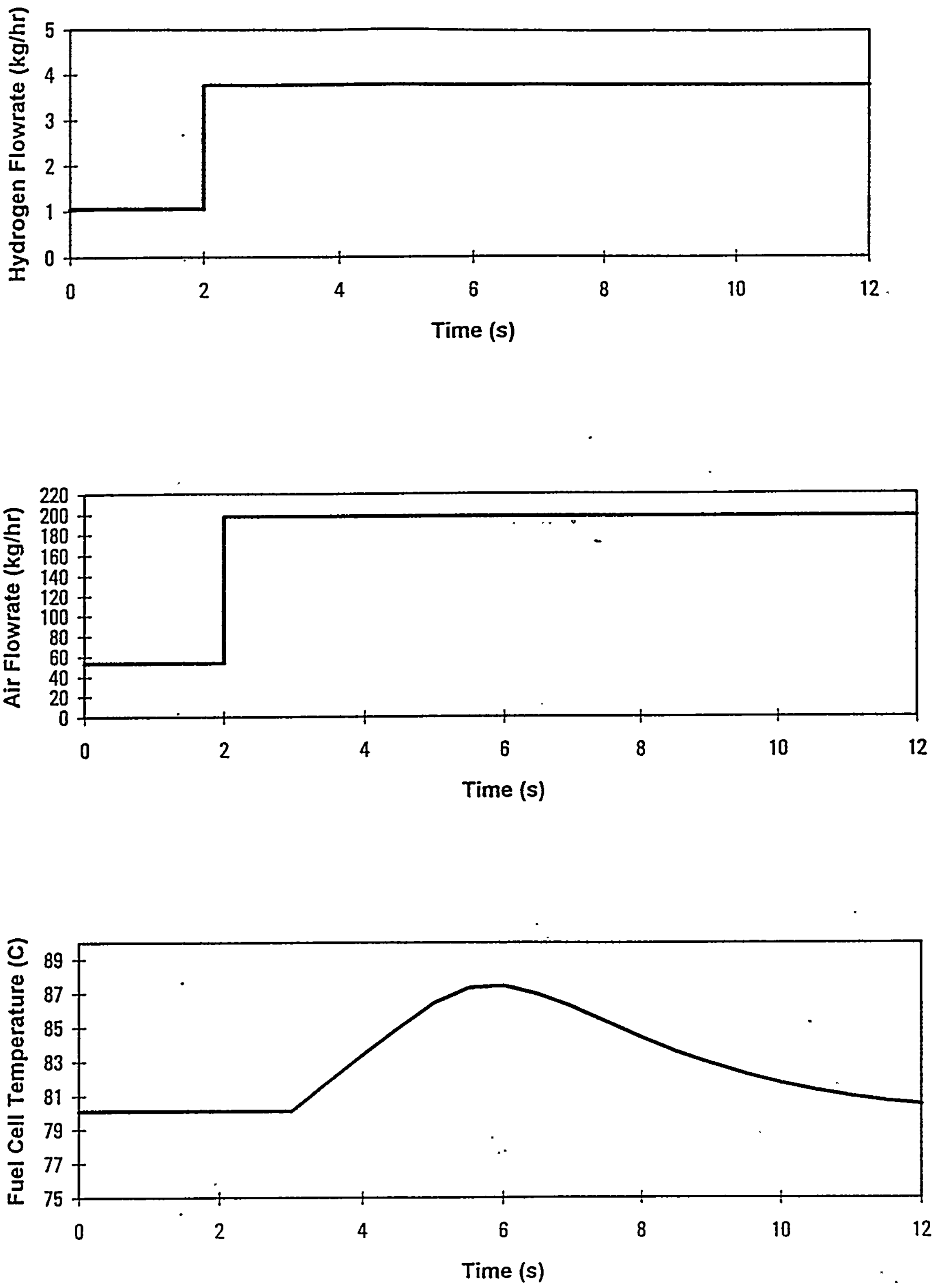

Figure 3-12. Fuel Cell Subsystem Transient Response 20-50 kW Load Change (50 kW Stack)

3.5 Gas Management Subsystem Description

The GMS in development at AlliedSignal is based on results from the steady-state and dynamic modeling of the FCS subsystem. The GMS supplies the FCS with hydrogen fuel and air at the correct temperature, pressure, and humidity to deliver optimum power from the fuel cell. It also contains the controls required to operate the GMS and to provide FCS and GMS status to the DPHV system power controller. A schematic of the GMS is shown in Figure 3-13 and in Appendix C, Figure C-1.

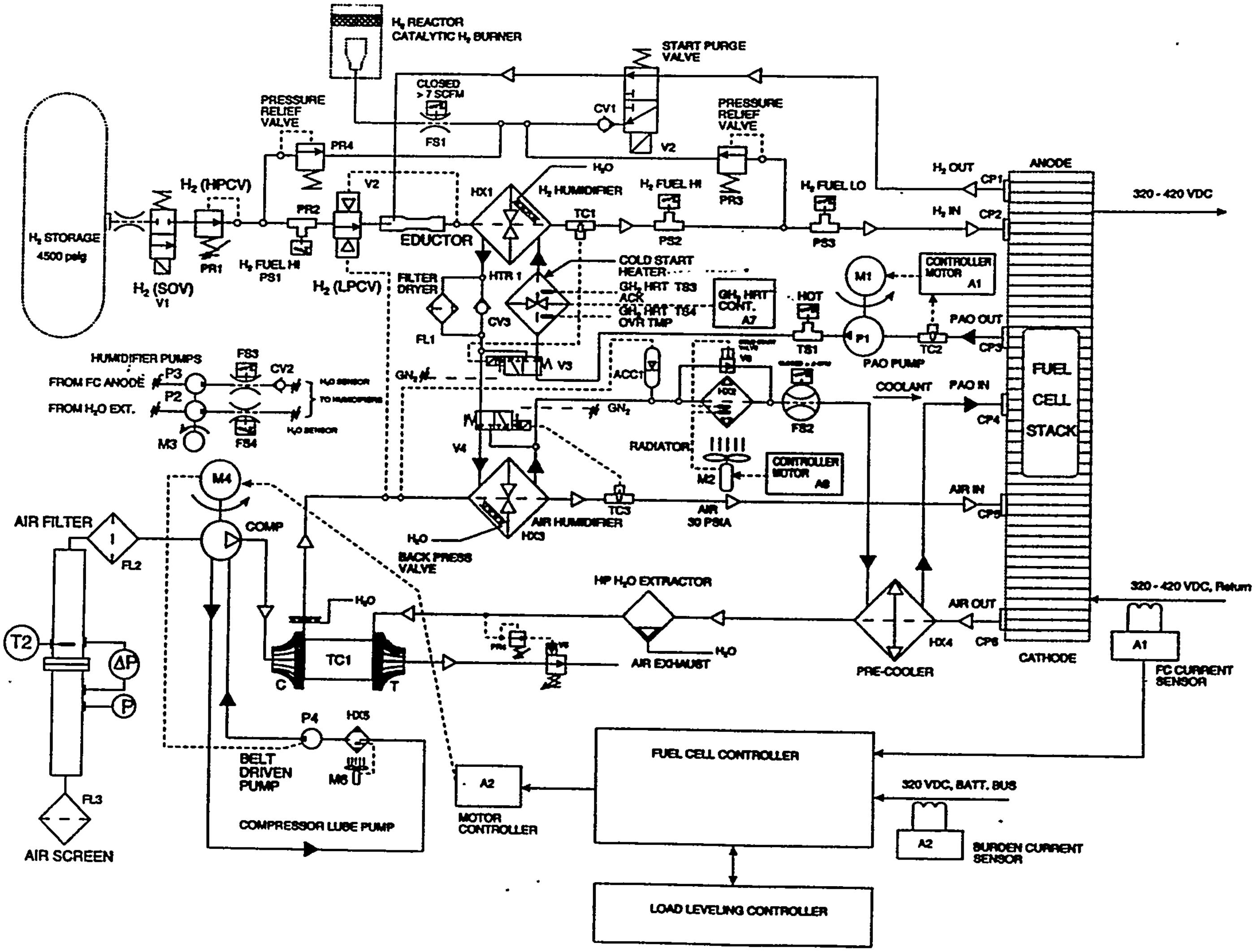
H_2 REACTOR
CATALYTIC H_2 BURNER
START PURGE VALVE
CLOSED > 7 SCFM
FS1
CV1
V2
PRESSURE RELIEF VALVE
PR4
PRESSURE RELIEF VALVE
PR3
H_2 STORAGE 4500 psig
H_2 (HPCV)
H_2 (SOV) V1
PR1
PR2
H_2 FUEL HI PS1
H_2 (LPCV)
V2
EDUCTOR
HX1
H_2O
H_2 HUMIDIFIER
TC1
H_2 FUEL HI
PS2
H_2 FUEL LO
PS3
H_2 OUT
CP1
H_2 IN
CP2
ANODE
320 - 420 VDC
FILTER DRYER
HTR 1
CV3
FL1
COLD START HEATER
GH_2 HRT TS3 ACK
GH_2 HRT TS4 OVR TMP
GH_2 HRT CONT. A7
HOT
TS1
M1
CONTROLLER MOTOR A1
P1
PAO PUMP
TC2
PAO OUT
CP3
FUEL CELL STACK
HUMIDIFIER PUMPS
FROM FC ANODE
FROM H_2O EXT.
P3
P2
M3
FS3
FS4
CV2
H_2O SENSOR
TO HUMIDIFIERS
H_2O SENSOR
GN_2
V3
ACC1
V6
HX2
FS2
COOLANT
PAO IN
CP4
GN_2
V4
RADIATOR
M2
CONTROLLER MOTOR A6
M4
AIR FILTER
FL2
COMP
AIR HUMIDIFIER
HX3
H_2O
BACK PRESS VALVE
TC3
AIR 30 PSIA
AIR IN
CP5
HP H_2O EXTRACTOR
H_2O
AIR EXHAUST
H_2O
AIR OUT
HX4
CP6
CATHODE
PRE-COOLER
320 - 420 VDC, Return
A1
FC CURRENT SENSOR
T2
ΔP
P
TC1
C
T
P4
HX5
BELT DRIVEN PUMP
M6
COMPRESSOR LUBE PUMP
FL3
AIR SCREEN
A2
MOTOR CONTROLLER
FUEL CELL CONTROLLER
320 VDC, BATT. BUS
A2
BURDEN CURRENT SENSOR
LOAD LEVELING CONTROLLER

Figure 3-13. Optimal PEM FCS Configuration

3.5.1 Operating Modes

The GMS contains the controls and logic required to interact with the LLU subsystem to control the fuel cell in the following modes.

- **Pressure** — Pressure control is achieved by using mechanical control valves. These valves regulate the 300-340 atm (4500-5000 psia) hydrogen to 2 atm (30 psia) in two stages. The pressure is determined by the valve settings and sensed using a set of Hi-Lo pressure switches. These switches are set at the maximum and minimum operating pressure tolerances.

- **Temperature** — Both the hydrogen and air feed streams are preheated to the required temperatures (85°C and 75°C, respectively) by the polyalphaolefin (PAO) coolant loop. The temperature control of the PAO at the FCS outlet is set at a nominal value of 90°C.

- **Humidity** — A 100 percent relative humidity is desired for the hydrogen and air entering the FCS. Ultrasonic transducers/humidifiers are used to humidify the gas streams.

- **Hydrogen Leak Detection** — Detection of hydrogen leakage is performed by shutting off the hydrogen supply and measuring the pressure decay. This may be used as a Built-In Test (BIT) test during actual operation, or as a Power On/Off Self-Test (POST) test.

3.5.2 Hydrogen Component and System Descriptions

The hydrogen control system consists of the following components:

- **Hydrogen Pressure Control Valves** — The hydrogen Hi Pressure Solenoid Valve (SOV) is an electrically controlled, pilot operated, slow opening, fast closing solenoid valve. The hydrogen Hi Pressure Control Valve (HPCV) is an industrial pressure regulating valve. It regulates hydrogen input pressures between 300 and 340 atm. (4500-5000 psia) down to 14-18 atm (200-250 psia) output pressures. When an electrical signal is received, the solenoid valve opens, and the regulator begins operations controlling the pressure to the hydrogen Low Pressure Regulating Valve (LPRV) at the nominal 14-18 atm (200-225 psia) level. The LPRV is a dome-loaded control valve that regulates hydrogen flow to the FCS at a nominal 2 atm (30 psia). The actual pressure at the inlet of the FCS is determined by the compressor outlet pressure.

- **Hydrogen Start Purge Valve (SPV)** — This valve is a three-way valve located in the hydrogen recirculation loop. This valve vents the fuel cell anode to atmosphere through a catalytic reactor, in order to remove any gases (N_2, O_2) that diffuse through the MEA to the anode side during shutdown. This valve opens only during start-up.

- **Pressure Switches** — Two normally closed, hermetically-sealed pressure switches are used to verify that hydrogen pressure is maintained within the operating limits. The hydrogen Hi Pressure Switch opens when the hydrogen exceeds the maximum allowable pressure and verifies that the HPCV is functioning properly. The Low Pressure Switch (LPS) opens when hydrogen pressure drops below the minimum allowable pressure. The LPS, in conjunction with a timer circuit in the GMS controller, verifies that hydrogen consumption is normal and that no hydrogen leakage through the lines is present.

- **Hydrogen Heat Exchanger/Humidifier (HX1)** — This heat exchanger/humidifier transfers heat from the PAO coolant loop to the hydrogen feed stream and supplies the water required for humidification in order to maintain an 85°C FCS inlet temperature at 100 percent relative humidity.

- **Hydrogen Humidifier Tube Pump (HTP) (P3) (Peristaltic Pump)** — The HTP pumps water from the FCS to HX1. The tube pump has no shaft sealing, an indefinite run dry capability, and is self-priming. It feeds water directly to the ultrasonic humidifier.

- **Hydrogen Recirculation Subsystem** — The eductor system is necessary to distribute the hydrogen evenly throughout the FCS. The eductor (venturi jet pump), powered by high-pressure hydrogen, recirculates the unreacted hydrogen from the FCS to the hydrogen humidification system.

3.5.3 Air Component and System Descriptions

- **Turbocompressor Subsystem (TCS)** — The TCS under development at AlliedSignal consists of a motor-driven air compressor in series with a turbocharger, because currently available dynamic turbocompressors do not offer a wide flow range at the required pressure. The subsystem consists of the following components:

  - **Motor-Driven Air Compressor (COMP)** — The air compressor is a Roots compressor powered by a standard AC electric motor. The air compressor motor speed is controlled via a 0-10 VDC signal. The motor controller is powered by the 320 VDC power bus. The motor speed is controlled by varying the voltage and frequency of the power provided to the motor in accordance with the input control signal.

  - **Turbocharger (TC1)** — The turbocharger is an air-bearing turbocharger that extracts energy from the cathode exhaust stream and uses it to compress the COMP outlet pressure to 2 atm. Water is injected into the outlet of TC1 to pre-humidify the air stream.

- **Heat Exchanger/Humidifier (HX3)** — This heat exchanger/humidifier transfers heat from the PAO coolant loop to the air feed stream and supplies the water required for humidification in order to maintain a 75°C FCS inlet temperature at 100 percent relative humidity.

- **Air Humidifier Tube Pump (P2)** — The tube pump transfers water from the FCS to the HX3 subsystem.

- **Precooler Heat Exchanger (HX4)** — The vitiated air discharged from the FCS is cooled by the PAO coolant loop to condense water contained in the air stream within this heat exchanger.

- **Water Extractor** — The vitiated air exhaust from HX4 is spun by the guide vanes in the water separator. This causes the water vapor to separate from the air stream and flow into the receiver for the humidification subsystem.

3.5.4 FCS Subsystem Coolant Loop

A centrifugal PAO pump forces the coolant through the FCS at a rate determined by the thermostat at the FCS outlet. The nominal pump output is 2 atm. absolute, which matches the gas pressures in the stack. The coolant pump motor speed is controlled via a 0-10 VDC signal derived from the coolant temperature and fuel cell control input. The motor controller is powered by the 320 VDC power bus. The PAO coolant (90°C) exiting the FCS flows through the heat exchanger/humidifiers to preheat the hydrogen and air feed streams to 85°C and 75°C, respectively. A radiator further cools the PAO to 70°C. The radiator fan is thermostatically controlled and contains an internal valve to bypass the radiator when necessary.

3.5.5 FCS Electrical Isolation

In order to achieve and maintain optimal subsystem performance, it is vital to ensure proper electrical isolation in the PEM FCS subsystem. Current losses in the gas flow lines can be avoided by insulating electrically gas lines and fittings, and grounding the GMS. In addition, high dielectric strength materials for the fuel cell canister need to be used to present current leakage through physical mounts. Shunt currents in the cooling loop are minimized by use of the high dielectric strength coolant, PAO.

3.5.6 FCS Subsystem Operation

- **Startup Sequencing** — In a normal startup sequence (22°C ambient temperature), the events are sequenced by the GMS controller. Initially, the humidifier tube pumps start and supply water to the ultrasonic atomizers. The Power Off recirculation fan starts and supplies air to the air side of the FCS.

  The hydrogen pressure control valves open and fuel is fed to the anode. The hydrogen entering the fuel cell provides the energy for the eductor to recycle unreacted fuel. Experimental studies have shown that energy 20-25 percent of the rated power can be achieved at ambient conditions (22°C FCS, 1 atm. pressure). A fraction of that power is used to drive the Roots compressor, which exhibits very rapid startup. Additional power is diverted to the electric coolant heater located at the outlet of the stack. The hot coolant is then used to bring the heater/humidifiers and the FCS up to the required temperatures. The electric heater is turned off when approximately 40 percent of the rated power is achieved. The total time required to achieve the optimal operating conditions (80°C at 2 atm.) is estimated to be under 30 seconds.

In cases where the ambient temperature is below freezing (cold startup), the cold start electric heater uses energy from the LLU (≈ 4 kW) to melt the ice in the FCS subsystem and preheat the coolant loop. Seven to twelve minutes are required to bring the subsystem up to its operating temperature. Design efforts are under way to reduce this startup time.

- **Power Control** — The current output of the stack is continuously monitored through a feedforward signal by the GMS controller. When the controller senses a steady-state demand for power, it adjusts the speed of the compressor to provide the required air flow rate, and the hydrogen valves adjust accordingly. As hydrogen demand increases, the eductor increases the H_2 recirculation rate as more H_2 is supplied.

- **Idling/Deceleration** — When the Hall-effect current sensor detects an idle current demand, the compressor is ramped up to provide the load necessary to maintain fuel cell voltage. This also prepares the FCS for rapid power demand for acceleration, if necessary.

- **Shutdown** — The HPCV closes and cuts off hydrogen flow to the FCS. The compressor is at idle and depletes the remaining hydrogen from the stack. The cooling system is then shut down and the Power Off recirculation fan intermittently turns on as commanded by the Power Off oxygen sensor to react the residual hydrogen and to maintain proper conditioning of the FCS.

- **Operating Limits** — Optimal performance of the FCS subsystem for automotive applications is achieved at 2 atm., 80°C FCS temperature, and 85/75°C humidification temperatures for hydrogen and air, respectively. Maintenance of these operating conditions within tight tolerances ensures consistent subsystem performance. Operating pressures in excess of 2.5 atm. result in improved fuel cell performance. However, overall subsystem performance degrades due to increasing compression requirements. Low operating pressures, on the other hand, require additional water for the humidification process. As a result, water balance at the subsystem level is not achieved at pressures lower than 1.5-1.8 atm. unless air is fed to the FCS at very low stoichiometries (1-15), which in turn leads to diminished FCS performance.

The effect of fuel cell temperature on overall performance is minimal in the 70-90°C range. Dynamic modeling of the FCS subsystem has shown that an adequate temperature control algorithm would maintain the temperature of the stack within this range, even in case of significant disturbances such as abrupt power load changes. The state of the water entering the FCS with the feed gases has a significant effect on fuel cell performance. Liquid water at the anode/cathode entry points can lead to flooding of the electrodes. As a result, the temperatures of both humidifiers need to be maintained at their optimal values. Experimental studies suggest that a maximum deviation of 2-3°C can be tolerated in the humidifiers.

3.5.7 FCS Control

A diagram of the FCS subsystem controller is shown in Appendix C, Figure C-2. The controller communicates fuel cell status with the vehicle power controller via discrete and analog signals to the LLU controller (LLC). The FCS subsystem controller is divided into three sections.

- **Control Logic**

  Sequences Start-Up

  Controls Purge

  Sequences Shut-Down

  Inhibits System if Critical Faults Exist

- **Fault Detect and Annunciator**

  Monitors Critical Temperatures, Pressures, and Flows

  Transmits Critical Faults to Control Logic Section

  Communicates System Status with the LLC via Discrete Signals

- **Servo Control**

  Monitors Fuel Cell Burden Electrical Current

  Transmits Burden Overcurrent to Fault Detect Section

  Controls Air Flow in Proportions to Fuel Cell Outlet Temperature

  Generates an Analog Signal Representing Hydrogen Fuel Quantity On-Board

The schematic for the Fuel Cell Controller shown in Figure C-2 in Appendix C provides a representation of the logic and not a final design. The Fuel Cell Controller logic is described below.

3.5.8 FCS Control Logic

- **Subsystem Startup Logic** — The controller receives a FUEL CELL ON discrete signal from the LLC. The start sequence is controlled by a Start Timer. The Start Timer enables the purge circuit to purge the fuel cell of spectator gases on the anode side, and inhibits faults such as low coolant flow, low humidification water, and low pressure until these parameters stabilize. The Start Timer is valid for 10 seconds. At the end of the start sequence, the fuel cell is capable of delivering 10 kW of power. Power delivered depends on the demand by the LLC. Full power is available when the coolant temperature is stabilized at the set point of 85°C on the outlet of the FCS.

The time the fuel cell requires to heat the coolant is dependent on the load placed on the fuel cell by the LLC. The more load placed on the fuel cell, the more self-heating is induced, and the faster the fuel cell PAO coolant temperature will reach the required set point.

Two provisional inputs are provided to the LLC for off-design operation. The AIR FC FEED FWD allows the LLC to force a greater stoichiometric airflow through the fuel cell. This ratio is normally controlled by the electrical current feedback signal from the output current transducer.

The COOLANT FC FEED FWD allows the LLC to increase the PAO flow regardless of fuel cell PAO outlet temperature. The COOLANT FC FEED FWD typically works in conjunction with the PUMP OVRD signal. These signals have been designed into the system for the sub-zero cold start system that is currently being modeled. Both the AIR FC FEED FWD and the COOLANT FC FEED FWD are provisional inputs, and may not be used unless required by the dynamic system model.

- **Subsystem Control** — After the initial system startup sequence, the FCS subsystem controller monitors the fuel cell current output. The hydrogen fuel is controlled by mechanical pressure regulators, with hydrogen being recirculated using an ejector pump. The fuel cell controller only needs to monitor hydrogen fuel pressure to verify proper operation. Coolant temperature is controlled by a thermostat on the inlet side of the fuel cell. This thermostat controls the cooling airflow across the radiator, with a valve that bypasses the radiator for cold start. The fuel cell controller monitors the PAO coolant temperature on the outlet side of the fuel cell, and increases the flow to maintain the correct outlet temperature. Correct coolant inlet temperature is critical for the operation of the pre-cooler, which is the source of the humidification water. Correct outlet temperature is critical to the operation of the fuel cell and air and hydrogen humidifiers.

- **Subsystem Shutdown** — The preferred shutdown sequence is to place the INTEGRITY TEST, 12 Volt discrete signal high. This keeps the fuel cell running, but causes the hydrogen shut-off solenoid valve to close. The H_2 PRESS LO and MASTER CAUTION discretes are then sensed. These indicate that the hydrogen fuel is being consumed, creating a low pressure condition on the anode side. This low pressure condition indicates that the fuel cell is not leaking internally. This condition should result in approximately five seconds from the INTEGRITY TEST discrete being activated. At the end of this test, the FUEL CELL ON discrete may then be placed LO, shutting down the system.

3.5.9 FCS Subsystem Inhibit and Fault Isolation

There are five errors that will result in the closing of the Hydrogen Shut-Off Solenoid Valve (SOV), shutting down the fuel cell. The errors latch a relay and require a reset signal to re-enable the system.

Unrecoverable Errors

- Humid Water (NOT)
  - No humidification water flow from the air humidifier pump
  - No humidification water flow from the hydrogen humidifier pump
- H_2 Press Hi
  - High hydrogen pressure before main hydrogen pressure regulator
  - High hydrogen pressure at the inlet to the fuel cell
- H.O.T. (High Oil Temperature)
  - PAO coolant exiting the fuel cell is above acceptable limits. Fuel Cell overheating
- Ovr Temp (Cold Start Heater)
  - The PAO coolant heater temperature is above acceptable limits
- Fc Burden Ovr Current
  - Excess electrical current draw by some component in the fuel cell auxiliary subsystem

Note: PAO COOLANT FLOW (NOT)

PAO coolant flow below low flow limit. This error may be used as an unrecoverable error in a later fuel cell controller design.

The errors shown above require a reset command before restarting which automatically shut down the fuel cell. These errors are expected to be generated by an equipment failure rather than a transient (out-of-tolerance) condition.

Recoverable Errors

- H_2 Press Lo
  - Induced by the INTEGRITY TEST
  - Low pressure regulator malfunction
  - Low hydrogen fuel quantity

- SOV Fail
    - Hydrogen shut-off SOV did not actuate when commanded, sending a feedback signal to the fuel cell controller
- Purge Fail
    - Purge flow not present when commanded, sending a purge flow signal to the fuel cell controller
- Htr Fail
    - Humidification PAO coolant heater has not reached the desired set point

These error may reflect a transient out-of-tolerance condition reflecting a system error. The LLC has the option of shutting down fuel cell operations if these errors occur.

SECTION 4
HYDROGEN STORAGE SUBSYSTEM REQUIREMENTS

4.1 Hydrogen Storage on Board Vehicles

4.1.1 Hydrogen As An Automotive Fuel

A low-cost, compact means of storing hydrogen is needed for successful commercialization of the Direct Hydrogen-Powered PEM fuel Cell Stack Hybrid Vehicle (DPHV) electro-chemical engine for electric vehicles. Hydrogen is appealing as an automotive fuel because the only byproduct of a low-temperature reaction is water, with no pollutants or greenhouse gases. Hydrogen can either be stored on board a vehicle in its pure form, or produced by reforming a hydrocarbon such as methanol. For the present program, a direct-hydrogen-fueled mandate was part of AlliedSignal's contract in developing a fuel delivery system for the vehicle.

4.1.2 Goals For Hydrogen Storage On Vehicles

The main goal for hydrogen storage on board a vehicle is to achieve a driving range of 380 miles with an EPA fuel economy of 80 MPG (see Section 1.1.2). The deliverable amount of hydrogen fuel has been estimated at 12.5 lbs. The cost target for the hydrogen storage system is $300, which is in accordance with the goal set forth by the Partnership for a New Generation of Vehicles (PNGV).

4.1.3 Methods For Storing Hydrogen On Vehicles

Four hydrogen storage methods have been studied as part of the storage system design process. These methods are described below:

- **Pressurized Gas Storage** — Gaseous hydrogen is the most simple and direct approach, but requires high storage pressures to achieve a reasonable packaging volume. This technology is based on the deployment of compressed natural gas for light duty vehicle use. For automotive applications, lightweight composite fiber wrapped pressure vessels with metallic or plastic liners represent a potential solution in a technically and economically viable storage system. Storage in vehicle systems is presently limited to 3000 psia. However, storage systems with pressures of up to 10,000 psia have been achieved in aerospace applications.

- **Cryogenic Liquid Hydrogen Storage** — This technology is based on the existing distribution and dispensing of hydrogen and other cryogenic fluids. Liquid hydrogen at cryogenic temperatures provides a much higher packaging density than gaseous storage. However, a significant energy penalty is associated with the liquefaction process.

  Liquid hydrogen storage involves the use of a vacuum jacketed super-insulated storage vessel commonly known as a dewar. Many established U.S. suppliers fabricate stationary dewars and support equipment for large and small quantity cryogenic applications. A few suppliers produce liquid methane dewars for automotive applications.

- **Carbon Molecular Sieve** — The objective of the carbon molecular sieve is to increase the storage capacity of compressed gas hydrogen by the addition of activated carbon to the pressure vessel. The carbon material is based on that developed for methane purification pressure swing absorbers. The use of activated carbon to augment pressurized methane storage has been considered recently. A similar approach has been suggested for hydrogen storage. It has been demonstrated that the physical absorption of pressurized hydrogen gas on activated carbon will increase a pressure vessel's storage capacity within a particular temperature and pressure range.

- **Metal Hydride Storage** — This concept is based on the chemical reaction of hydrogen with a metal alloy to form a hydride. Metal hydride storage can be accomplished at low pressures (2 to 7 atm) and at room temperature. However, the low hydrogen capacity of existing metal hydrides (1 to 1.5 percent by weight) results in heavy storage systems. The heavy weight required to store a sufficient quantity of hydrogen might, therefore, prove to be prohibitive for automotive applications. This, in addition to their excessive cost and the need for considerable heat transfer, renders the use of existing metal hydride technologies unattractive for automotive applications.

- **Summary of Storage Method Selection** — Pressurized gas storage has been selected as the best near term choice for development for the DPHV program. Advantages include significantly developed and demonstrated technology, simplicity, low weight, simple refueling and no boil-off losses. Liquid storage will also continue to be investigated since it provides the potential of reduced cost, volume and weight as compared to compressed gas. However, significant technical and safety issues must be resolved for this technology to be deployable to the general public. Continued research and development of Carbon Molecular Sieve (CMS) technology is ongoing as a cost sharing effort. At present, however, the CMS materials offer no advantages over compressed gas storage. As for metal hydride storage systems, their weight and cost are prohibitive for automotive applications.

4.1.4 Specifications For Hydrogen Storage

No codes or specifications particular to automotive hydrogen fuel systems presently exist. Specifications from the Compressed Natural Gas Vehicles (CNGV) environment were used as guidelines in the formation of the hydrogen system requirements. Such CNGV specifications include: NGV-1, NGV-2, (published by the American Gas Association [AGA]), NHTSA FMVSS 301, Fuel System Integrity (for liquid fueled automobiles), NHTSA 303 Fuel System Integrity (for gaseous fueled automobiles), NHTSA 304 Vehicle Pressure Vessels (produced by the National Highway Traffic Safety Administration) and NFPA-52, CNG vehicular Fuel Systems (produced by the National Fire Protection Association). A complete hydrogen-specific system and component product specification for performance, design, qualification, and production quality is being assembled as part of the design and development effort. Existing codes for compressed flammable gases for industrial settings are available and are applicable to the hydrogen infrastructure facilities. Some of the applicable codes and standards for on and off board storage are given in Appendix F, Figure F-1.

4.2 Gaseous Hydrogen Storage System Concept

The gaseous hydrogen storage system is being modeled on existing CNGV storage system configurations, such as that used on the CNG powered Dodge Ram Van. Key system performance goals are summarized in Table 4-1.

Table 4-1. Gaseous Hydrogen Storage System Design Goals

Hydrogen Storage Capacity	12.5 lbs
Total Syst em Weight	217 lbs
Total System Cost	$300
Total Volume	< 9 ft3
Mile Life	100,000 Miles
Operation	Tr ansparent
Refueling Time	5 Minutes
Safety	Equivalent to Gasoline

Installation studies performed by Chrysler Liberty and Technical Affairs determined the maximum external storage volume to be 12 cubic feet. This was determined by iterating the size and number of typical pressurized cylinder shapes within the existing vehicle design architecture. The 12 cubic foot installation was then iterated with storage pressure assuming carbon fiber overwrapped vessels and ambient temperature storage. A storage pressure of 5000 psia is required to achieve the technical requirements of 12.5 lbs H_2 with an external volume of 12 ft^3 (9 ft^3 internal storage volume).

4.2.1 System Schematic - Gaseous Hydrogen

The present gaseous storage system schematic is shown in Figure 4-1. A combination of three storage tanks was found to provide the optimum installation within the vehicle. The baseline design consists of all-composite pressure vessels with carbon fiber overwrap. CNG vessels are commercially available in this configuration (i.e. 3000 psia). Tests conducted with hydrogen using these vessels have shown encouraging results. The increased pressure required for hydrogen storage and the cost of the carbon fiber material present the main technical challenges.

Each tank is shown with manual valve and pressure relief devices. The manual valves are typically provided for tank service considerations. The flow fuse operates in a similar fashion to an electrical fuse. That is, in the event of a downstream leak and flow increases beyond a predetermined level, the flow fuse will stop the flow completely. A single manual valve is provided in series with the flow fuse to provide a shut-off means in case of a minute leak, too small to actuate the flow fuse.

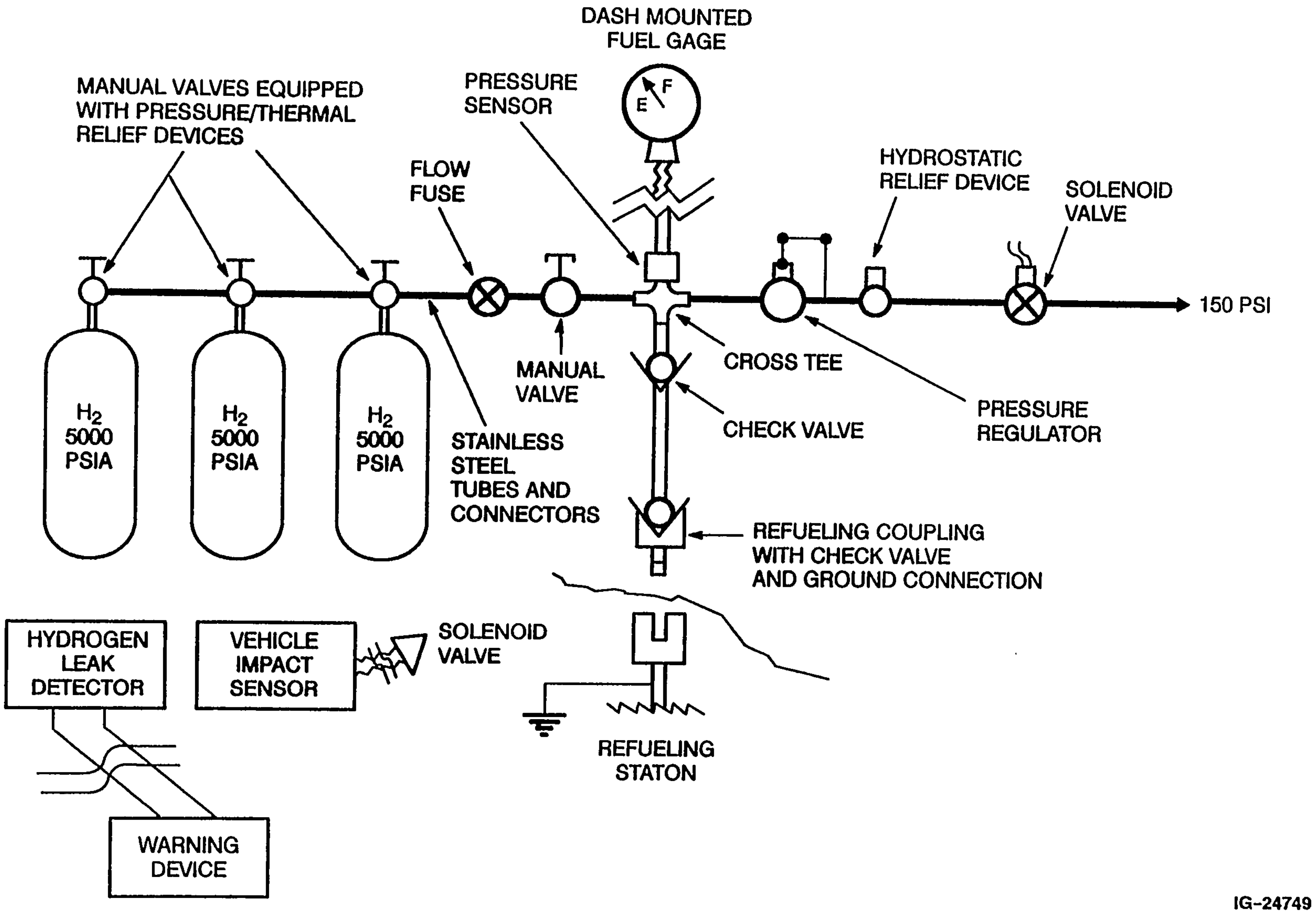
DASH MOUNTED
FUEL GAGE
F
E
MANUAL VALVES EQUIPPED
WITH PRESSURE/THERMAL
RELIEF DEVICES
PRESSURE
SENSOR
FLOW
FUSE
HYDROSTATIC
RELIEF DEVICE
SOLENOID
VALVE
150 PSI
H_2
5000
PSIA
H_2
5000
PSIA
H_2
5000
PSIA
MANUAL
VALVE
CROSS TEE
CHECK VALVE
PRESSURE
REGULATOR
STAINLESS
STEEL
TUBES AND
CONNECTORS
REFUELING COUPLING
WITH CHECK VALVE
AND GROUND CONNECTION
HYDROGEN
LEAK
DETECTOR
VEHICLE
IMPACT
SENSOR
SOLENOID
VALVE
REFUELING
STATON
WARNING
DEVICE
IG-24749

Figure 4-1. Gaseous Hydrogen Storage System Schematic

A refueling coupling which resembles, in appearance and operation, a gasoline nozzle is being investigated. A refueling coupling must incorporate a ground in order to provide electrical grounding for the vehicle during refueling operations. NGV-1 is being used as a guideline in the design of the refueling coupling. The Refuel Proximity Switch shown in the schematic prevents the vehicle from accidentally being driven while the refueling hose is connected. The Quantity Sender senses tank pressure and temperature, and provides a signal to a dash-mounted "fuel level" indicator gage. Both these functions will be integrated with the Fuel Cell System Controller. A normally closed/fail closed electric shut-off valve actuates the hydrogen flow to the pressure regulator. A flow limiter, or restriction, may be needed to attenuate the sudden pressure spike resulting from the opening of the shut-off valve. The pressure regulator reduces the vessel pressure to a working pressure of 150 psia. The shut-off valve could alternatively be placed down stream of the pressure regulator to reduce the average load on the valve and eliminate pressure spiking the regulator. However, leakage from the regulator could also result in a pressure spike down stream. Further analysis is required to optimize the placement of the valve.

4.2.2 Storage Vessel Size Estimate

A storage pressure of 5000 psia is required for ambient temperature storage, as shown in Figure 4-2. The design point demonstrates a density of approximately 1.4 lb per ft^3, which corresponds to a volume of 9 ft^3 for 12.5 lbs of storage. This translates into an external pressure vessel volume of approximately 12 ft^3.

4.2.3 Installation Concepts

A single pressure vessel would be most desirable in terms of minimizing both cost and complexity. An installation concept of a large tank combined with a much smaller cylinder is shown in Appendix F, Figure F-2. However, this configuration negates all usable trunk space. As a result, the viability of single tank assembly is limited to trucks or large station wagons, where volume is not a significant issue. Numerous layouts for mid-size passenger vehicles have been generated by Chrysler engineering.

Figure F-3 in Appendix F shows a concept with nine pressure vessels, which utilizes available volume adequately but greatly increases complexity and cost. Alternative layouts considered in this study are shown in Appendix F, Figures F-4 and F-5. However, the optimal configuration for storage of the required volume of hydrogen is shown in Figure 4-3. This system is being modeled in the trunk of the Chrysler LH Sedan and consists of three identical pressure vessels, each 15 inches OD and 39.4 inches long.

With some minor modifications, such as moving the rear seat cushion forward three inches (same position as the standard LH model), and repositioning of the spare tire, 16.5 ft^3 of trunk space is available along with 9.0 ft^3 of hydrogen storage.

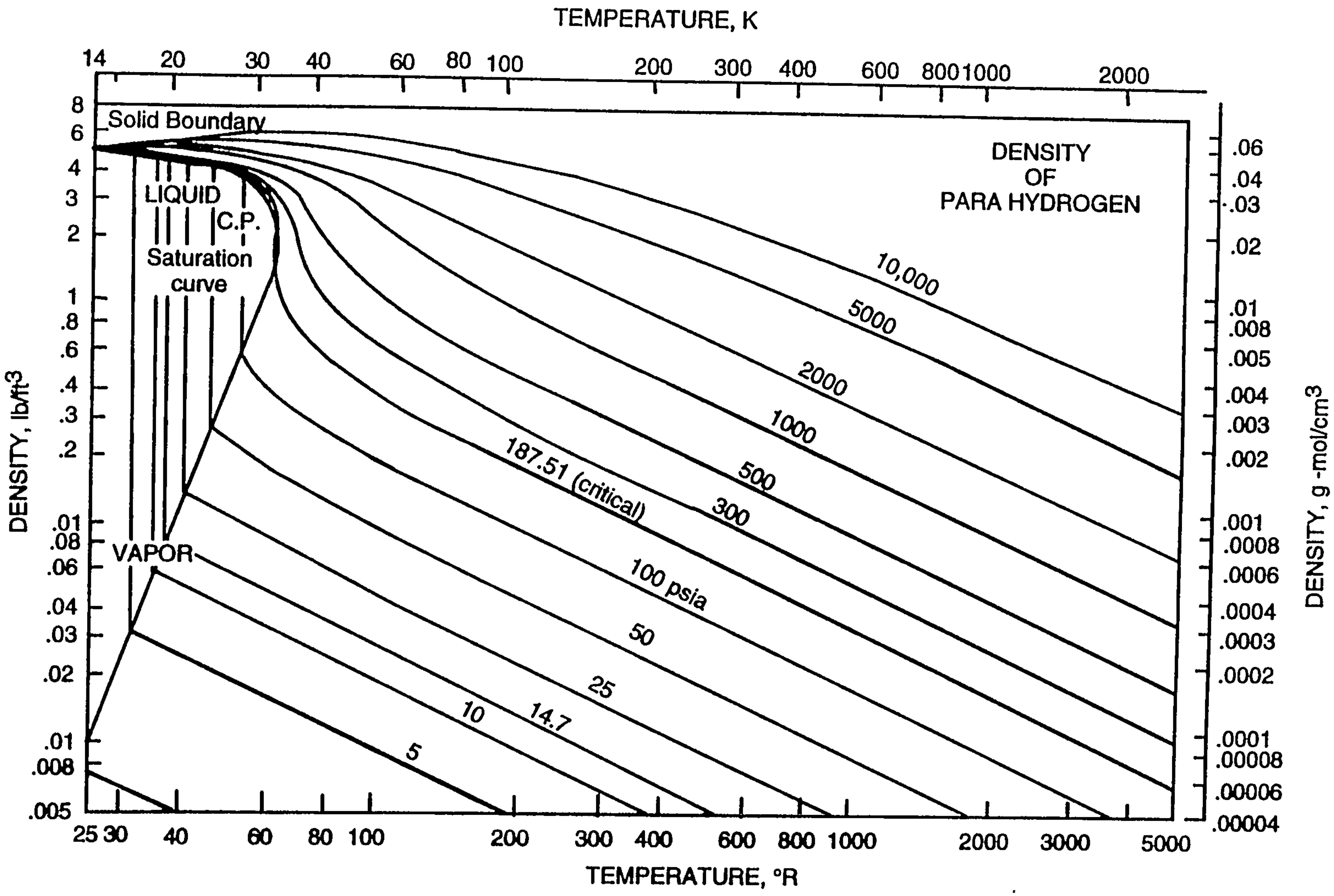

M-03747

Figure 4-2. Hydrogen Density as a Function of Pressure and Temperature

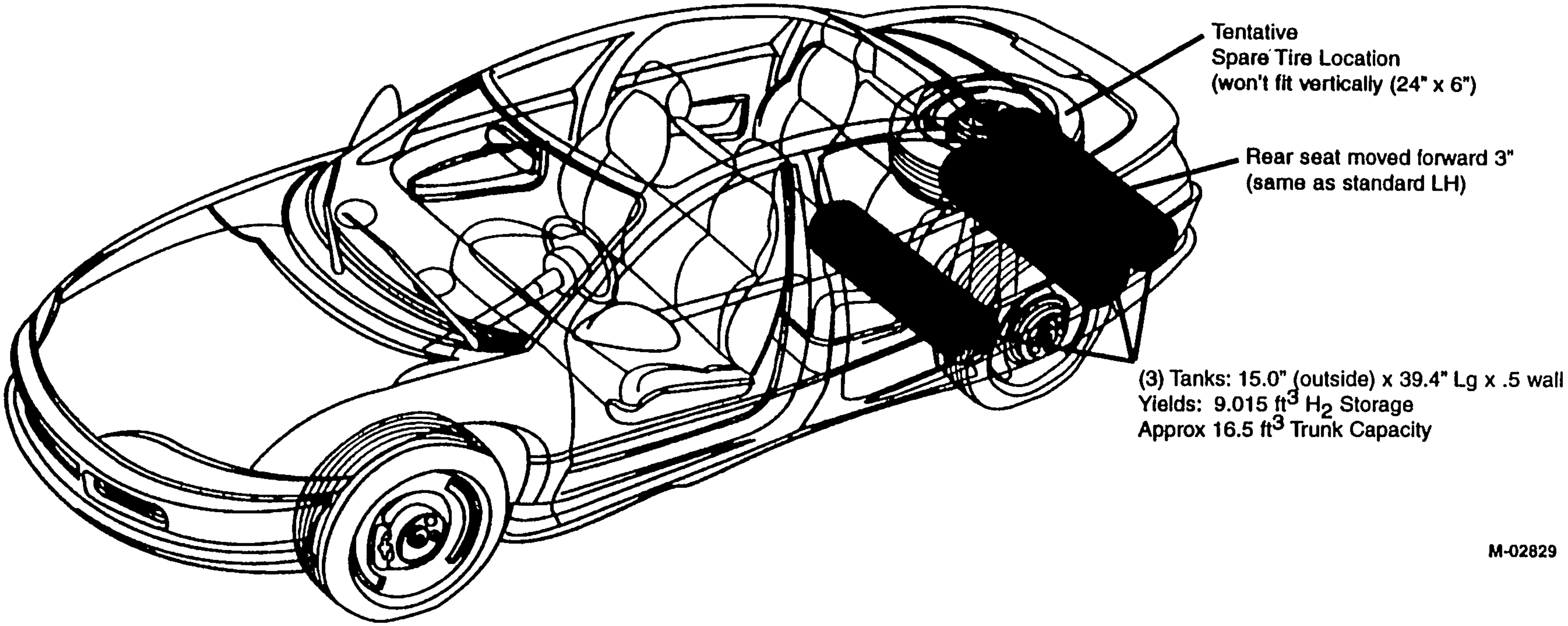
Tentative
Spare Tire Location
(won't fit vertically (24" x 6")
Rear seat moved forward 3"
(same as standard LH)
(3) Tanks: 15.0" (outside) x 39.4" Lg x .5 wall
Yields: 9.015 ft^3 H_2 Storage
Approx 16.5 ft^3 Trunk Capacity
M-02829

Figure 4-3. Best-Fit Gaseous Hydrogen Installation Layout

4.2.4 Gaseous Hydrogen Safety Issues

Sudden pressure release and fire constitute the primary safety considerations for gaseous hydrogen storage systems. Hydrogen's very low ignition energy and broad range of flammability in air make it susceptible to easy ignition. Hence, leakage will have to be kept to a minimum. Minimal connection interfaces are included in the system design to lessen the potential for leakage. In addition, flexible gas lines minimize leaks during crash impacts by allowing for displacement of components. The feasibility of several on board hydrogen sensing technologies is being evaluated. Gas release after crash impacts should be demonstrated to be consistent with NHTSA FMVSS 301 and 303 at the vehicle test level in future development phases. The ability to shut-off the hydrogen supply in case of an emergency will be incorporated into the FCS subsystem controller logic. This can be integrated in to the vehicle operation logic and activated by any number of conditions such as crash impact, leak detection, operator command, refueling, as well as any fuel cell operational failure. Also, in the case of a system leak, hydrogen shut-off will be accomplished by the flow fuse. An electronic leak detector will be mounted in the vicinity of the hydrogen storage subsystem. This device will warn the driver in the event of a hydrogen leak. Safe containment of the mechanical pressure energy will be demonstrated to be consistent with the bullet impact testing of NGV-2. Since auto-ignition of sudden hydrogen releases is possible, a demonstration test to characterize this event is planned for the first phases of development testing. Means to mitigate risks associated with this type of event will be developed and demonstrated as soon as practical. Since durability of composite CNG vessels has proven to be acceptable, equivalent or better failure rates will be targeted for the hydrogen storage system by providing the same safety factors and structural integrity.

Several fiberglass wrapped compressed natural gas pressure vessel failures have been studied and the lessons incorporated into the design of the hydrogen storage system. Specific installation conditions to be avoided have been identified in the failure analyses. In addition, the baseline hydrogen vessels, which are carbon fiber overwrapped, are less susceptible to the failure mechanism associated with the subject fiberglass CNG vessels.

4.2.5 Refueling Thermodynamics

As a result of the continuing effort to make the system indistinguishable to the user from a conventional gasoline automobile, a five minute refueling time goal has been established. When a pressure vessel is filled, compression energy is dissipated as heat. Due to its negative Joule-Thompson Effect coefficient, the temperature of hydrogen gas rises across a throttle valve. Computational analyses of the thermodynamics of the refueling process indicate that for the adiabatic condition, the temperature of hydrogen gas in the vehicular storage system rises about 270°F to 400°F when cascade filled from a worst case 130°F ambient temperature stationary 6000 psia vessel (Figure 4-4).

The results of an analysis which includes heat transfer to the vessels and environment show that the heat transfer is too slow to markedly reduce gas temperature until well after the refueling process is complete. A five minute simulated refueling with heat transfer is shown in

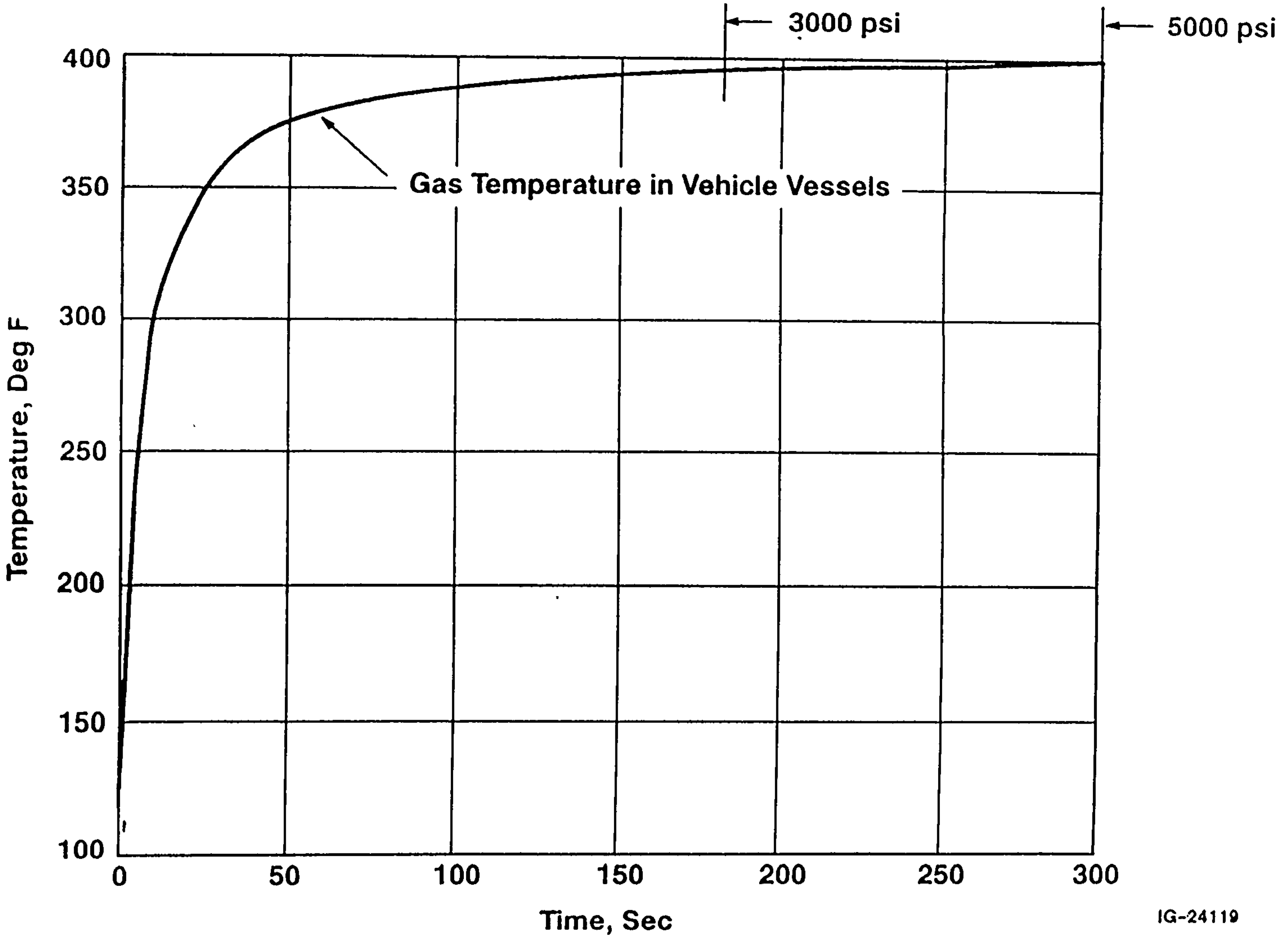

Figure 4-4. Tank Refuel Adiabatic Temperature Response

Figure 4-5. The temperature spike which results during the refueling operation could result in a 30 percent reduction in storage capacity for a single refueling. Multiple refuelings, such as filling the vessels to 70 percent of mass capacity, allowing them to cool, then performing a top-off fill would eliminate the temperature spike problem. Very slow filling of the vessels overnight would also eliminate a temperature spike problem. However, a single five minute refueling procedure is the goal of this program. Minimization of the effect of the temperature spike is important in order to avoid increased volume and cost for the system. One potential solution is to expand the stored hydrogen through a turbine in place of a throttle as it enters the storage vessel, which would result in a temperature drop due to the work removed.

However, as shown in Figure 4-6, compressor inefficiencies negate the beneficial effect. The prospect of adding a heat sink media to the inside of the vessels is prohibitive since the quantity of heat generated is very large. About 100 lb of aluminum would have to be added to the pressure vessels to reduce the temperature of the gas by 100 F. Several hundred pounds would have to be added to have any marked beneficial effect.

A technically viable solution to the refueling heat problem is to supply refrigerated hydrogen gas for refueling. Computational analysis has revealed that a hydrogen supply gas temperature of -100°F will eliminate the temperature spike. The energy of compression will raise the temperature of the -100°F gas to an average ambient temperature of 70°F as it is compressed in the vessel. Figure 4-7 shows that for various initial fill conditions, a supply temperature of -100°F results in ambient temperature within the bottle with no danger of over-pressurization.

While technically viable, the cost of refrigerating a gaseous hydrogen supply to -100°F is prohibitive. However, a liquid hydrogen supply system, such as that shown in Figure 4-8C, could provide hydrogen at reduced temperature with little cost impact to the system or fuel. A refrigeration system would not be required since the liquid hydrogen's extreme cold temperature could be utilized. This is most likely the best long-term solution to the fast fill problem since it has been projected that large scale delivery of hydrogen will have to be in liquid form to be economical.

For a gaseous hydrogen supply system the most cost effective method to achieve a complete fill in five minutes is to over-pressurize the vessels. The pressure will diminish to the rated operating pressure when the vessels cool down to ambient temperature. This scheme is currently used for CNG-powered vehicles. CNG refueling dispensers are temperature compensated such that a complete fill is assured up to an ambient temperature of 72°F. An overpressurization of as much as 25 percent is done to accomplish the complete fill. A similar approach could be taken for the hydrogen storage vessels. However, a greater over pressurization would be required for hydrogen due to its negative Joule-Thompson coefficient and its unfavorable compressibility factor characteristics. It has been computed that a 7000 psia fill at 72°F would be required to ensure a complete fill for 5000 psia ambient temperature storage, thus requiring a 40 percent overpressure.

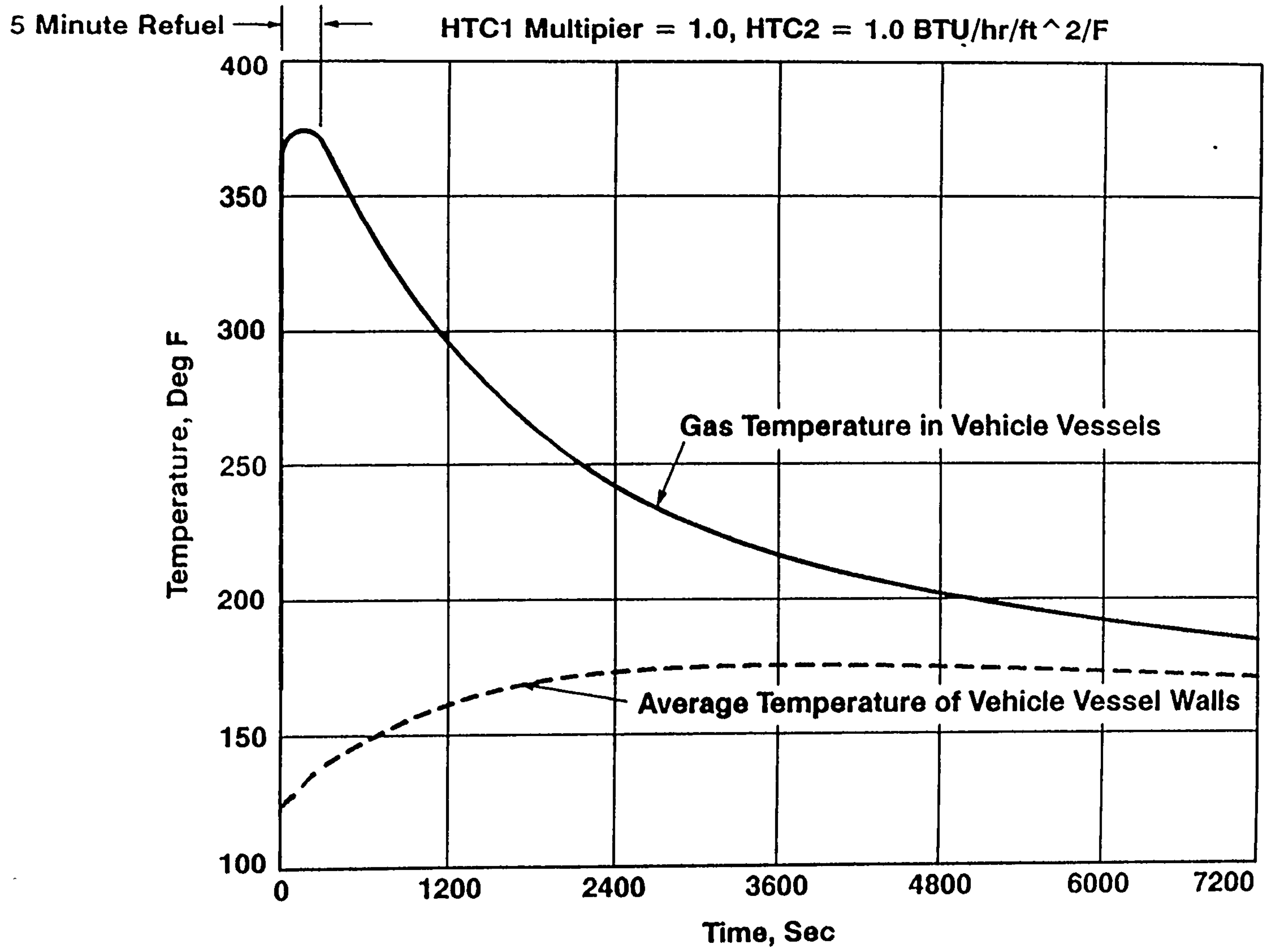

Figure 4-5. Refuel Temperature Response with Heat Transfer

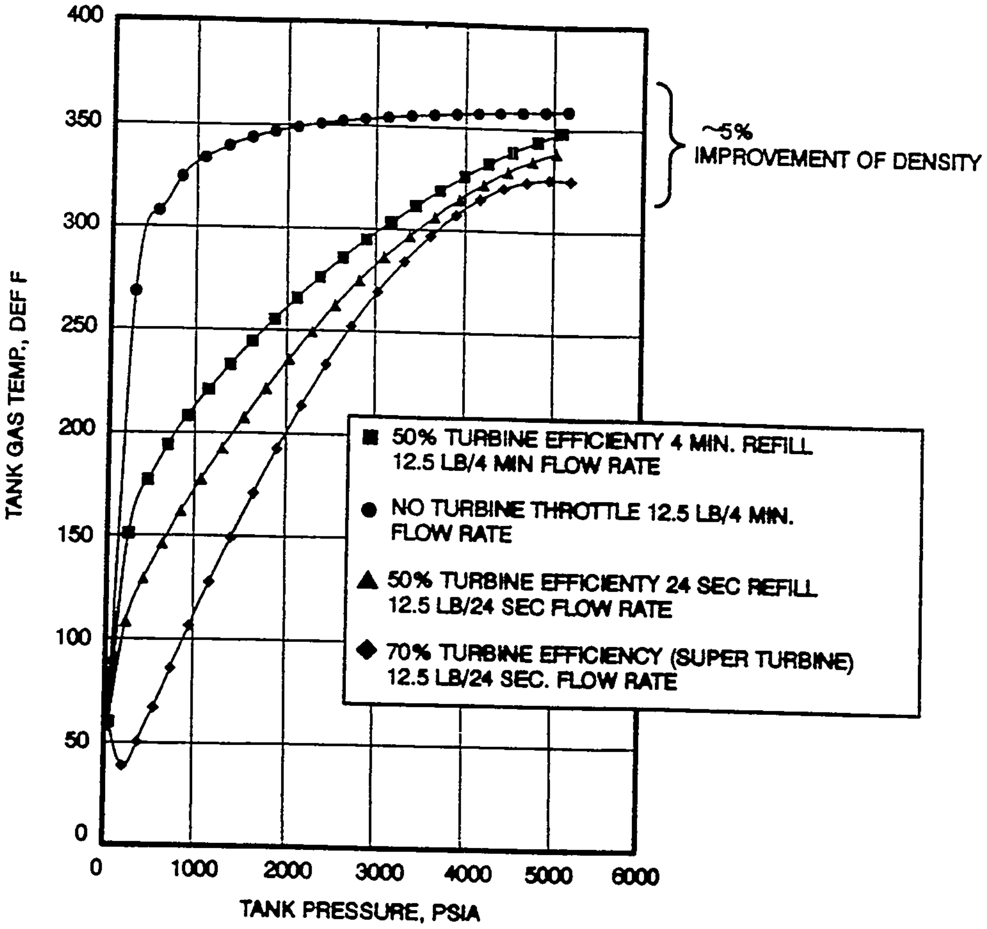

Figure 4-6. Hydrogen Tank Refueling Temperature Rise

As part of the development research on the Hydrogen Storage Subsystem, an EDO LiteRider, Model 45L, cylinder was subjected to a hydrogen fast fill (5000 psia) and discharge test. The purpose of the test was threefold:

- To determine the overpressure required to achieve a 5000 psia fill
- To determine overpressure relief thermal temperature requirements
- To investigate the vessel material compatibility with hydrogen.

Temperature data was recorded from thermocouples placed inside the bottle. The hydrogen was supplied by five 6000 psia hydrogen storage cylinders connected by 3/8" stainless steel tubing. The cylinder was filled to approximately 5150 psia within 30 seconds. The cylinder was then left at pressure for approximately four hours. Finally the hydrogen was rapidly discharged. The vessel was then cut into sections for analysis.

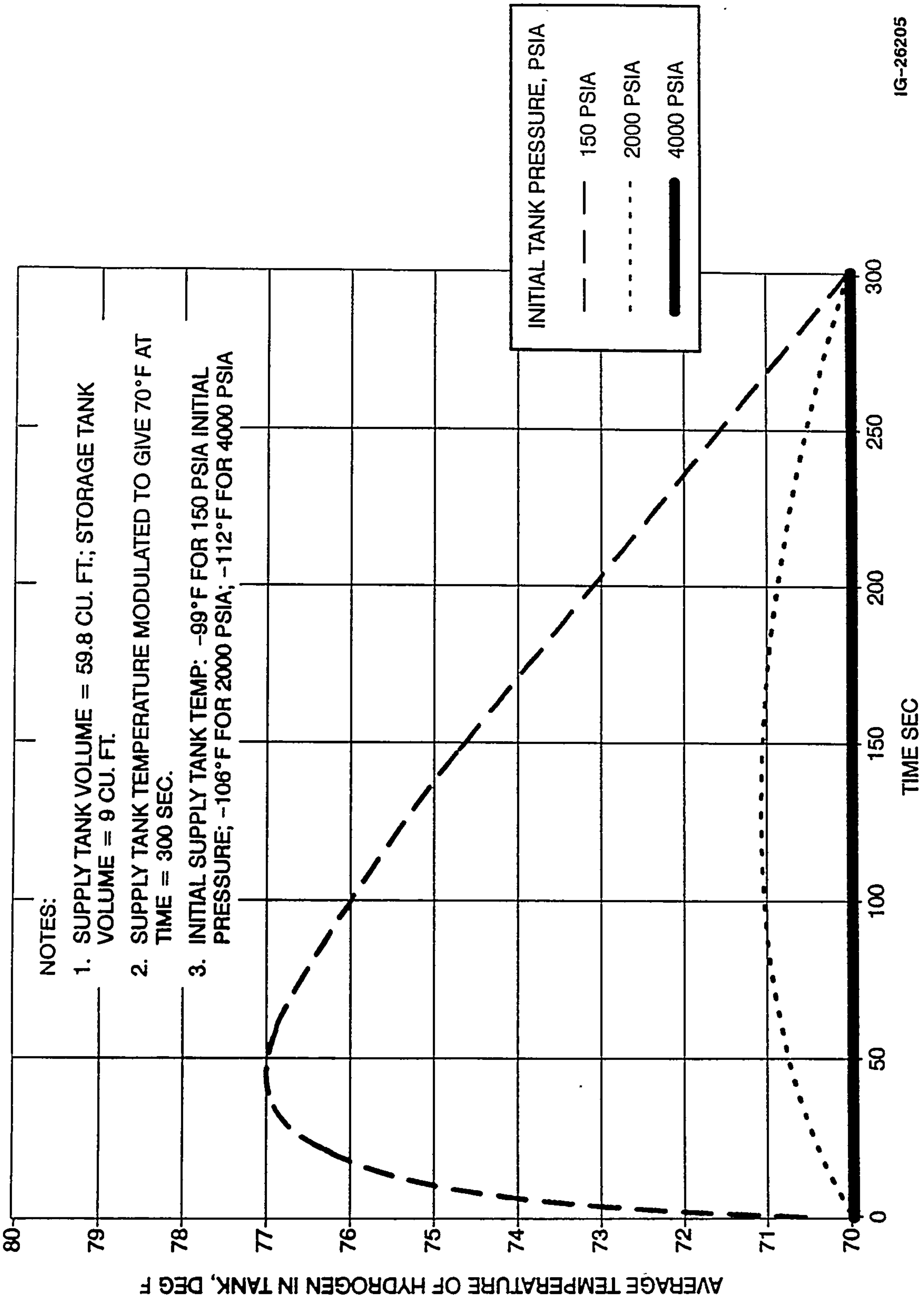

NOTES:

1. SUPPLY TANK VOLUME = 59.8 CU. FT.; STORAGE TANK VOLUME = 9 CU. FT.
2. SUPPLY TANK TEMPERATURE MODULATED TO GIVE 70°F AT TIME = 300 SEC.
3. INITIAL SUPPLY TANK TEMP: −99°F FOR 150 PSIA INITIAL PRESSURE; −106°F FOR 2000 PSIA; −112°F FOR 4000 PSIA

Figure 4-7. Refueling Tank Temperature Rise without Turbine

The results of the test procedure are especially encouraging. The test indicates that an overpressure of 800 psia (5800 psia total) is required to achieve a settled pressure of 5000 psia. This pressure is much less than the overpressure which was analytically determined. Actual heat transfer from the entering hydrogen to the vessel is far better than that which was calculated. Samples of the liner material from the test vessel and from an untested vessel were taken to AlliedSignal for analysis. Laboratory analysis indicates that no changes were detected in the liner material due to the hydrogen pressurization, soak, and rapid depressurization cycle.

4.2.6 High Pressure Refueling Schemes

Three potential refueling schemes are shown in Figure 4-8. The first utilizes a 60 cubic foot 8000 psia reservoir which feeds gas through a throttle and a heat exchanger to produce the -100°F hydrogen to the tank at 5000 psia. The second scheme is similar to the first except that a cascade of two reservoirs is used to reduce total compression costs. The 4000 psia reservoir fills the tank partly, followed by the 8000 psia reservoir. The third system employs a liquid stationary reservoir which pumps liquid hydrogen to a vaporizer in order to refrigerate the hydrogen to -100°F. An economic analysis of the alternative schemes is necessary to determine the optimal configuration.

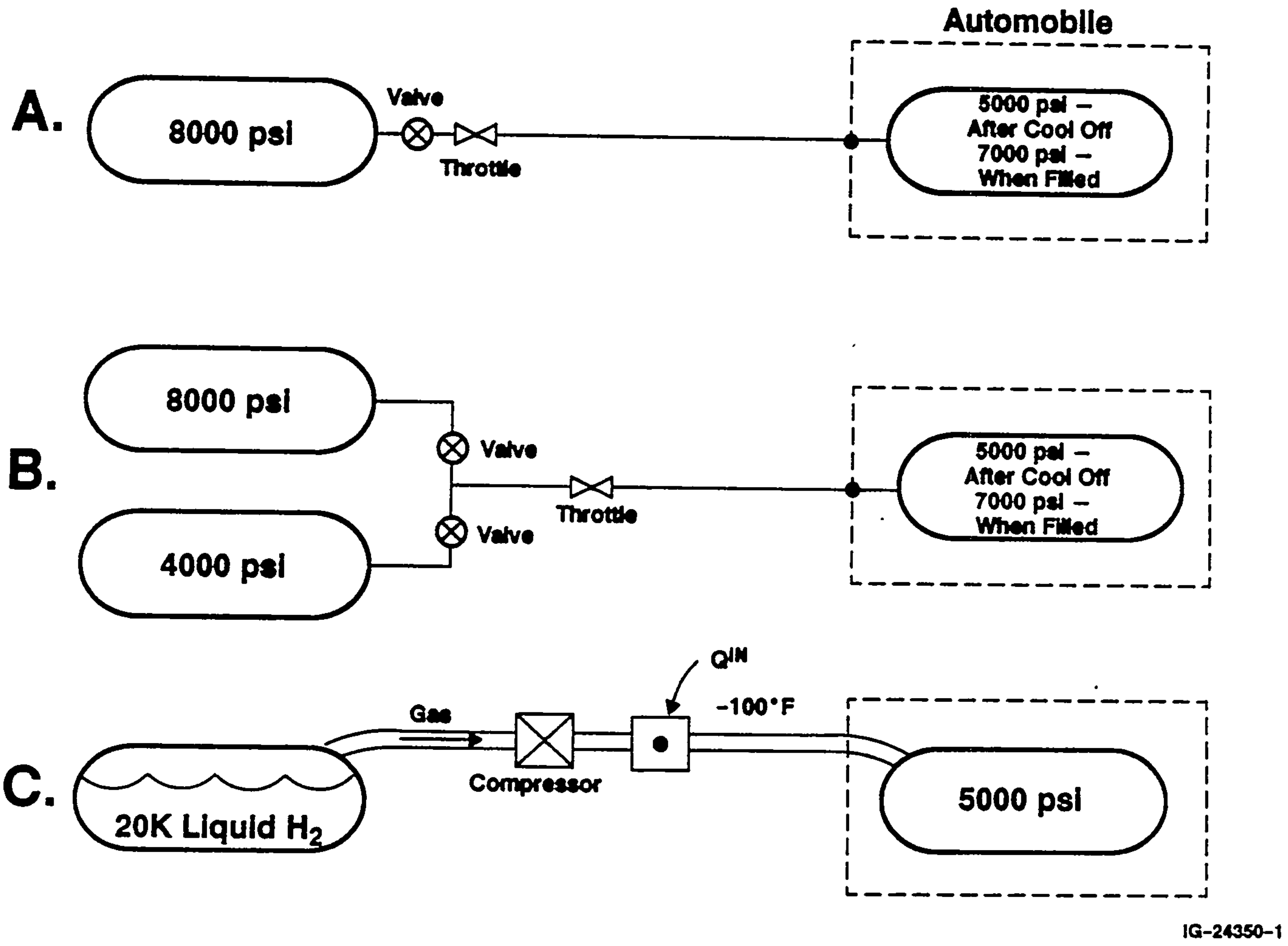
Automobile
A.
8000 psi
Valve
Throttle
5000 psi –
After Cool Off
7000 psi –
When Filled
B.
8000 psi
Valve
Throttle
Valve
4000 psi
5000 psi –
After Cool Off
7000 psi –
When Filled
C.
Q^{IN}
-100°F
Gas
Compressor
20K Liquid H_2
5000 psi
IG-24350-1

Figure 4-8. Potential Refueling Schemes for Pressurized Gas Storage Systems

4.2.7 Barriers To Commercialization

The primary barrier to the large-scale commercialization of this technology is cost. The pressure, weight, and volume requirements for effective hydrogen storage restrict vessel materials to the strongest and lightest pressure vessel overwrap fibers. The carbon fiber utilized in the pressure vessels is the primary cost driver in the hydrogen storage system. Current carbon fiber world production capacity would have to double in order to support production of 100,000 vehicles per year. Evaluation of the potential cost reductions achievable through economies of scale for carbon fibers is necessary.

The thermal issues involved in the refueling process pose some additional technical challenges. Compression heating during refueling results in a significant increase in gas temperature in the vessel, thus reducing storage efficiency. Providing an overpressure to the storage system is necessary to achieve a complete refuel within five minutes. The cost impact of a thermally-managed sub-ambient hydrogen supply needs to be investigated.

Safe operation of pressurized hydrogen storage systems must also be demonstrated. Issues of flammability due to leakage and sudden release of pressure must be dealt with in the detailed design of the system and demonstrated prior to commercial deployment and customer acceptance.

4.3 Liquid Hydrogen Storage System Concept

Liquid hydrogen storage on the vehicle has been identified as an alternative approach to pressurized gas storage, with potential advantages in both cost and volume. However, challenges posed by operational and renewable-source infrastructure considerations must be taken into account in evaluating the viability of this system. Key system performance goals are summarized in Table 4-2.

Table 4-2. Liquid Hydrogen Storage System Design Goals

Hydrogen Storage Capacity	12.5 lbs
Total Subsystem Weight	100 lbs
Total Subsystem Cost	$300
Total Volume	< 6 ft3
Mile Life	100,000 Miles
Operation	Transpare nt
Refueling Time	5 Minutes
Safety	Equivalent to Gasoline

4.3.1 System Schematic - Liquid Hydrogen

A schematic of a liquid hydrogen storage system is given in Appendix F, Figure F-6. The storage dewar is connected to the fuel cell via a manual service valve, a pressure relief valve, and a pressure regulator. A pressure switch is connected to a tank heater which may be required to boil off hydrogen gas for maximum-rate consumption.

4.3.2 Liquid Hydrogen Safety Issues

The refueling of a liquid hydrogen dewar can potentially be severely hazardous. In addition to frostbite, liquid hydrogen (20°K) can cause nitrogen and oxygen in the air to liquefy if not properly insulated and isolated. Liquid oxygen is extremely hazardous when in contact with various substances. In addition, the risk of oxygen entering a liquid hydrogen storage system is very serious.

4.3.3 Refueling of a Liquid System

Refueling a dewar is more complicated and time consuming than a pressurized gas vessel. An empty dewar will boil off significant amounts of hydrogen as it is being cooled to the temperature of liquid hydrogen. Measuring the hydrogen retained by the dewar is also difficult, particularly in the high-pressure system where the liquid/gaseous boundary can become indeterminate. Significant engineering efforts to automate the refueling process are required in order for liquid hydrogen systems to attain commercial viability.

A schematic of the proposed liquid refueling system is shown in Figure 4-9. Liquid is pumped by pressure in the reservoir or the pump, as required. A vent return line sends gas from the automobile tank back to the reservoir.

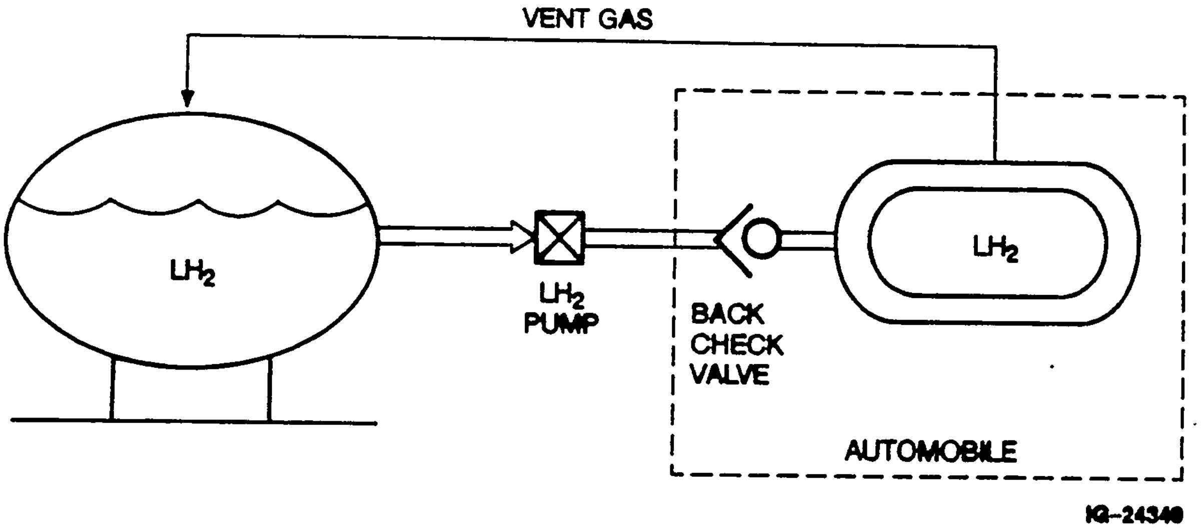

Figure 4-9. Proposed Liquid Refueling Scheme

4.3.4 Barriers To Commercialization

A number of technical challenges currently impede the wide-spread commercialization of liquid hydrogen storage systems. As heat leaks into the dewar, hydrogen gas must be vented after a "lock-down" time has elapsed to avoid bursting of the vessel; vaporization of liquid hydrogen can generate pressures as high as 20,000 psia if fully restrained to ambient temperature. Boil-off of liquid hydrogen raises several operational issues. Boil-off gas must not be directly vented due to the associated flammability hazard; this is particularly true in parking structures. The boil-off gas could be reacted in a small fuel cell, a catalytic reactor, or a combustor. Such a device has not yet been designed and demonstrated for this application.

The boil-off rates also affect the economics of liquid hydrogen storage systems. With current technology, boil-off rates of about two percent per day are achievable. This translates into a hydrogen loss of 0.25 lbs per day for a storage of 12.5 lbs. Therefore, if the vehicle were totally idle, the dewar would begin to vent after one day and would be empty in 50 days. An adequate solution to the boil-off problem would be to increase the lock down time by increasing the vent pressure of the dewar. Computational Analyses have shown that by using a vent pressure of 2000 psia, the lock down time could be increased to 80 days.

However, this would require a dewar with a substantially reinforced internal tank in order to withstand the additional pressure, thus increasing cost and complexity. Cryogenic refueling hazards and complexity also pose some serious barriers to commercialization of the on-board liquid hydrogen storage system.

4.4 Dewar Size Estimates

The volume required to store 12.5 lbs of hydrogen in liquid form is less than 3 ft^3. Based on currently available designs, this translates into an external dewar volume of about 6 ft^3, as shown in Appendix F, Figure F-7 (most of the additional 3 ft^3 required is for a vacuum void insulation jacket). Hence, a significant reduction in storage volume can be achieved with liquid hydrogen storage. A schematic of the installation for a liquid hydrogen system is shown in Figure 4-10.

Liquid dewars are operated at relatively low pressures (typically less than 150 psia). As a result, a significant cost reduction can be achieved compared to pressurized gas storage, since no high strength reinforcing materials are required for a dewar. They are typically constructed of stainless steel sheet and welded together.

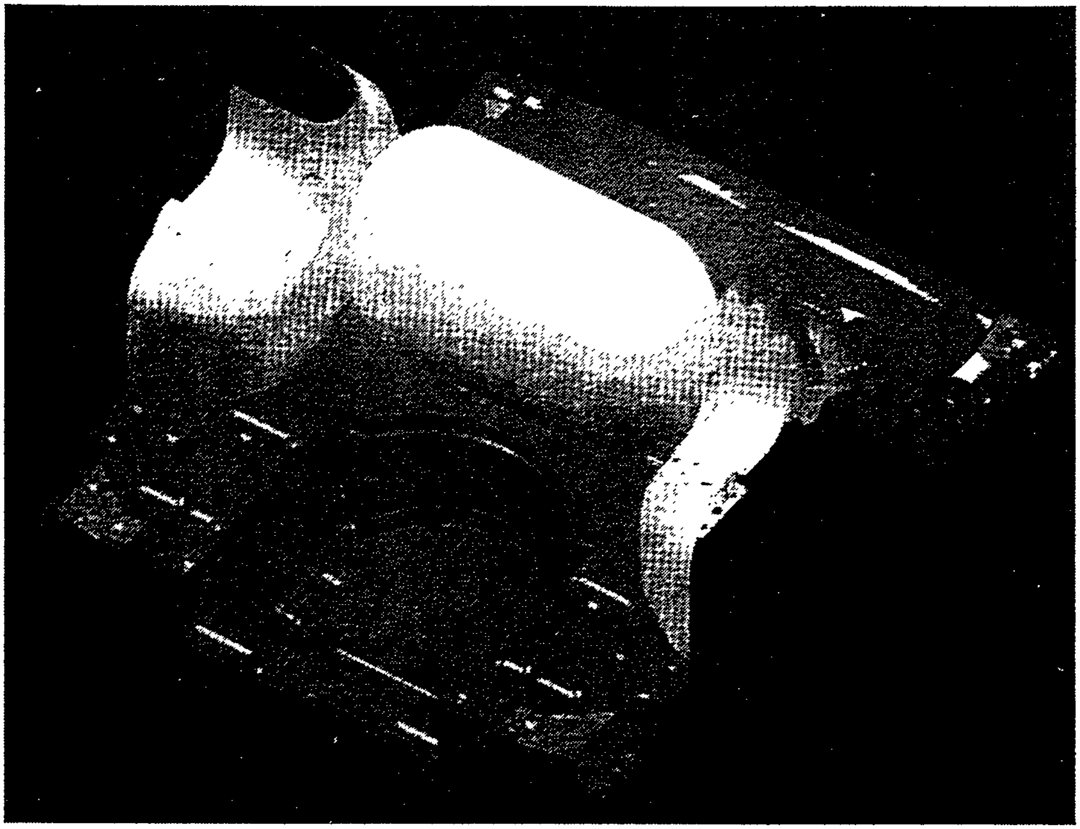

Figure 4-10. Liquid Hydrogen Installation Layout (1-Tank)

SECTION 5
LOAD LEVELING UNIT SUBSYSTEM

The Fuel Cell Stack (FCS) provides the DC Power Bus with a continuous energy source for normal operations, while the Load Leveling Unit (LLU) provides energy to supplement the FCS when transient power demands are requested. A trade study to select the LLU that is best suited for the Direct Hydrogen Fueled Proton Exchange Membrane Fuel Cell System for a Hybrid Vehicle (DPHV) system has been performed. The three technologies that were considered as candidates included the use of batteries, flywheels, and capacitors to provide the energy for transient conditions. After consideration of cost, availability, weight, and other factors, the battery technology was selected for the DPHV system.

Once the LLU power source was selected, the requirements for the electronics necessary to interface the LLU with the FCS, power bus and motor controller were defined. The requirements, circuit selection, and operation are discussed in the following paragraphs.

5.1 Load Leveling Unit Concept

The most cost effective way to realize the high efficiency and low emissions of a direct hydrogen-fueled fuel cell-powered vehicle and still retain the performance characteristics inherent in today's Internal Combustion Engine (ICE) is through the use of an auxiliary power source. This technique allows the fuel cell to provide power efficiently to the electric motor for most vehicle drive situations, while the auxiliary power source provides power to augment the fuel cell during peak vehicle load situations such as acceleration. Following these peak load periods, the auxiliary source is recharged from the fuel cell using excess power not required for the motor. As an added bonus, the auxiliary power source is available as "bootstrap" power for the fuel cell start-up.

Figure 5-1 illustrates the major components required for the operation of the LLU, the Load Leveling Controller (LLC), the chopper/regulator, and the battery pack. The key element in the successful and efficient operation of the LLU is the LLC. Although the FCS subsystem performs in a closed loop fashion for optimal efficiency for any given load, the LLC imposes that load via the chopper/regulator based on the vehicle power or battery recharge needs at any given moment. The LLC uses inputs from the power bus (current and voltage), battery State of Charge (SOC) and FCS status as the bases for its control algorithm outputs to the chopper/regulator. The controller's main control output is a duty cycle control signal to the chopper/regulator, which forces more or less average current onto the vehicle primary power bus and thus places a larger or smaller electrical load on the FCS.

The battery pack is the "leveler" part of the LLU. It stores electrical energy provided by the FCS during non-peak power modes, by the motor during regenerative braking or from an external power source when the vehicle is non-operational. The battery gives up its energy under the following conditions:

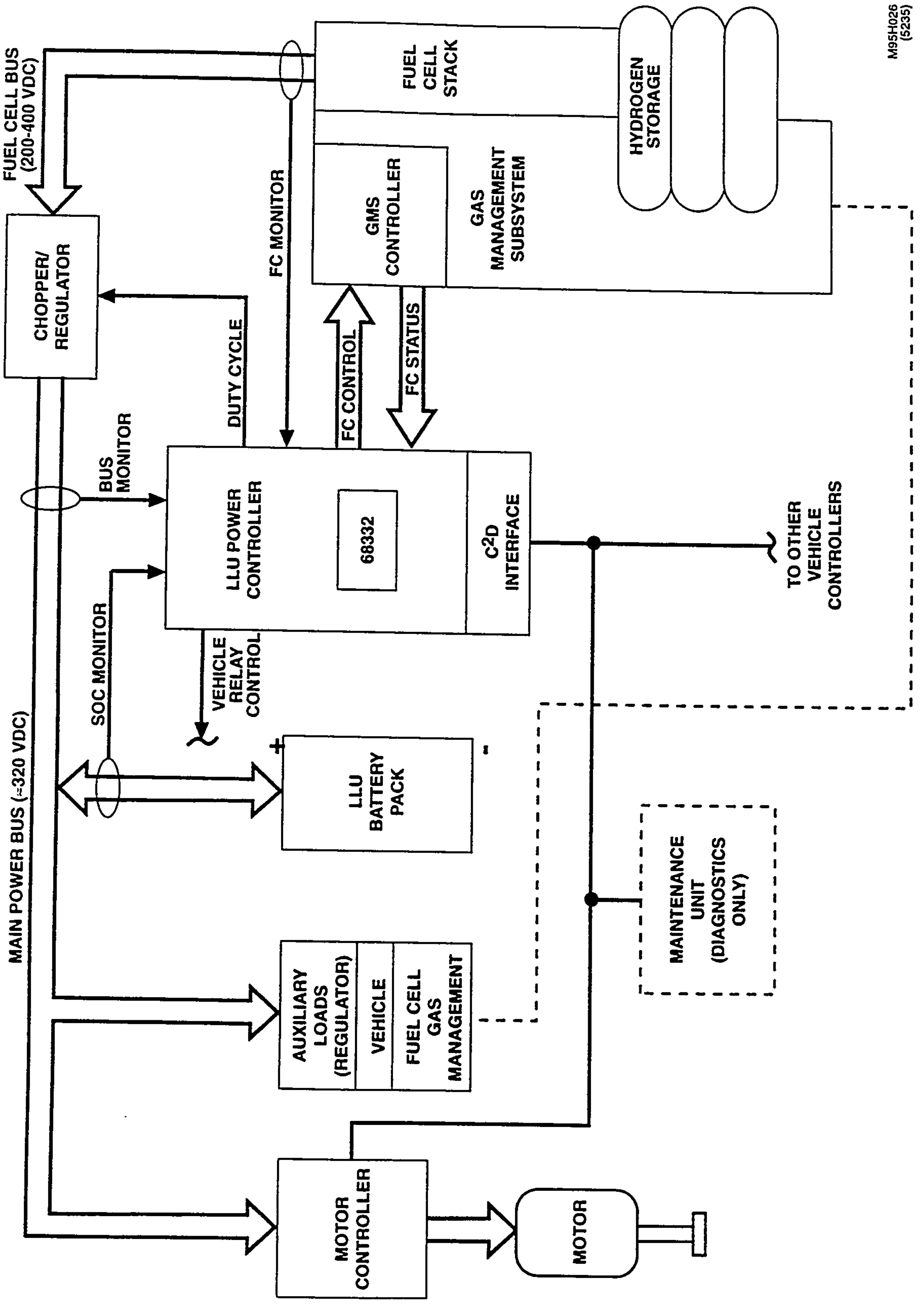
FUEL CELL BUS
(200-400 VDC)
FC MONITOR
FUEL CELL STACK
HYDROGEN STORAGE
M95H026
(5235)
GMS CONTROLLER
GAS MANAGEMENT SUBSYSTEM
CHOPPER/ REGULATOR
DUTY CYCLE
FC CONTROL
FC STATUS
BUS MONITOR
LLU POWER CONTROLLER
68332
C²D INTERFACE
TO OTHER VEHICLE CONTROLLERS
SOC MONITOR
VEHICLE RELAY CONTROL
MAIN POWER BUS (≈320 VDC)
+
-
LLU BATTERY PACK
MAINTENANCE UNIT (DIAGNOSTICS ONLY)
AUXILIARY LOADS (REGULATOR)
VEHICLE
FUEL CELL GAS MANAGEMENT
MOTOR CONTROLLER
MOTOR

Figure 5-1. LLU Component Configuration

- When FCS power is unavailable during start-up and power is required for auxiliary vehicle and FCS components.
- When the FCS is unable to provide the necessary power for required vehicle performance during peak power cycles such as rapid acceleration.

The system architecture with the batteries located directly on the motor controller power bus was chosen due to the lower impedance (60 mohm in a 320 VDC stack) and relatively constant voltage characteristics of the battery packs which are available as compared to those characteristics of the FCS subsystem. Because the battery pack repeatedly is charged and discharged during a drive cycle, impedance is critical to the vehicle's operating efficiency. Energy losses for these charge/discharge cycles are thus minimized with the battery directly on the motor controller power bus.

The FCS, with a voltage variation from 200 to 400 VDC over its load range and with a nominal impedance of 125 mohm, operates more efficiently as an average power device with its output regulated by the chopper/regulator.

5.2 LLU Subsystem Description

Because LLU operation is determined by vehicle modes of operation, an overview of LLU operation is best illustrated by a typical drive cycle. Figure 5-2 illustrates the various modes the LLU will undergo and the relationship of FCS and the LLU battery power outputs during these modes. The optimization of system performance by the LLC for each mode is critical to achievement of the overall desired efficiency (and thus vehicle range).

5.2.1 Overall System Overview

The 9 modes of system operation are shown in Table 5-1 and are described in the following pages. Each of these descriptions include the system status and a brief summary discussion of the mode.

- **System Dormant Mode (Mode 1)**

  Status:

  - FCS Power: OFF, unless supporting battery recharge
  - FCS Ancillaries: OFF, unless supporting battery recharge
  - Regeneration: None
  - Vehicle Velocity: N/A, vehicle stopped
  - Vehicle Ancillaries: Off

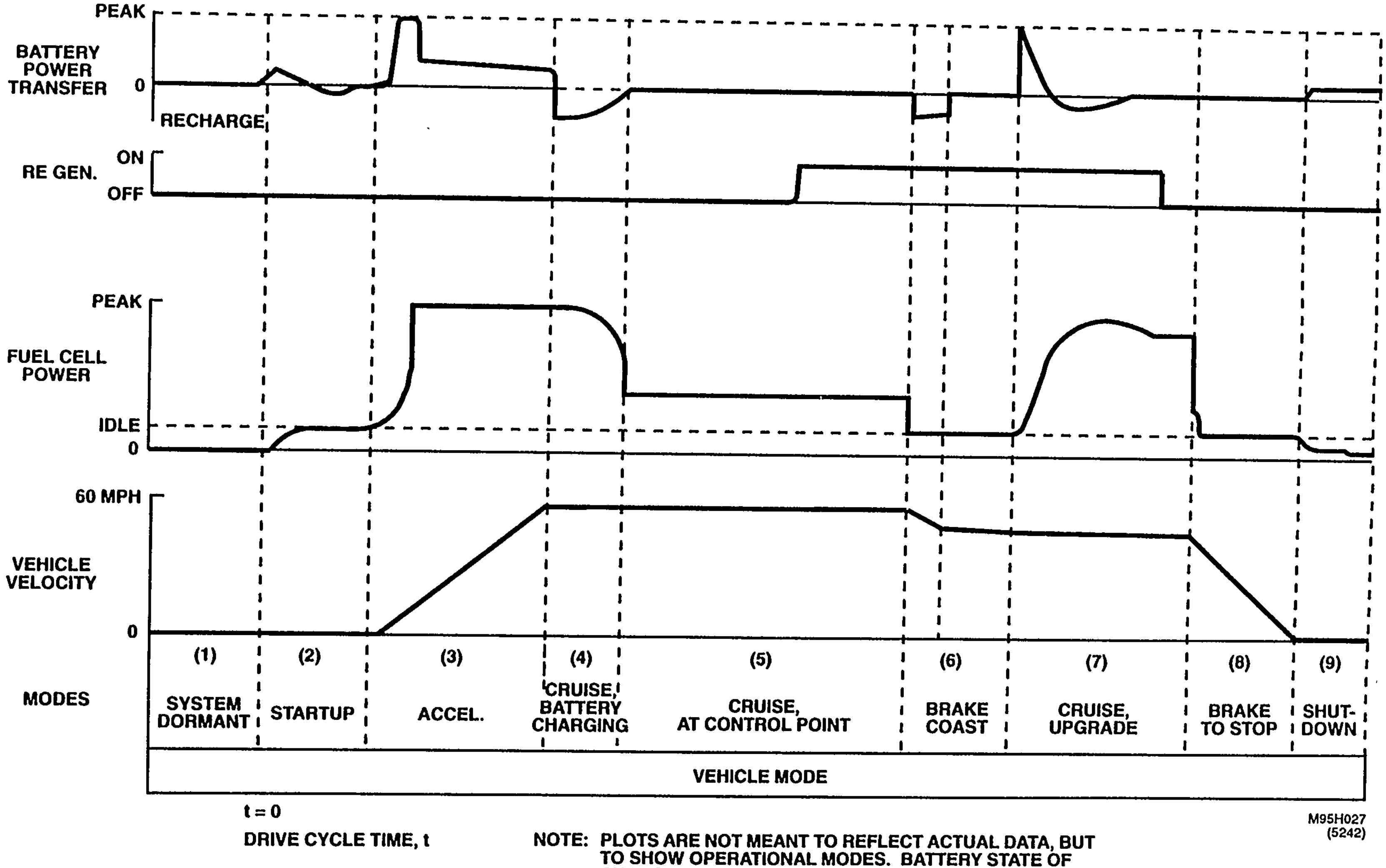

NOTE: PLOTS ARE NOT MEANT TO REFLECT ACTUAL DATA, BUT TO SHOW OPERATIONAL MODES. BATTERY STATE OF CHARGE CONTROL POINT IS APPROXIMATELY 80% SOC

M95H027
(5242)

Figure 5-2. Vehicle Operational Effects on LLU Operation

Table 5-1. DPHV Mode Description

Mode Number	Title	FCS Power	LLU Batteries
1	System Dormant	Off	Charging if source available
2	System Start-up	On	Provides power to FCS and vehicle
3	System Acceleration	Full Power	Provides power to motor as required
4	Cruise	Full Power then Cruise Power	Recharge from accelerate, then no power output
5	Cruise	On	No power output required
6	Brake, Coast	Idle	Recharge if required, receive regen brake energy
7	Cruise, Up grade	Increased Power	Provide power during FCS ramp up, then recharge, then idle.
8	Braking	Idle	Recharge from motor
9	System Shutdown	Off	Idle (assume regen braking has been manually turned off)

During this mode, the primary concerns are that the FCS subsystem is in a safe shutdown, and that the LLU battery pack be left in a SOC range so that the vehicle will be ready for the next drive cycle. Preparation for system shutdown is carried out in mode 9.

- **System Start-up (Mode 2)**

Status:

- FCS Power: On, but not yet delivered to motor
- FCS Ancillaries: On
- LLU Batteries: Providing energy to FCS and vehicle accessories
- Regeneration: N/A
- Vehicle Velocity: N/A, vehicle stopped
- Vehicle Ancillaries: On, if required.

During this mode, the FCS subsystem is beginning coolant flow, air flow, and the stack is warming up, using energy from the battery pack to run the FCS ancillary subsystems. Additionally, the battery pack may also be required to provide energy to the vehicle ancillaries such as the dome light or dashboard indicators. Built-In-Test (BIT) status will be provided to the operator during start-up.

The duration of this mode will be dependent on how much time is required before the FCS is able to provide usable power. Thirty seconds is considered the maximum acceptable time from initiation of start-up until the FCS is ready to provide power. If further testing of the FCS indicates start-up times longer than this, the battery pack, will be required to provide the additional energy thereby increasing the Ah capacity requirement of the LLU.

- **Acceleration (Mode 3)**

  Status:

  - FCS Power: Full power (worst case)
  - FCS Ancillaries: On
  - LLU Batteries: Providing “make-up” power to achieve desired acceleration
  - Regeneration: N/A
  - Vehicle Velocity: Moderate acceleration but requiring more power than the fuel cell can provide.
  - Vehicle Ancillaries: On, as required.

During this mode, the FCS may be required to provide the maximum power available, with the battery pack augmenting this power to give the desired acceleration. The LLU dictates this mix of power based on battery SOC and FCS status. The worst case for this mode is the 0 to 60 MPH acceleration in 12 seconds, which was used to determine maximum system power (and thus maximum energy requirements from the battery pack). The LLU battery pack is sized at 2.7 kWh, 60 kW peak power so that the acceleration is achieved in 12 seconds as required and the battery drops only to a SOC shown below.

$$\text{SOC} = 95\% - \frac{(60\ \text{kW} * 12/3600)}{2.7\ \text{kWh}} * 100\% = 88\%$$

assuming a 95 percent SOC at the beginning of the acceleration cycle.

Other variations on this mode are:

- The acceleration rate is lower than the maximum, in which case the FCS requires little or no energy from the LLU batteries
- The FCS is still in its start-up cycle and is not ready to provide full power when acceleration is initiated, and the batteries must provide most or all of the energy for acceleration and cruise until the FCS comes on line

- **Cruise, Battery Charging (Mode 4)**

  Status:

  - FCS Power: Cruise Power plus Battery Charging Power - decreasing as battery returns to control point
  - FCS Ancillaries: On
  - LLU Batteries: Accepting charge from FCS to return to control point state of charge
  - Regeneration: N/A
  - Vehicle Velocity: Constant
  - Vehicle Ancillaries: On, as required

  In this mode, the FCS provides the necessary power to the drive train to maintain speed. It also provides power to recharge LLU to replace energy consumed during Mode 3. The amount of recharge is determined by the LLC control algorithm which maintains the LLU state of charge at a specified level. The further the LLU is from this control point the more aggressive the charge. As the LLU returns to normal energy level, the power from the FCS approaches the cruise power level.

- **Cruise (Mode 5)**

  Status:

  - FCS Power: On at Cruise Power Level
  - FCS Ancillaries: On
  - LLU Batteries: Recharging, if required, but not providing power
  - Regeneration: N/A
  - Vehicle Velocity: Constant
  - Vehicle Ancillaries: On, as required.

  In this mode, the FCS provides the necessary power to the DC power bus. The FCS ancillaries are optimized for efficiency for that point on the fuel cell performance curve. The worst case for this mode is the Baker Grade drive cycle. Simulation models have determined a sustained requirement for almost 40 kW output from the FCS for this case. This information was used to size the FCS. The average power required for the cruise mode for normal highway conditions is expected to be in the 10-20 kW range.

- **Brake, Coast (Mode 6)**
  - FCS Power: On, idle mode
  - FCS Ancillaries: On, minimal power draw
  - LLU Batteries: Accepting Regenerative Braking Power (SOC increasing above control point)
  - Regeneration: On (if enabled) delivering energy to the battery proportional to the deceleration rate.
  - Vehicle Velocity: Decreasing
  - Vehicle Ancillaries: On, as required

  This mode represents vehicle braking followed by a no power coast. While the brake is depressed, a proportional amount of energy is recovered and directed to the battery for recharging. If the LLU was previously at the SOC control point, the SOC would increase above this point. When traction power was again needed, the LLC would allow this excess energy to be consumed prior to requesting additional power from the FCS. If the LLU remains below the control point after braking, normal operation resumes immediately upon application of traction power.

- **Cruise on Grade (Mode 7)**

  Status:

  - FCS Power: On at elevated power level
  - FCS Ancillaries: On at elevated power level
  - LLU: Provide supplemental power while FCS ramps up. Recharge after FCS assumes full power requirement
  - Regeneration: N/A
  - Vehicle Velocity: Constant
  - Vehicle Ancillaries: On, as required.

  This mode is representative of reapplication of traction power after a short term idle situation such as coast or while waiting at a stop. Initially the LLU provides supplemental power until the FCS ramps to the required power level. The FCS then provides traction power plus recharging power to return the LLU to the control point.

If the grade exceeds 8 percent, then the FCS will be incapable of supplying all the required power so the LLU will continue to provide supplemental power as required - similar to Mode 3.

- **Brake to Stop (Mode 8)**

  Status:

  - FCS Power: On in idle mode
  - FCS Ancillaries: On at minimal power
  - LLU Batteries: Recharging, if required
  - Regeneration: Disabled (for this example)
  - Vehicle Velocity: Decreasing by mechanical braking and road/zero losses
  - Vehicle Ancillaries: On as required

  This mode represents a braking action without regenerative braking. Here traction power is zero and all braking energy is dissipated as heat with no recovery. If the LLU has been providing supplemental power during Mode 7, the FCS would provide recharging energy during this mode.

- **System Shutdown (Mode 9)**

  Status:

  - FCS Power: Preparing to Power Down
  - LLU Batteries: Recharging, if required
  - Regeneration: None
  - Vehicle Velocity: Stopped
  - Vehicle Ancillaries: On until shutdown complete.

  During this mode, the GMS is performing an orderly shutdown of its FCS. Dependent on the results of further safety studies (particularly for the case of leaving a parked vehicle with the FCS running at a low idle), the system may stay on long enough to bring the LLU battery pack to full SOC and possibly to perform an equalization charge. The LLC will "supervise" this orderly shutdown and will store the last SOC measurement before it is also shut down. Safety concerns may prevent continued operation of the fuel cell after the ignition is turned off. In this case it may be necessary to recondition the LLU during periods of opportunity while driving the vehicle.

5.2.2 Battery Pack Assembly

The DPHV program will require a battery pack to supplement the energy being supplied by the PEM FCS. PEI has performed a series of computer modeling exercises, as discussed in Section 2.0, to determine the required battery pack capacity. The results of this modeling effort indicate LLU battery pack requirements as shown in Table 5-2.

Table 5-2. LLU Battery Requirements

Requirement	Value
Nominal Battery Pack Voltage	320 VDC
Minimum Operational Battery Voltage	240 VDC
Peak Battery Power (6-10 Seconds)	60 kW
Maximum Battery Energy	2.7 kWh

Additional desired characteristics include:

- Good recharge performance of less than 60 minutes from a 50 percent SOC
- High specific energy; greater than 30 Wh/kg
- High volumetric energy; greater than 80 Wh/liter
- Good peak power; greater than 0.2 kW/kg
- Availability by the third quarter of 1995

Existing batteries available for electric and/or hybrid vehicles typically target some but not all of the Table 5-2 requirements. Batteries with high peak power will not have adequate energy, those with sufficient energy will be excessively heavy, those with good recharge capabilities degrade from excessively deep discharge cycling. The "Perfect" battery is currently not available but several companies are working toward solutions to meet the hybrid electric vehicle needs.

PEI has performed a study of numerous battery technologies including the following: Lead-Acid, Nickel-Cadmium, Nickel Metal Hydride, Nickel-Iron, and Lithium Monosulfide. Although some of these technologies show promise in meeting the needs of Hybrid Vehicles their maturity of design, cost, or other limiting constraints make their use in current vehicle development prohibitive. The selection process focused not only on the battery's ability to provide pack performance to meet the requirements detailed in Table 5-2 but also on the volume, weight, and packaging flexibility. Additionally the availability of batteries for near term applications has made certain battery types and manufacturers more appealing than others.

The battery pack, implementation, battery selection, and conclusions are discussed below:

- **Battery Implementation**

  The battery pack selected will supply 320 VDC to the vehicle power bus to meet the requirements of the motor selected for this program (see Section 1.0). Most of the battery manufacturers surveyed supply their products in 2 VDC individual cells which, in most cases, are packaged into a 12 VDC module. Figure 5-3 shows the typical configuration for the battery pack and the instrumentation necessary for battery pack monitoring.

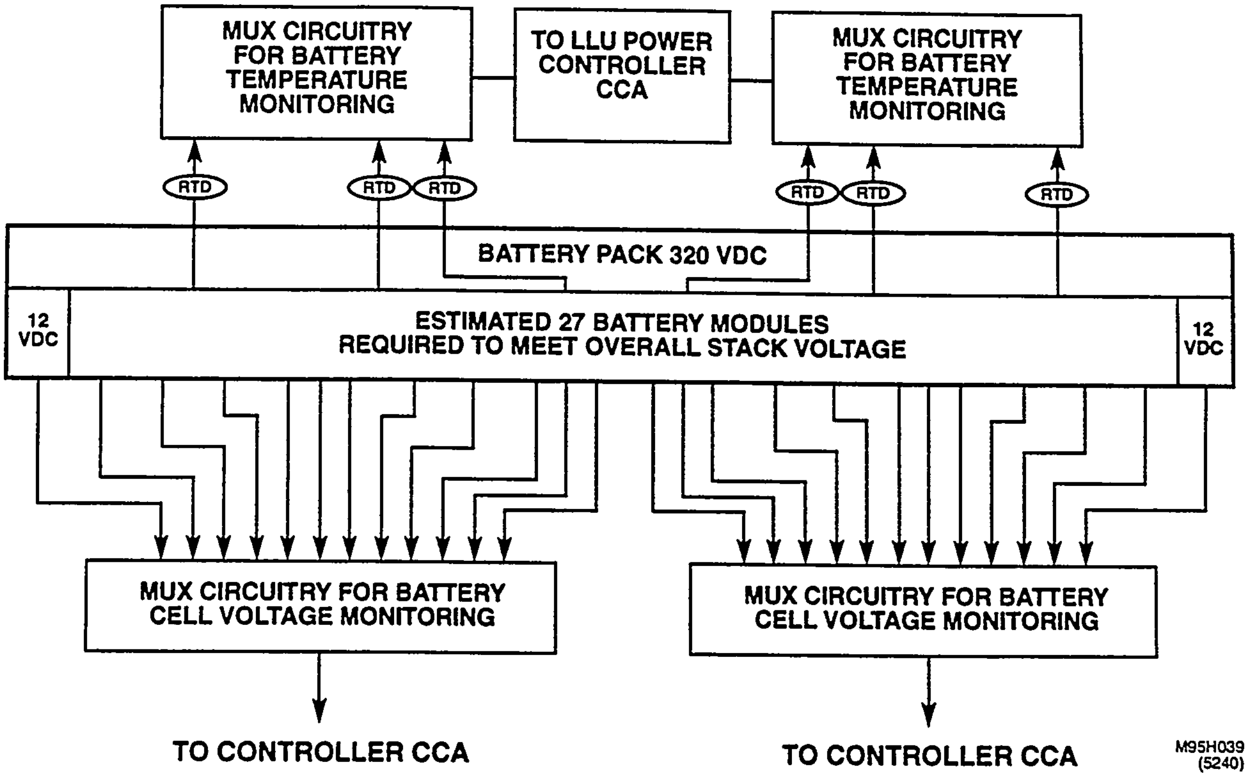
MUX CIRCUITRY FOR BATTERY TEMPERATURE MONITORING
TO LLU POWER CONTROLLER CCA
MUX CIRCUITRY FOR BATTERY TEMPERATURE MONITORING
RTD
RTD
RTD
RTD
RTD
RTD
BATTERY PACK 320 VDC
12 VDC
ESTIMATED 27 BATTERY MODULES REQUIRED TO MEET OVERALL STACK VOLTAGE
12 VDC
MUX CIRCUITRY FOR BATTERY CELL VOLTAGE MONITORING
MUX CIRCUITRY FOR BATTERY CELL VOLTAGE MONITORING
TO CONTROLLER CCA
TO CONTROLLER CCA
M95H039 (5240)

Figure 5-3. DPHV Battery Configuration for Cell and Stack Monitoring

The battery pack will be monitored at intermediate points within the pack using a simple voltage measurement scheme to determine each cell's condition and to identify any performance degradation within the pack. Temperature monitoring will be implemented within the pack using a thermistor bead configuration as shown in Figure 5-4. Additionally, the overall battery pack will be periodically returned to 100 percent SOC to avoid degradation of individual cells. This equalization cycle serves to prolong the life of the pack in the hybrid vehicle environment of repeated charge/discharge cycles.

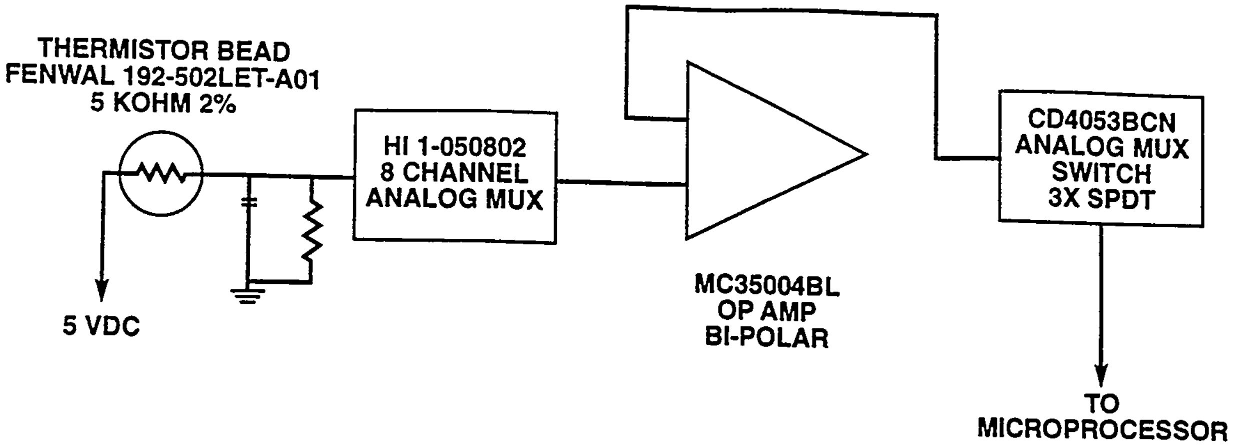

Figure 5-4. Typical Battery Temperature Sensing Circuitry

M95H043
(5240)

- **Battery Selection**

PEI's investigation has led to a focus on the Lead-Acid type batteries. Over the past few years, innovations in Lead-Acid batteries have improved energy density, power, and cycle life. Integral to these innovations has been the development of composite materials for use in the battery plate designs. In several instances companies are using a composite lead wire to form a mesh to make up the battery grid system with individual layers separated by an insulating material. Among the companies leading in these technological innovations are Electrosource and Bolder Technology.

The Bolder Technology design incorporates a spiral wound approach, Figure 5-5, and their resulting batteries are showing a high peak power output in the range of 0.8 to 1.0 kW/kg. At present they have developed a 1.2 Ah cell with an individual cell voltage of 2.0 VDC. Bolder currently has capability to supply a battery "string" consisting of four individual battery mini-stacks to provide 320 VDC at 4.8 Ah. Bolder is also working toward a 10 Ah pack design which better suits the needs of DPHV. However, this effort is currently not a high priority and requires additional research funds to promote an accelerated design effort. As Table 5-3 shows, the Bolder Battery compares very favorably to the other choices because of the high peak power capability. Additionally, the Bolder Battery is stated to be a sealed device which makes the mounting options more flexible. Availability, however, may be a problem for the current DPHV program. Bolder has indicated a mid-1995 availability for a prototype battery pack. The total output of 4.8 Ah would not be adequate for PEI to test all aspects of the vehicle drive cycles but could be used for approximately 50 percent of the testing to provide data concerning the feasibility of using this technology in its later development stages.

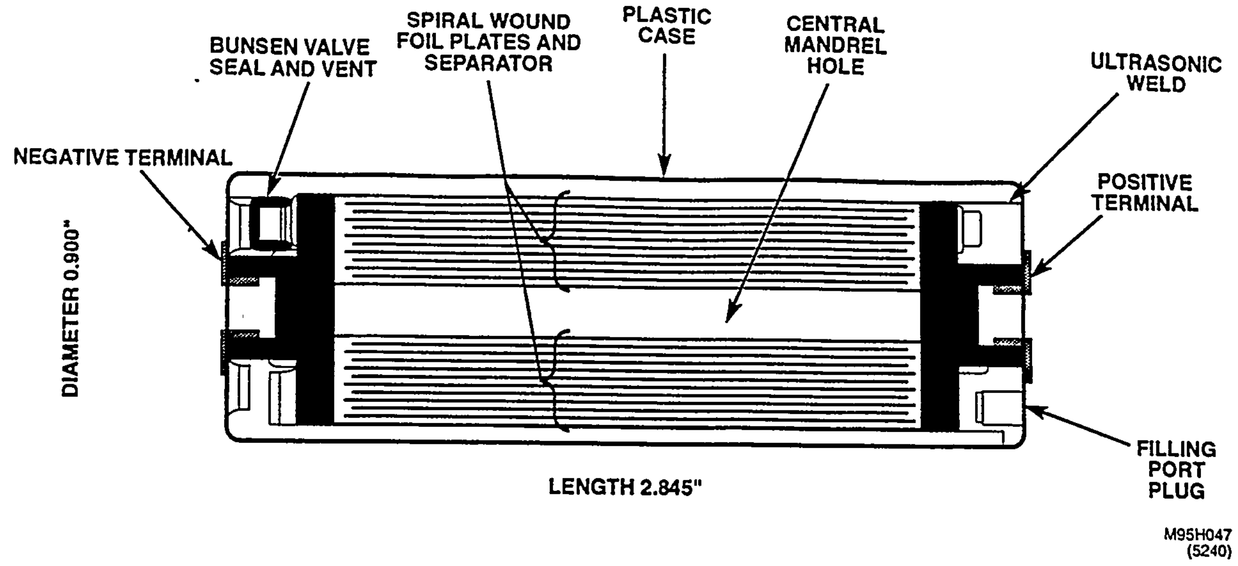
BUNSEN VALVE SEAL AND VENT
SPIRAL WOUND FOIL PLATES AND SEPARATOR
PLASTIC CASE
CENTRAL MANDREL HOLE
ULTRASONIC WELD
NEGATIVE TERMINAL
POSITIVE TERMINAL
DIAMETER 0.900"
LENGTH 2.845"
FILLING PORT PLUG
M95H047
(5240)

Figure 5-5. Bolder Spiral-Wound Battery Technology

Table 5-3. Battery Technology Comparison Trade-Off Matrix

Electric Chemistry	Nickel Cadmium	Lead Acid	Lead Acid
Source	SAFT STM5-200	Electrosource Horizon 12N85 is baseline	Boulder Technology
Specific Energy (W-hr/kg)	55	41	~ 30
Volumetric Energy (W-hr/l)	104	83.9	~ 85
Peak Power (kW/kg)	.175	.240	.8-1.0
Self-Discharge Loss		.0 03% per day @ 27 °C	< .3% per day
Price/Output ($/kW-hr)	2000	150	TBD
Reliability/Life Cycles	> 900	TBD	TBD
Impedance (Ohms)		< .0015 per 12 Volt Module	.0016 per 1.2 A-hr Cell
Mounting Orientation	Plates must be vertical	Plates must be horizontal sealed	Flexible since cells are
Overcharge Capability	Low gassing at High SOC	Thermal and gassing and life considerations	Good up to 1 Coulomb
Individual Cell Voltage	1.2 volts	2.0 volts	2.0 volts
Weakness	Very expensive	No hybrid batteries being developed currently	Not currently available
Strength	Environmentally insuitable	High energy, rapid recharge, sealed low impedence	High power density, rapid recharge, sealed, flexible mounting
Technology Maturity (10= mature)	10	8	2

The Electrosource "Horizon" battery incorporates the composite lead wire technology which is woven into grids which are then interconnected by wire to form a bipolar unit (see Figure 5-6). One grid is pasted as a positive and the other as a negative with the paste being a proprietary material which does not require hydro-setting. Electrosource currently is producing a valve regulated lead-acid battery specifically tailored for pure electric vehicle applications where higher specific energy is a critical requirement. Electrosource currently has in production their "N" series of batteries (12N95 and 12N85) with the 12N95 being the battery designed for Chrysler for the TEVan programs. The 12N85 is a second generation design using the same technology but with improvements in the case and connectors to reduce the overall size and weight of the battery pack.

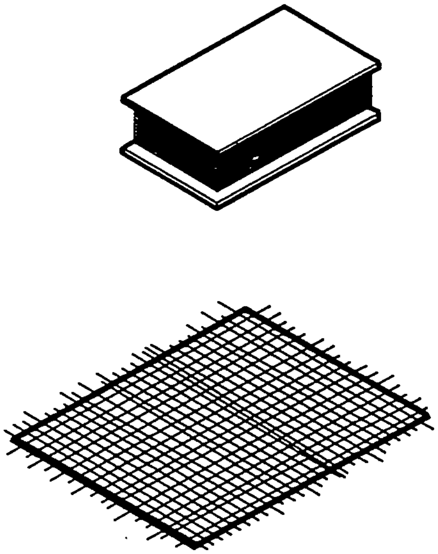

HORIZON HORIZONTAL PLATE ORIENTATION

- ELIMINATES SHEDDING OF ACTIVE MATERIAL FROM GRIDS
- ELIMINATES INTRA-PLATE ACID STRATIFICATION
- IMPROVES HEAT DISTRIBUTION
- IMPROVES OXYGEN RECOMBINATION

HIGH TENSILE STRENGTH MATERIAL STABILIZES PLATE DIMENSIONS ELIMINATING GRID GROWTH

- ALLOWS USE OF PURE LEAD OF LOW TIN CONCENTRATION ALLOYS TO MINIMIZE CHARGE GASSING AND POSITIVE PLATE CORROSION
- GLASS-FILAMENT CORE ELIMINATES NEED FOR ANTIMONY,CALCIUM OR OTHER ALLOYS TO INCREASE GRID STRENGTH
- CO-EXTRUSION OF LEAD WIRES PRODUCES EXTREMELY FINE GRAIN STRUCTURE HIGHLY RESISTANT TO GRID CORROSION

M95H062
(5244)

Figure 5-6. Electrosource "Horizon" Battery Features

Electrosource is also addressing the unique needs of Hybrid vehicles by developing their new "U" series of batteries. The "U" series is being developed to produce better peak power performance with reduced size and capacity. Electrosource is currently in a position to immediately supply their 12N85 model batteries for use during the DPHV development phase with intentions of having the "U" series available for the integration phase.

As currently configured, the Electrosource 12N85 will meet the power requirements identified for DPHV but will exceed capacity in terms of battery energy (20.4 kWh supplied versus 2.7 kWh required). This battery will also exceed the desired weight but this should not be a problem in the initial developmental phase.

The best that industry has to offer is still not the "Perfect" battery for the DPHV application. During this phase of the program, certain trade-offs will have to be made. The most critical of these trade-offs will be the ratio of energy to weight/volume. The weight of a battery stack which is currently available, with sufficient capacity to meet system requirements, will be detrimental to overall performance if implemented into the vehicle. This issue will be addressed as the program continues.

- **Conclusions**

  PEI has determined that the Electrosource "Horizon" battery will be the battery of choice during the development phase. It will be a program goal to test a battery pack from Bolder later in the program. Additionally PEI will continue to investigate the available technologies as new battery designs mature and approach a point of manufacturing viability.

5.2.3 Chopper/Regulator Assembly

Requirements for the Chopper/Regulator subsystem are shown in Table 5-4. The implementation of the design to satisfy these requirements are discussed below.

Table 5-4. Chopper/Regulator Requirements

Requirement	Value
Maximum Output Power	40 kW
Minimum Output Power	0 kW
Output Voltage	240 to 320 VDC
Input Voltage	200 to 400 VDC
Non-isolated	***
Current Regulator	***

- **Circuit Selection**

  The LLU chopper/regulator is required to supply a voltage to the bus that can be either higher or lower than the FCS output. This prevents the use of either a basic step-down or a step-up regulator only. By combining the two basic regulator circuits, a step-up/step-down configuration can be created that employs only one simple inductor. The combined configuration is shown in Figure 5-7.

- **Current Mode Control**

  The system design requires that the output current of the chopper/regulator be controlled. Current mode control methods used in typical power supplies are well suited for this application. A current request is determined by the LLC and a control voltage proportional to the required current is sent to the chopper/regulator. A simplified current control circuit is shown in Figure 5-8. When the switching device is commanded

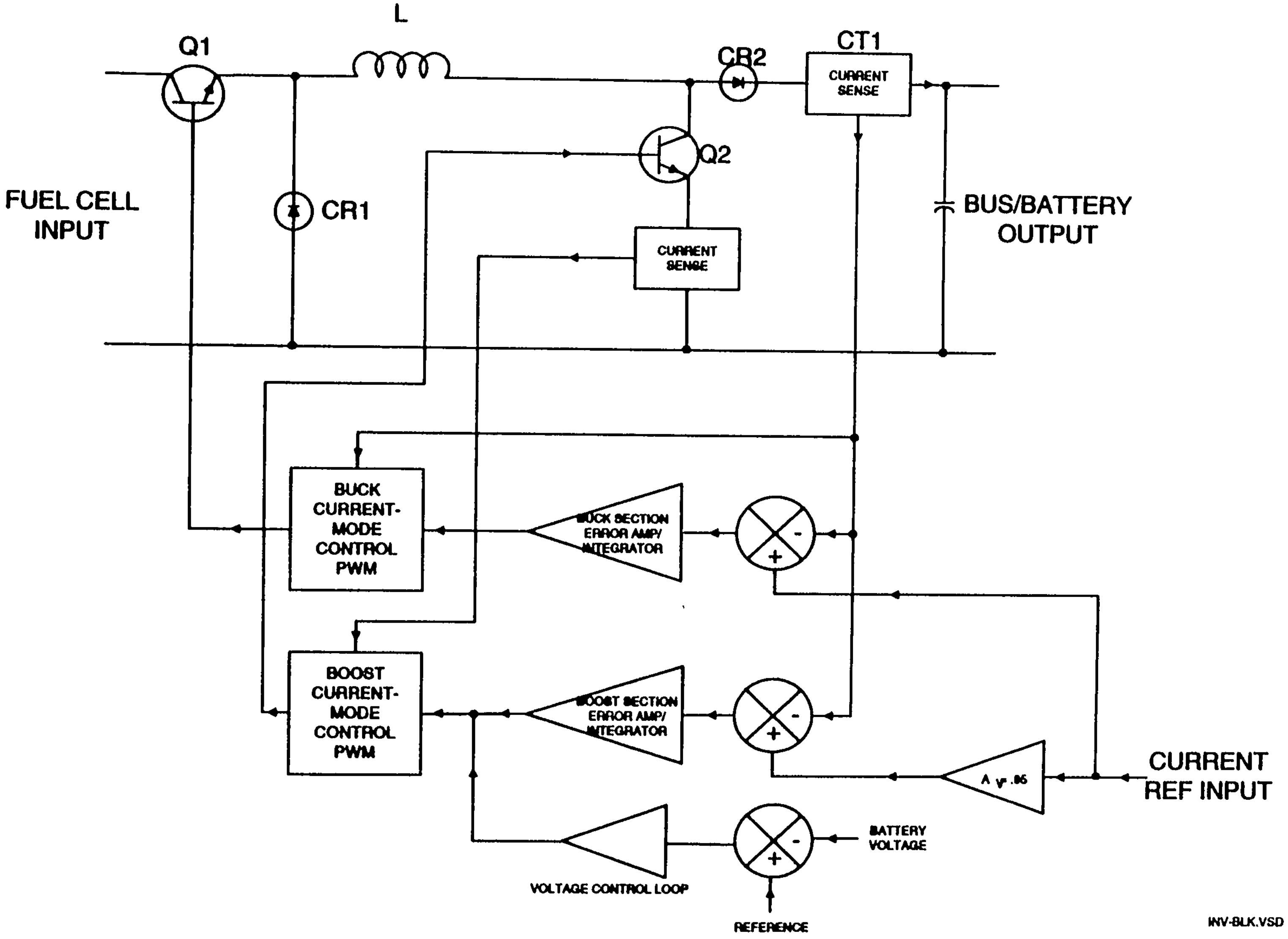
L
Q1
CR2
CT1
CURRENT SENSE
Q2
FUEL CELL INPUT
CR1
CURRENT SENSE
BUS/BATTERY OUTPUT
BUCK CURRENT-MODE CONTROL PWM
BUCK SECTION ERROR AMP/ INTEGRATOR
-
+
BOOST CURRENT-MODE CONTROL PWM
BOOST SECTION ERROR AMP/ INTEGRATOR
-
+
A v= .86
CURRENT REF INPUT
BATTERY VOLTAGE
-
+
VOLTAGE CONTROL LOOP
REFERENCE
INV-BLK.VSD

Figure 5-7. Chopper/Regulator Configuration

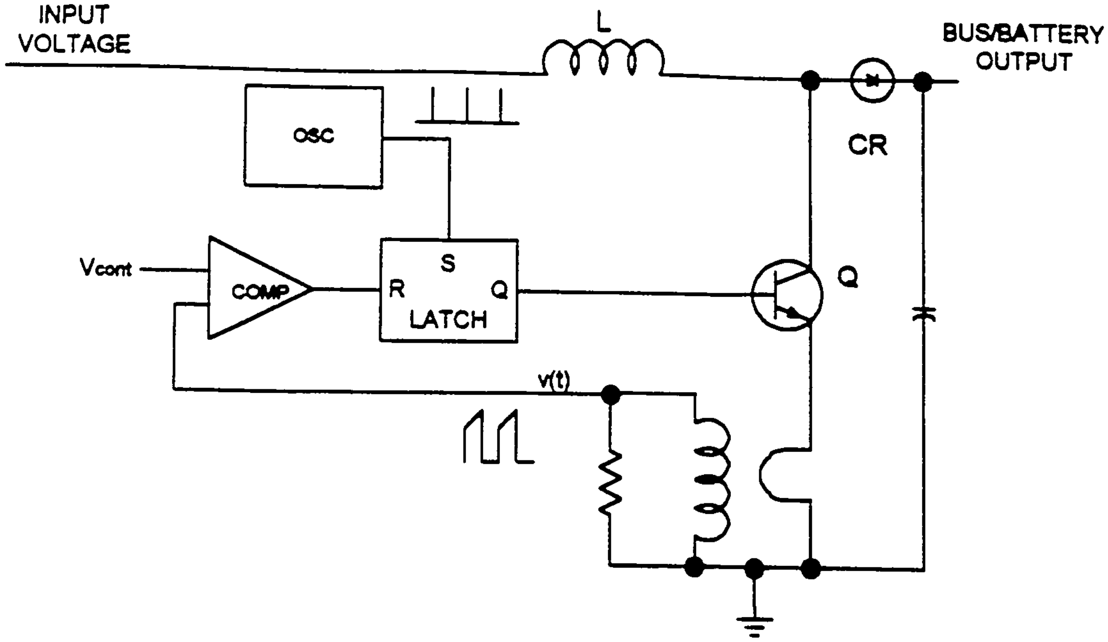

Figure 5-8. Current Control Circuit

"ON" by the oscillator, the upward ramping inductor current is monitored with a current transformer and converted to a voltage, v(t), that is a scaled replica of the inductor current.

When this voltage reaches the control voltage ,Vcont, the switching device is turned "OFF". The switching device remains "OFF" until the next oscillator pulse triggers the circuit "ON". Therefore, the control loop regulates the peak current through the switch and through the inductor. The peak current is averaged and compared to the request from the controller, and a resulting error signal is generated to provide the degree of accuracy required by the system.

Some advantages of the current mode control are:

- Excellent open-loop D.C. and dynamic line regulation result because current sources inherently reject input voltage changes.
- Automatic pulse-by-pulse current limiting.
- The inductor pole and 2nd order characteristics are eliminated, resulting in a simplified control loop. Extremely high closed loop gain-bandwidth can be safely used.

- No conditional loop stability problems exist when the effective battery capacitance changes.

- **Boost Operation**

If the output voltage to provide the requested current is greater than the fuel cell voltage, the circuit is automatically configured as a boost (step-up) regulator by circuits internal to the chopper/regulator. Specifically this is accomplished by turning the switching device Q1 "ON" for the entire time. This mode allows the output voltage to be adjusted to any value that is greater than the input. The simplified circuit for this mode is shown in Figure 5-9.

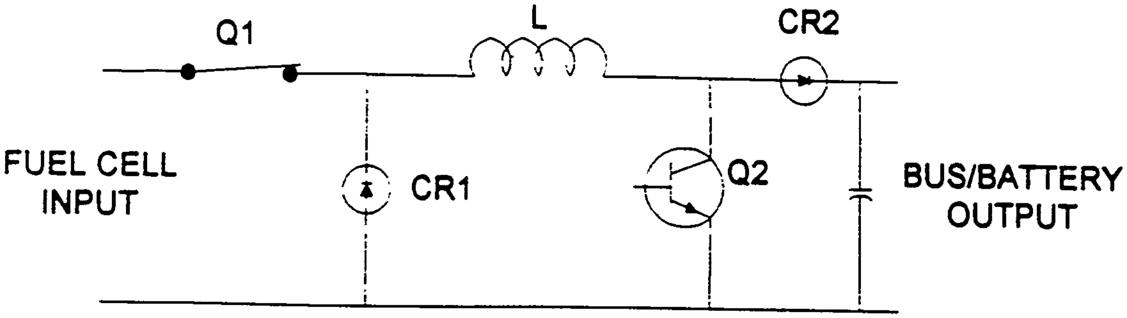

Figure 5-9. Simplified Boost Current Circuit

The circuit operation can be described as follows. When Q2 is in the "ON" state, the current in the inductor L ramps from zero current to a value:

Eq 5-1) $Il = (Vin \times ton) /L$

where ton is the time Q2 is turned "ON".

After Q2 has been on for ton seconds, Q2 is turned "OFF" and the magnetic field in the inductor will start to collapse generating a reverse voltage that forward biases diode CR2. For this design, the system operates in a discontinuous mode where the inductor current is allowed to completely decay to zero each cycle. All energy that was stored in the inductor is then transferred to the output. The output voltage becomes:

Eq 5-2) $Vout = Vin (ton/ toff) + Vin$

Equation 5-2 shows that the output is always greater than Vin and is controlled by the ratio of the ton to toff.

- **Buck Operation (Step-Down)**

If the required output voltage is less than the fuel cell voltage, the circuit is configured as a buck (step-down) regulator by inhibiting switching device Q2 "ON" for the entire time. This configuration allows the output voltage to be adjusted to any value that is less than the input. The simplified circuit for this mode is shown in Figure 5-10.

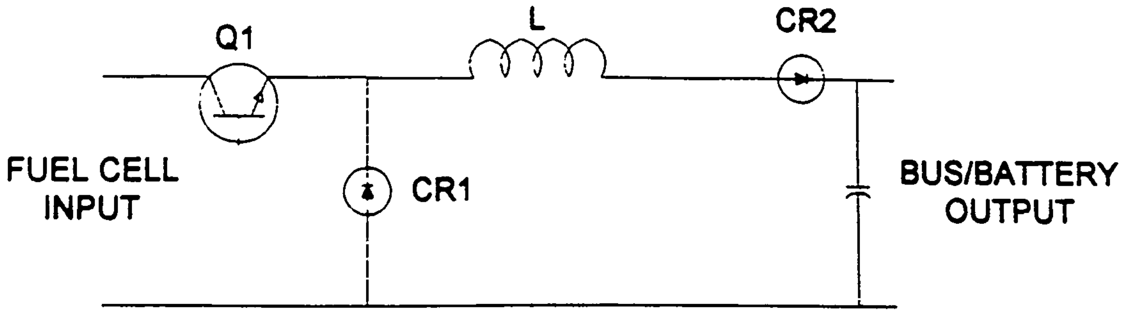

Figure 5-10. Simplified Buck Current Circuit

The circuit operation can be described as follows. Switching device Q1 provides a variable duty cycle square wave to an output filter. The filter averages the waveform and produces a DC output. When Q1 is in the "ON" state, the current in the inductor L increases to a value:

Eq 5-3) $Il = ((Vin - Vout) x\ ton) / L$

where ton is the time Q1 is turned "ON".

After Q1 has been on for ton seconds, Q1 is turned "OFF" and the magnetic field in the inductor will start to collapse generating a reverse voltage that forward biases diode CR1. The peak current will decay at a rate of Vout/L. Since the inductor is sized to not completely discharge during the cycle, the circuit operates in a continuous mode. Energy that was stored in the inductor is then transferred to the output. The output voltage becomes:

Eq 5-4) $Vout = Vin \times ton / (ton + toff)$

This equation shows that the output is always less than Vin and is controlled by the ratio of the ton to the switching period.

- **Operational Tradeoff Discussion**

Transformer isolated topologies were rejected as candidates. The application does not require input-to-output isolation, and the addition of typical transformers would decrease the efficiency by two to three percent. For a 40 kW throughput power, this would result in an additional 800 to 1200 watts to be dissipated by the thermal management system. Three non-isolated topologies were compared to determine the optimum choice for this application. The three methods were:

1) Non-isolated flyback type – This type is capable of both step-up and step-down operation as required by the application, but develops negative output voltages. To use this circuit would require that the fuel cell return be connected to the positive terminal of the battery.

   Major advantages – simple control circuit; inherently power limited.

   Major disadvantages – right half plane zero, difficult to compensate for all required operating conditions; negative output voltage.

2) Combined step-up/step-down, single controller – The basic circuit connections are shown in Figure 5-8. However, it is possible to use a single controller to simultaneously modulate both switching devices.

   Major advantage – simple single control circuit; Since a switching device is in series with Vout, current limiting can easily be implemented.

   Major disadvantages – Two switching devices operating simultaneously doubles switching losses. While this is not a problem for low input voltages (< 50 VDC), it becomes a major power loss for this application since the input voltage is 200 to 400 VDC.

3) Combined step-up/step-down, dual controllers – The basic circuit is shown in Figure 5-7. Two separate controllers are use, one for the buck section and one for the boost.

   Major advantage – Since a switching device is in series with Vout, current limiting can easily be implemented. Unlike the configuration discussed in 2) above, only one power switch is modulated at any one time. Switching losses (a serious problem for high input voltages) are limited to one device.

   Major disadvantages – Requires two separate control circuits. Requires additional low level circuits to determine when to configure as a buck or a boost circuit.

The combined step-up/step-down topology discussed in 3) above has been chosen for implementation. The disadvantage discussed for this method does increase the control electronics. However, the cost of these small signal devices is insignificant compared to the reduction in switching losses. The higher losses would reduce the reliability of the power devices, and also result in increased heatsink and thermal management costs. Design considerations for the chopper/regulator are discussed in Appendix A.

5.2.4 Power Controller

The LLC will be a microprocessor based system used to monitor and control the energy system of the DPHV project. Requirements for the LLC are described in the following pages.

The LLC will have the following capabilities:

a) Regulate chopper power via an analog output

b) Maintain battery environment

c) Maintain communication with controllers on the Chrysler Collision Detection (CCD) bus

d) Optimize GMS control as defined and matured during the test phase

e) Control and report on the prognostic and diagnostic activity for the Energy Control System

f) Process computations of critical data relating to control algorithms

g) Monitor the chopper/regulator status via a discrete input

- **LLC Implementation**

  The PEI controller approach is based upon utilizing a previous processor design with some modifications for the DPHV project. This design includes a Motorola MC68332 micro-controller, a 32-bit integrated micro-controller which combines high-performance data manipulation capabilities with powerful peripheral subsystems. The MC68332 features fully static, high-speed complementary metal-oxide semiconductor (CMOS) technology. Based upon the 68020 CPU32 instruction set, the MC68332 provides enhanced system performance and utilizes the extensive software base for the Motorola family of processors (see Figure 5-11 for the MC68332 block diagram).

  The MC68332 contains intelligent peripheral modules such as the Time Processor Unit (TPU), which provides 16 microcoded channels for performing time related activities ranging from simple input capture to complex motor control. High-speed serial communications are provided by the Queued Serial Module (QSM) with synchronous and asynchronous protocols available. Two kilobytes of fully static standby Random Access Memory (RAM) allow fast two-cycle access for system and data stacks and vari-

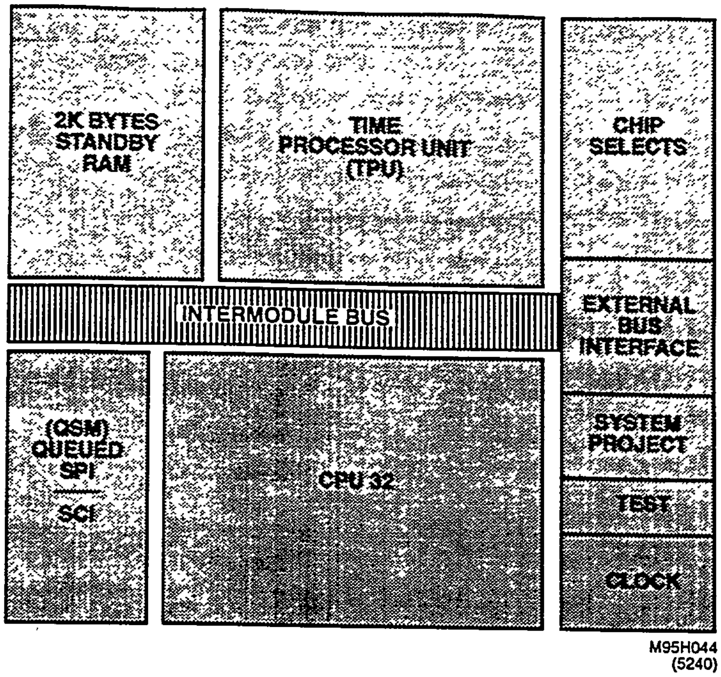
2K BYTES STANDBY RAM
TIME PROCESSOR UNIT (TPU)
CHIP SELECTS
INTERMODULE BUS
EXTERNAL BUS INTERFACE
(QSM) QUEUED SPI
SCI
CPU 32
SYSTEM PROJECT
TEST
CLOCK
M95H044
(5240)

Figure 5-11. MC68332 Block Diagram

able storage with provision for battery backup. Twelve chip selects enhance system integration for fast external memory or peripheral access. These modules are connected on-chip via the Inter-Module Bus (IMB).

The LLC will provide the integrated monitoring and control of the energy system for the DPHV project. See the tables in Appendix B for the Input/Output definition details. Data is gathered from analog and discrete measurements. The LLC will use this data to control a wide range of battery-related functions such as heating and cooling. The LLC will monitor and regulate the power delivered to motor bus from the FCS. Power regulation will be accomplished by supplying an analog input to the chopper/regulator and by supplying an analog signal to the GMS feed forward input. This regulation is based upon battery conditions (SOC and temperature), current, and anticipated motor bus requirements with the operational goal being to provide smooth peak power surges in the most efficient manner possible.

Another goal is to recoup, conserve, and optimize energy usage to obtain the 380 mile range goal and to insure long battery life.

The following are some processing items and relationships that must be considered to achieve our overall system goals.

a) Open Circuit Pack Voltage vs State of Charge

b) Pack Voltage vs Rate of Discharge

c) Cell Capacity vs Cell Temperature

d) Specific Energy vs Specific Power Performance

e) Cell Impedance vs State of Charge

f) Stand Loss Characteristics

g) Optimized Charging Algorithm for the Selected Batteries

h) Optimized Methods of State of Charge Determination

i) Optimization of Fuel Cell power request

j) Optimized Methods of anticipating power needs

k) Controlling the fuel cell feed forward airflow

It is anticipated that significant fuel stack testing will be required before the control algorithms are fully optimized.

The LLC will be designed to provide the following functionality:

1. Determine the Battery SOC based on a number of critical parameters such as Battery Amp Hour Capacity, the current total number of Amp Hours discharged from the battery, and Amp Hours provided by regeneration or the FCS subsystem.
2. Measure total pack voltage.
3. Measure individual module voltage.
4. Measure battery charge and discharge currents.
5. Supervise all charging activities based on a unique algorithm for the specific battery used.
6. Determine battery capacity.
7. Determine battery impedance.
8. Maintain the battery thermal environment during charging if required.
9. Maintain the battery environment within prescribed limits.
10. Supervise a ventilation system to control the accumulation of battery gases if required.

11. Maintain communications with the Motor Controller and other off-board monitoring devices (i.e. Maintenance Unit [MU] or Data Acquisition System [DAS]).
12. Maintain and regulate requested power from the GMS via the chopper/regulator and feed forward signal. The requested power will be based upon SOC of the battery pack. This will be a linear algorithm since the power requested is interpolated linearly between two SOC endpoints.
13. Provide runtime error detection and reporting. This shall be accomplished using an error prioritization method. The system would be shutdown upon detecting a fatal error.
14. Provide Diagnostics of the LLC.

Software has been written and verified on a prototype system to maintain the battery environment, communicate with other controllers, and process computations of some critical data. The balance of software will be written to complete the functionality discussed above. This software will utilize a mixture of C and 68332 Assembly as appropriate and the RXTC Operating System (OS).

5.3 DTC Considerations for LLU

From the onset of the DPHV program, the realization of a vehicle which is cost competitive with existing ICE-powered vehicles has been considered critical to program success. Each major component of the system is being selected or designed with attention to the following factors:

1) Present performance and cost
2) Eventual production cost
3) Obstacles to be overcome or technology which must be advanced prior to the commercial production of a viable system.

The LLU items being considered for DTC purposes include:

1) LLU Power Controller CCA: This includes the Circuit Card Assembly (CCA) on which the microprocessor, memory and signal conditioner, and serial bus interface circuity reside.
2) Battery Pack: This includes the batteries, the tray or enclosure, any venting or forced air accessories, and temperature or voltage transducers.
3) Chopper/Regulator: Includes the CCA and any chassis mounted components related to performance of this circuit.

4) Packaging and Interconnects: Includes housing, cables, relays, heat sinks, and special cooling components, if required.

DTC considerations for each of these items are discussed below.

- **LLU Power Controller**

  The cost improvements for production will come primarily from the consolidation of functions into fewer components through hybridization or incorporation of functions into Application Specific Integrated Circuits (ASICs). Also as the development program progresses and control of the system is optimized, it may be possible to reduce the circuitry implemented in the development LLC and thus reduce the cost.

- **Battery Pack**

  Major technology and producibility improvements are needed in this area to meet the overall DTC cost goals for the system. Present battery systems for electric vehicles are designed for high specific energy so that range can be maximized. Requirements for this and other hybrid vehicle systems force battery developers toward high peak power, reasonable energy density, and light weight. Although there is a market in the portable power tool industry for this type of battery, the vehicle market is new for this area of development. The battery industry, however, is accelerating development and when the market matures, there should be significant cost reductions. Other items within the battery pack such as transducers, packaging, and cooling accessories are fairly mature technologies and will not see much cost improvement.

- **Chopper/Regulator**

  The major cost drivers for this circuitry are the high current carrying components such as the chopper transistors, diodes, and the inductor. These must be high current and high voltage devices. There is still some room for maturity in the Isolated Gate Bipolar Transistor (IGBT) technology, the selected switching devices for the development phase and a chance for breakthroughs in fabrication techniques for these devices is possible. Otherwise, one would expect only the reductions due to the broader market and higher production quantities brought about by the proliferation of these devices to the automotive market. Presently they are primarily used in stationary power switching stations in industrial applications.

- **Packaging and Interconnects**

  There are no known technology-driven items in this category which will benefit cost as component technology matures. The key to optimization of cost is to apply a strict DTC program to the design of the LLU enclosure and interconnects at the onset of the program and to keep production cost as a major factor in design decisions.

- **DTC Status**

Previous DTC estimates lumped the chopper/regulator and the LLC together and the packaging and interconnect elements were not broken out separately. In the future, these will be tracked as separate items as shown in Appendix D. The area of chief interest for the LLU is the battery pack. Technology advancements in the high power/ lightweight battery area is required before the needed drastic cost reductions can be obtained. Ultracapacitors are a possible replacement for the battery pack if the technology advancement/cost reduction progress is more rapid in this area. Both technologies will be tracked carefully through the course of the DPHV program for any advancements which may help the DTC effort.

SECTION 6
POWER TRAIN REQUIREMENTS

The power train for the DPHV will consist of a three-phase AC motor with its associated motor controller. This motor is spray oil-cooled. Vector control techniques are used for precise torque generation and exact matching of field to motor capability. The motor controller is powered by a nominal DC voltage of 324 VDC with an operational voltage range from 120 to 400 VDC.

The output torque from this motor is coupled to the wheels via a fixed speed reduction gear subsystem with a gear ratio of 9.34. Table 6-1 shows the design parameters for this motor.

Table 6-1. Westinghouse 3-Phase AC Induction Motor Design Characteristics

Full Load Parameter	Value
Rated Voltage (Leg-to-Leg)	160.0
Rated Voltage (Leg-to-Neutral)	92.38
Slip	1.5 %
RPM	8220
Power Factor	89 %
Rated Torque	123
Breakdown Torque	310
Rated Current	245
Efficiency	90.6 % (Minimum)
HP at 11000 RPM	56.0

6.1 Motor Operating Characteristics

Table 6-2 shows the full operating characteristics for the Westinghouse motor (NS308 MAC). The data shows the motor efficiency at various speed and load points (not all data points are shown in this table). At each RPM point, several electric motor output torques and powers are measured. The power into the motor and motor controller (labelled as Battery HP) is also measured. The efficiency of the motor and controller is then calculated from the ratio of the shaft HP to the Battery HP.

Table 6-2. Westinghouse Motor Operating Characteristics

RPM	In-lb	Shaft HP	Battery HP	Efficiency (%)
1026	3.1	0	0.4	14.0
1034	470.2	7.7	9.9	78.1
1048	973.1	16.2	20.4	79.2
1058	1491.3	25.0	32.5	77.0
1066	1970.5	33.3	44.7	74.5
2043	78.7	2.5	3.2	78.8
2051	471.8	15.4	17.8	86.2

Table 6-2. Westinghouse Motor Operating Characteristics (Continued)

RPM	In-lb	Shaft HP	Battery HP	Efficiency (%)
2062	1234.9	40.4	46.5	86.9
2075	1766.2	58.1	68.2	85.2
2080	1876.7	65.3	77.3	84.4
3039	104.4	5.0	6.1	93.2
3048	713.6	34.5	38.2	90.3
3057	970.8	47.1	52.0	90.5
3067	1502.7	73.2	81.6	89.6
3076	1977.3	96.5	109.5	88.2
4026	25.7	1.6	2.2	73.3
4031	428.0	27.4	30.3	90.5
4046	928.1	59.6	64.6	92.3
4057	1567.7	100.9	112.4	89.8
4061	1703.0	109.8	124.1	88.5
5037	45.4	3.6	4.6	78.3
5055	103.1	8.3	9.8	84.7
5061	880.9	70.8	77.3	91.5
5068	1243.1	100.0	113.8	87.9
6024	86.1	8.2	9.8	84.1
6030	324.4	31.0	34.4	90.3
6045	740.8	71.1	78.8	90.2
6053	8963.3	92.6	105.6	87.6
7060	8.5	1.0	1.7	55.0
7064	40.3	4.5	5.7	78.8
7070	276.7	31.1	33.9	91.5
7079	403.7	45.4	49.6	91.5
7088	617.6	69.5	78.0	89.1
7096	836.3	94.2	112.0	84.1
8056	23.8	3.0	4.2	72.3
8062	72.2	9.2	11.0	84.2
8068	237.0	30.3	32.5	83.3
8081	432.5	55.5	61.9	89.6
8089	591.2	75.0	87.5	86.7
8091	662.7	85.1	103.2	82.5
9037	24.7	3.5	4.7	75.2
9042	69.3	9.9	11.6	86.4
9048	211.4	30.4	33.1	91.8
9060	385.2	55.4	61.6	89.9
9069	515.1	74.1	88.3	83.9
10083	16.8	2.7	5.2	51.2
10092	78.2	12.5	13.6	92.3
10098	265.1	42.5	46.3	91.9
10104	377.6	60.6	69.9	86.7

SECTION 7
AUXILIARY SUBSYSTEM REQUIREMENTS

Three major subsystems comprise the auxiliary vehicle subsystem. These subsystems are the heating/cooling, regenerative braking and the electrical power, steering subsystems.

7.1 Heating/Cooling Subsystem Design

The goal for the design of the heating/cooling subsystem is to develop a heat pump system which will both heat and cool the interior of the vehicle.

System components include two refrigerant coils, one inside the HVAC subsystem and one in the motor compartment, an electric motor-driven compressor operating on 320 VDC, a combination expansion valve and receiver/drier which allows for bi-directional refrigerant flow (a new invention from Liberty and Technical Affairs), a four-way valve which controls the direction of refrigerant flow to put the system in the heating or cooling mode and a 134A refrigerant. The refrigerant, 134A, essentially is pure 1,1,1,2-tetrafluoroethane, commonly known as HFC-134A. This HVAC subsystem is designed to have power requirements between 3 and 5 kW. Figure 7-1 shows the HVAC heat pump refrigerant circuit diagram for this design.

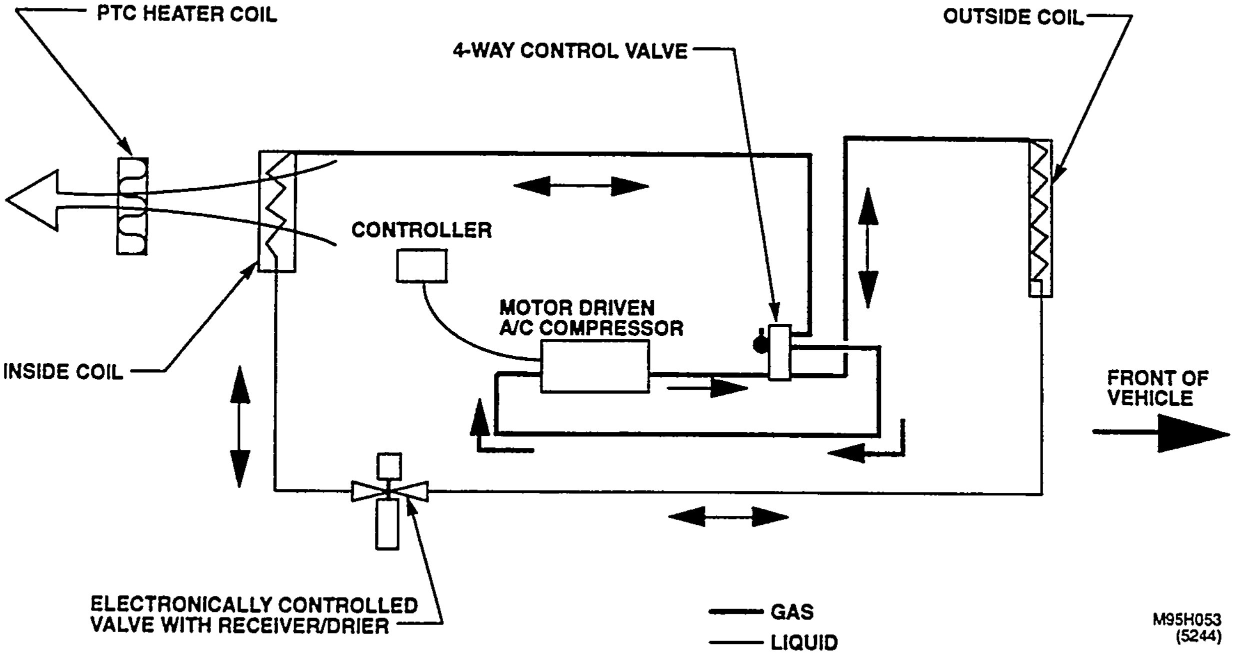
PTC HEATER COIL
OUTSIDE COIL
4-WAY CONTROL VALVE
CONTROLLER
MOTOR DRIVEN A/C COMPRESSOR
INSIDE COIL
FRONT OF VEHICLE
ELECTRONICALLY CONTROLLED VALVE WITH RECEIVER/DRIER
GAS
LIQUID
M95H053 (5244)

Figure 7-1. HVAC Refrigerant Circuit Diagram

The benefits of the HVAC design are to satisfy the customer's heating and cooling expectations while minimizing system energy usage. The heat pump system may be used in conjunction with PTC ceramic heaters to meet the federal defroster performance standard, MVSS-103.

The heat pump system has demonstrated heating capability at 5°F with a coefficient of performance of 1.5 (less than 2.0 is desirable) at the Valeo test laboratory.

7.1.1 Auxiliary Subsystem Power Allocation

Table 7-1 shows the auxiliary subsystem power and weight allocations.

Table 7-1. HVAC Subsystem Allocations

Component	Max imum Power (kW)	Supply Voltage (VDC)	Mass (kg)
Compressor	2.0	320	2.5
Condensor	N/A	2.4	
Evaporator	(5.23 Capacity)	1.8	
Heater HEX/Collector	(10.5 Capacity)	5.0	
Coolant Fan	2.0	2.0	
Heater Blower Fan	0.25	320	1.8
Expansion Valve	N/A	320	0.5
Actuators (2)	0.05	320	1.0
Ducts/Fasteners	N/A	10.0	
Seals	N/A	1.5	
Hoses/Fittings	N/A	2.4	
Controller	0.01	320	0.2
Total	**4.36**		**31.1**

7.2 Regenerative Braking Subsystem

The regenerative braking subsystem is designed and developed by AlliedSignal Automotive. The purpose for this subsystem is to maximize energy recovery during vehicle deceleration. The design incorporates antilock braking and traction control functions into the base braking system. This design provides a seamless transition between regenerative and friction braking. The subsystem design provides a brake-by-wire feature with dual system pedal actuated hydraulic brakes for fail-safe operation in case of electrical failure. Figure 7-2 shows the overall subsystem configuration.

Electrical specifications for the regenerative braking subsystem include operation on a 12 VDC voltage input, a periodic peak power draw of 0.42 kW, and an average power draw of 70 W.

7.3 Electrical Power Steering (EPS) Subsystem

The EPS subsystem is designed and developed by TRW. This subsystem operates on 320 VDC with maximum power requirements less than 1 kW in stall conditions. The design is a natural solution for electric vehicle power steering applications.

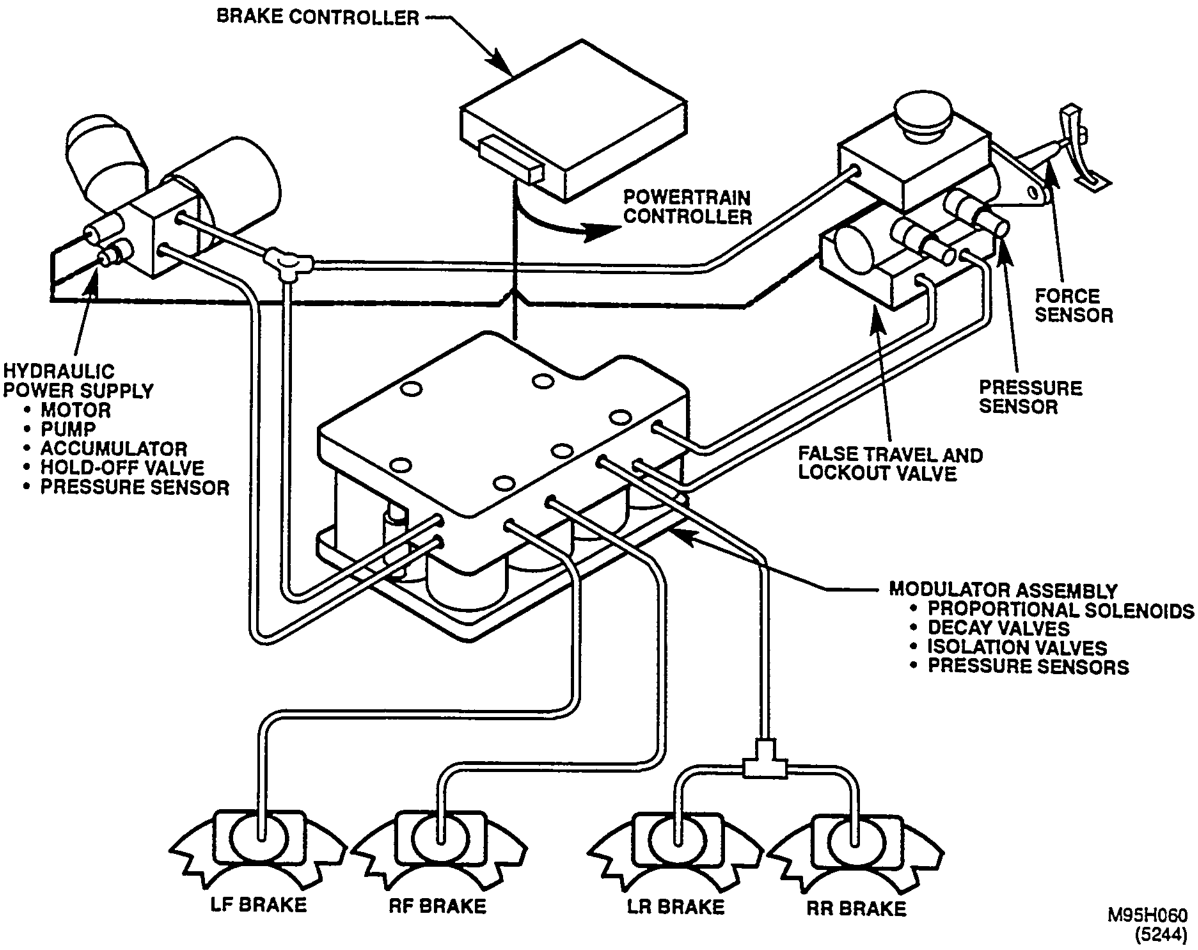
BRAKE CONTROLLER
POWERTRAIN CONTROLLER
HYDRAULIC POWER SUPPLY
• MOTOR
• PUMP
• ACCUMULATOR
• HOLD-OFF VALVE
• PRESSURE SENSOR
FORCE SENSOR
PRESSURE SENSOR
FALSE TRAVEL AND LOCKOUT VALVE
MODULATOR ASSEMBLY
• PROPORTIONAL SOLENOIDS
• DECAY VALVES
• ISOLATION VALVES
• PRESSURE SENSORS
LF BRAKE
RF BRAKE
LR BRAKE
RR BRAKE
M95H060
(5244)

Figure 7-2. Regenerative Braking Subsystem Configuration

The EPS is shown in Figure 7-3. This subsystem has been designed, developed, manufactured, and tested as a complete system. The subsystem provides an energy efficient operation which only uses power when steering is required. Fuel savings up to 0.6 mpg have been achieved on Internal Combustion Engine (ICE) vehicles. Steering subsystem operations have been shown to provide superior dynamic response since the EPS is highly programmable in response to torque, speed, and steer rate.

The design provides better optimization of assist, yaw stability, center feel, and returnability. Interaction of this subsystem with other chassis functions is possible.

Steering assist is available when the motor is not running with a possible 2200 lbs of rack force available. On-board diagnostics are available with better fault detection than conventional systems.

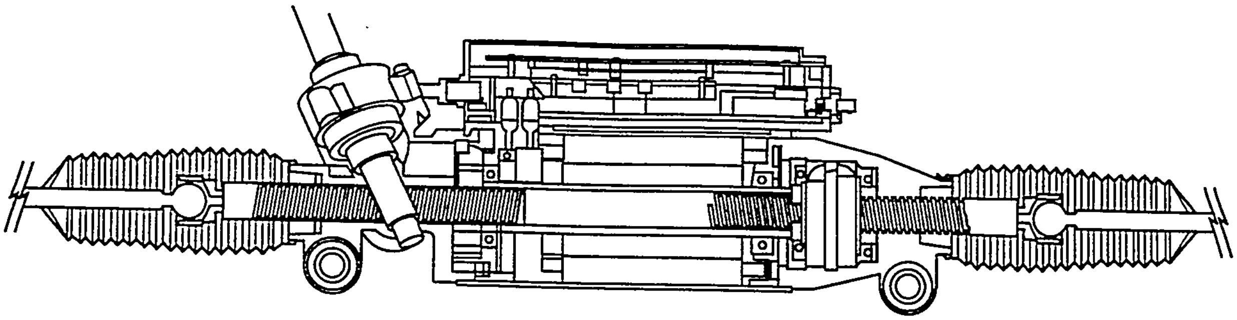

MJ95H032
(5241)

Figure 7-3. Electric Power Steering Subsystem

SECTION 8
ACRONYM LIST AND DEFINITIONS

Table 8-1 contains a list of acronyms and abbreviations used in this document. Column two of the table contains the definition of the acronym or abbreviation.

Table 8-1. List of Acronyms

Acronym	Definition
AC	Alternating Current
Ah	Ampere-Hour
ASIC	Application Specific Integrated Circuit
atm	At mosphere
BIT	Built-In Test
CCA	Circuit Card Assembly
CCD	Chrysler Collision Detection
CHYHV	CHrYsler Hybrid Vehicle
CMOS	Complementary Metal-Oxide Semiconductor
CNG	Compressed Natural Gas
CNGV	Compressed Natural Gas Vehicles
cm	Centimeter
CMS	Carbon Molecular Sieve
DAS	Data Acquisition System
dB	Decibel
DFMA	Design for manufacturing and assembly
DPHV	Direct-Hydrogen-Fueled Proton Exchange Membrane Fuel Cell System for a Hybrid Vehicle
DTC	Design-to-Cost
EPA	Environmental Protection Agency
EPS	Electrical Power Steering
FCS	Fuel Cell Stack
FUDS	Federal Urban Driving Schedule
GMS	Gas Management Subsystem
HP	Horsepower
HPCV	Hi Pressure Control Valve
HSS	Hydrogen Storage Subsystem
HTP	Humidifier Tube Pump
HVAC	Heating/Ventilation/Air Conditioning
Hz	Hertz (Cycles/Second)
ICE	Internal Combustion Engine
IGBT	Isolated Gate Bipolar Transistor
IMB	Inter-Module Bus
I/O	Input/Output
IPDS	Integrated Product Development System
kg	Kilogram

Table 8-1. List of Acronyms (Continued)

Acronym	Definition
kW	Kilowatts
kWh	Kilowatt-Hour
l	Liter
lbs	Pounds
LLC	Load Leveling Unit Controller
LLU	Load Leveling Unit
LPRV	Low Pressure Regulating Valve
LPS	Low Pressure Switch
MEA	Membrane Electrode Assembly
mg	Milligram
Mi	Miles
mohm	Milliohm
mpg	Miles per Gallon
MPH	M iles per Hour
MU	Maintenance Unit
mv	Millivolt
OS	Operating System
PAO	polyalphaolefin
PEM	Proton Exchange Membrane
PI	Proportional-Integral
PNGV	Partnership for a New Generation of Vehicles
POST	Power On/Off Self-Test
psia	Pounds per Square Inch Absolute
PWM	Pulse Width Modulator
QSM	Queued Serial Module
RPM	Revolutions per Minute
SOC	State of Charge
SOV	Solenoid Valve
SPV	Start Purge Valve
TPU	Time Processor Unit
VDC	Volts (Direct Current)
Wh	Watt-Hour

APPENDIX A
CHOPPER/REGULATOR DESIGN

Design Considerations

The chopper/regulator inverter provides an output current that is proportional to the CURRENT REFERENCE INPUT signal from the LLC circuitry. The inverter gain is 30 Amps/VDC for all combinations of battery voltages and output loads. A block diagram for the complete chopper/regulator is shown in Figure 5-7 and a schematic of the control circuit is shown in this Appendix. A discussion of the operation is presented below. Part identification reflects the schematic drawing located herein.

The output current from the chopper/regulator is continuously monitored by the current transformer, CT1. The output of CT1 is integrated to provide a DC signal proportional to the average current delivered to the load. The same device used to average (or integrate) the current signal functions as an error amplifier. The devices used for averaging (integrating) are U11 (U12). The resultant output signal from the error amplifier/integrator is a voltage which is proportional to the difference between the actual output current and the desired current requested by the LLC. This output signal is used to vary the pulse width of the signal to the chopper and hence regulates the current to the desired level.

Separate error amplifier/integrators are used for the buck and boost configurations, but both use CT1 to monitor the actual output current. The switch from buck to boost or vice versa is automatic. If the input voltage is less than that required to provide the required current, the buck control Pulse Width Modulator (PWM) causes Q1 to activate. The boost control PWM begins to step the input voltage to the required level to provide the necessary output current. Conversely, if the input voltage is higher than that required to provide the necessary output current, the buck PWM modulates the input voltage and the boost PWM never activates Q2.

A smooth transition for input voltages at the threshold modes is assured by reducing the current request signal applied to the boost error amplifier by 5 percent. This transition functions in much the same way as hysteresis operations with voltage comparators.

The reduction of output current by 5 percent for the boost mode has no effect on the overall system performance since the invertor is a gain block in the overall control system formed by the SOC monitoring circuit and the LLC. In addition to monitoring output load current, CT1 is also used to control the buck current mode PWM since the output is a scaled replica of the current switched by Q1. For the boost mode, a separate current transformer directly monitoring the current in Q2 is required for current mode control.

A voltage control loop is also used for protection should the battery and/or load be disconnected during operation. The details for this circuit are shown on sheet 6 of the schematics. The voltage loop is designed to regulate the output voltage (regardless of the current request) to 360

VDC. For normal operations, the output voltage is less than 360 VDC. Thus the voltage loop is saturated and is transparent to circuit operation. If, however, the battery/load is disconnected, the boost regulator would try to increase the output voltage as high as possible in attempt to provide the requested current and damage could occur. Sufficient output capacitance is provided to limit the amplitude of the output voltage transients until the voltage loop can automatically begin to operate and provide fail-safe conditions. A separate overvoltage comparator is used to turn the inverter off if the output exceeds 375 VDC as a redundant fail-safe mechanism. The comparator does not latch off and allows the unit to resume operation when the output voltage is reduced to values at or below 360 VDC.

A small signal model was developed for both the normal mode and for the voltage control mode for stability analysis. The low frequency, open-loop gain for the normal mode is 100 dB and the bandwidth is 2 Hz. The rate of closure is 6 dB/octave, resulting in stable operation. The voltage loop also closes at 6 dB/octave, however the bandwidth is 100 Hz to provide fast response time when activation is required. A model of the Electrosource Horizon Battery was used as an output load for the AC model.

An internal housekeeping supply is used to provide operational voltages for the control circuits. Three outputs are provided: +15 VDC, -15 VDC and an isolated +15 VDC bias voltage for the high voltage drivers. The topology for the supply is a current mode flyback design. A complete schematic for the design is shown on sheet 5. The supply is powered from either the battery or the FCS. This allows the unit to continue operations during various fault modes which might occur.

D

NOTES:

1. APPLICABLE STANDARD/SPECIFICATIONS:
   A. DOD-STD-00100D(AR)
2. FOR ASSEMBLY DRAWING SEE
3. UNLESS OTHERWISE SPECIFIED:
   RESISTANCE VALUES ARE IN OHMS
   CAPACITANCE VALUES ARE IN MICROFARADS
4. LEGEND:

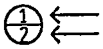

LOCATOR NUM,BER
SHEET NUMBER

5. PARTIAL REFERENCE DESIGNATORS ARE SHOWN, FOR COMPLETE DESIGNATION PREFIX WITH UNIT NUMBER OR SUBASSEMBLY DESIGNATION

HIGHEST REFERENCE DESIGNATION			
R57	C29	L1	Q2
T1	U17	CR28	P1
E3			

REFERENCE DESIGNATIONS NOT USED			

C

B

A

NEXT

4 3 2 1

REVISIONS			
REV	DESCRIPTION	DATE	APPROVAL
X0	ORIGINAL RELEASE	6-14-95	

D

C

B

JUNE 15, 1995

A

SSY	USED ON
APPLICATION	

MECHANICAL PROPERTIES
YP
TS
EL2
RA
BH
RH

DO NOT SCALE DRAWING
UNLESS OTHERWISE SPECIFIED
DIMENSIONS ARE IN INCHES
TOLERANCES ON DECIMALS ±
FRACTIONS ± ANGLES ±
THIRD ANGLE PROJECTION

ORIGINAL DATE OF DRAWING

DRAFTSMAN	CHECKER
ENGR	ENGR
ENGR	ENGR

PENTASTAR ELECTRONICS, INCORPORATED
HUNTSVILLE, ALABAMA 35807-0929

SCHEMATIC DIAGRAM,
40KW PRINTED WIRING BOARD

SIZE D
CAGE CODE 24290
SCALE NONE
UNIT WT ________
SHEET 1 of 7

8 7 6 5

D

C

B

NOTE: THIS PAGE RESERVED FOI

A

4 3 2 1

REVISIONS			
REV	DESCRIPTION	DATE	APPROVAL
X0	ORIGINAL RELEASE	6-14-95	

D

C

B

SPARE GATES, ETC.

A

SIZE	CAGE CODE	
D	24290	
SCALE NONE	UNIT WT ________	SHEET 2 of 7

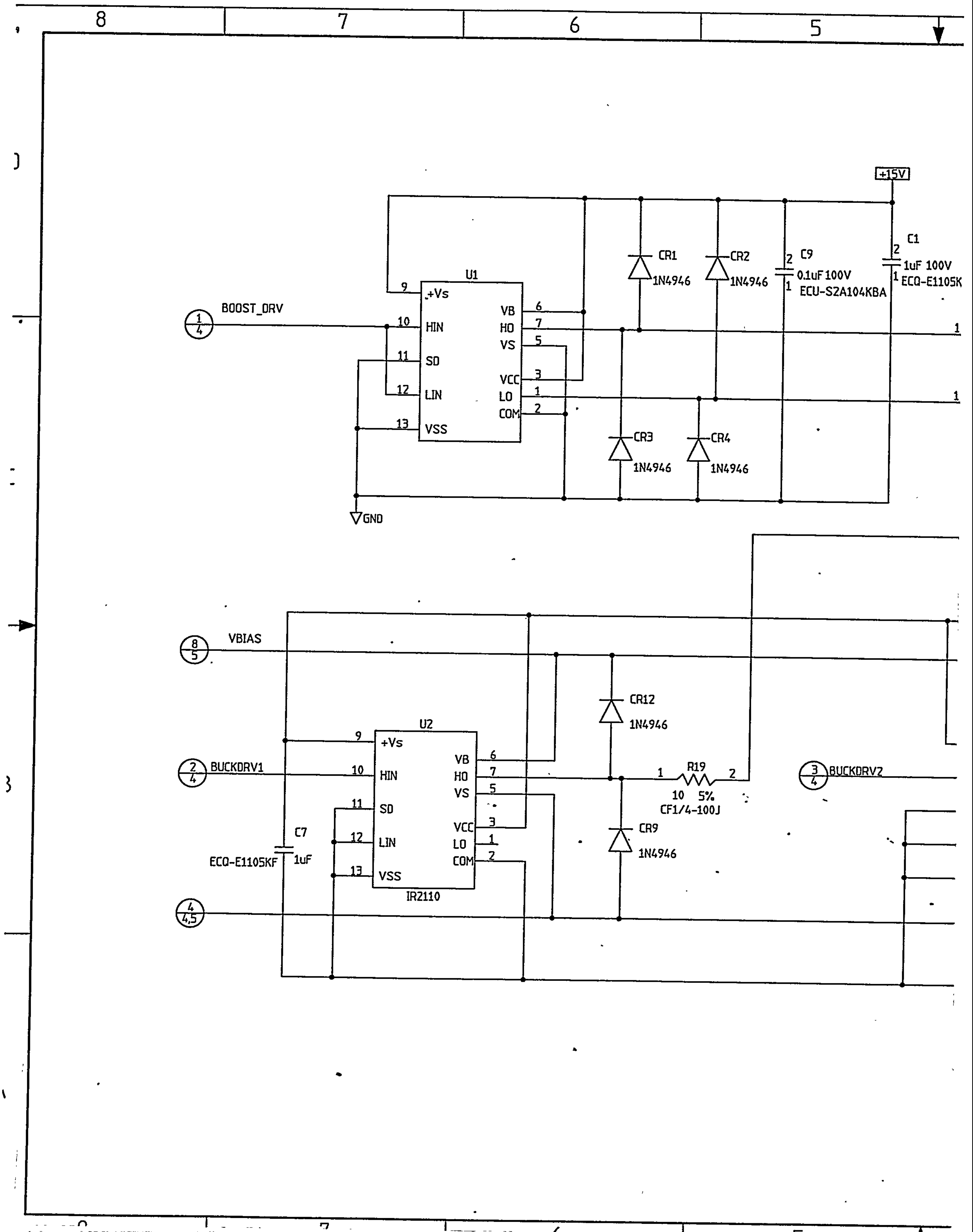
8
7
6
5
+15V
C1
2
1uF 100V
1
ECQ-E1105K
CR1
1N4946
CR2
1N4946
2
C9
0.1uF 100V
1
ECU-S2A104KBA
U1
9
+Vs
BOOST_DRV
1
4
10
HIN
11
SD
12
LIN
13
VSS
VB
6
HO
7
VS
5
VCC
3
LO
1
COM
2
CR3
1N4946
CR4
1N4946
GND
VBIAS
8
5
CR12
1N4946
U2
9
+Vs
BUCKDRV1
2
4
10
HIN
11
SD
12
LIN
13
VSS
IR2110
VB
6
HO
7
VS
5
VCC
3
LO
1
COM
2
C7
ECQ-E1105KF
1uF
R19
1
2
10 5%
CF1/4-100J
CR9
1N4946
BUCKDRV2
3
4
4
4,5

4 3 2 1

REVISIONS			
REV	DESCRIPTION	DATE	APPROVAL
X0	ORIGINAL RELEASE	6-14-95	

D

C

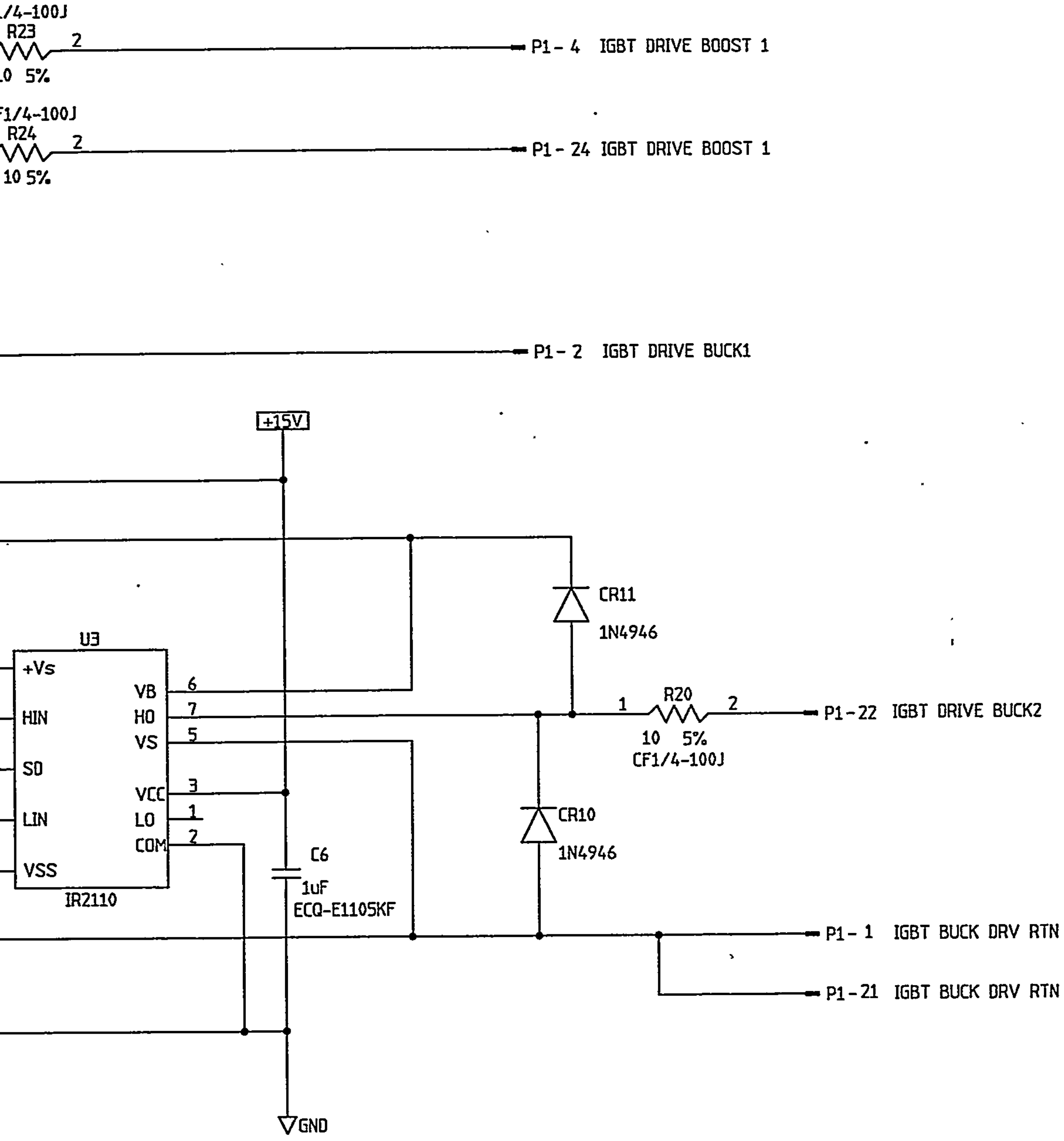

/4-100J
R23
2
0 5%
P1- 4 IGBT DRIVE BOOST 1
F1/4-100J
R24
2
10 5%
P1- 24 IGBT DRIVE BOOST 1
P1- 2 IGBT DRIVE BUCK1
+15V
CR11
1N4946
U3
+Vs
HIN
SD
LIN
VSS
VB
HO
VS
VCC
LO
COM
6
7
5
3
1
2
IR2110
1
R20
2
10 5%
CF1/4-100J
P1-22 IGBT DRIVE BUCK2
CR10
1N4946
C6
1uF
ECQ-E1105KF
P1- 1 IGBT BUCK DRV RTN
P1-21 IGBT BUCK DRV RTN
GND

B

A

IGBT DRIVERS FOR BUCK AND BOOST REGULATORS

SIZE D	CAGE CODE 24290	
SCALE	UNIT WT --------	SHEET 3 of 7

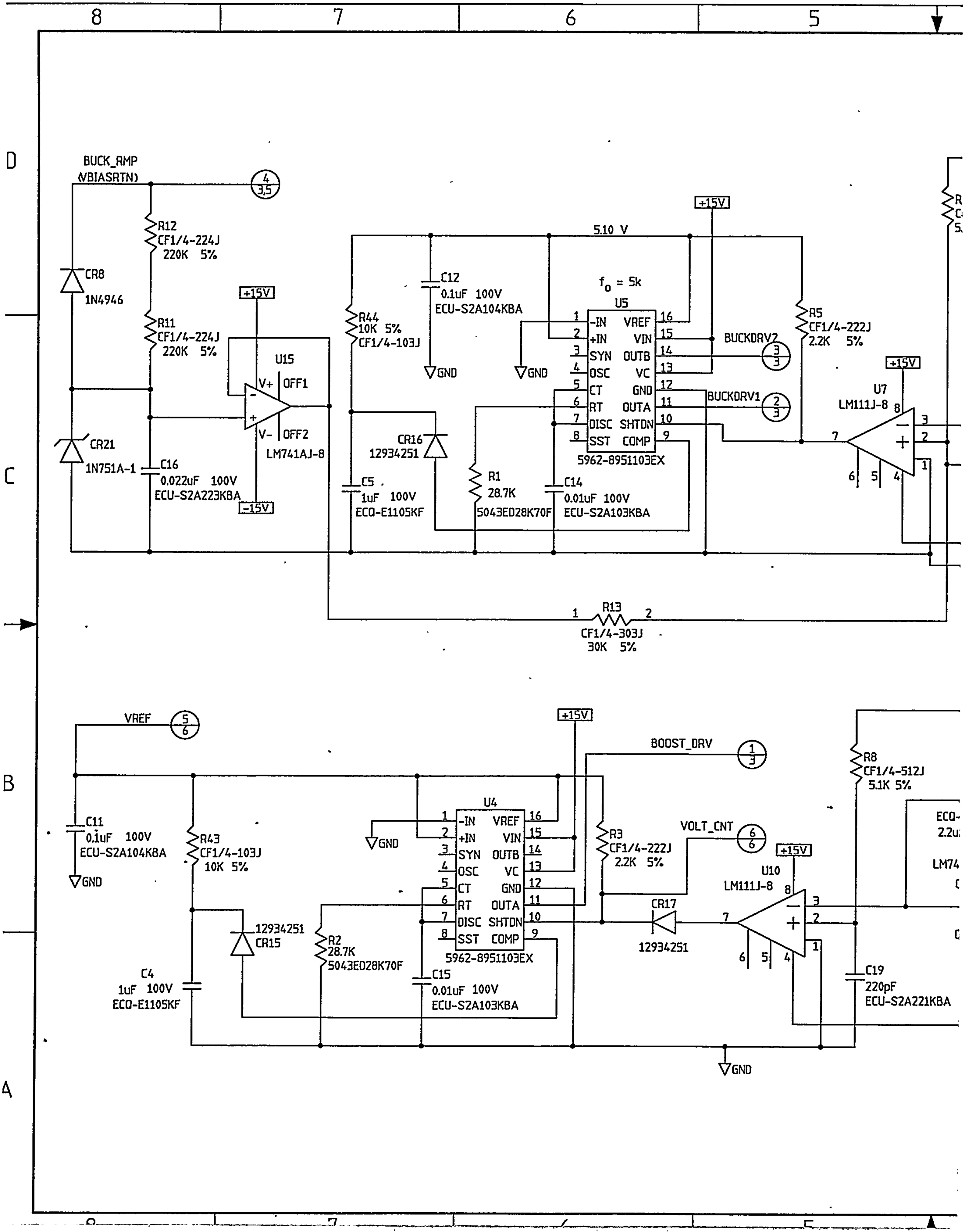
8
7
6
5
D
C
B
A
BUCK_RMP
(VBIASRTN)
4
3,5
R12
CF1/4-224J
220K 5%
CR8
1N4946
R11
CF1/4-224J
220K 5%
+15V
U15
V+
OFF1
V-
OFF2
LM741AJ-8
-15V
CR21
1N751A-1
C16
0.022uF 100V
ECU-S2A223KBA
R44
10K 5%
CF1/4-103J
C12
0.1uF 100V
ECU-S2A104KBA
GND
CR16
12934251
C5
1uF 100V
ECO-E1105KF
R1
28.7K
5043ED28K70F
5.10 V
f$_0$ = 5k
U5
-IN
+IN
SYN
OSC
CT
RT
DISC
SST
VREF
VIN
OUTB
VC
GND
OUTA
SHTDN
COMP
5962-8951103EX
C14
0.01uF 100V
ECU-S2A103KBA
BUCKDRV2
3
3
BUCKDRV1
2
3
R5
CF1/4-222J
2.2K 5%
U7
LM111J-8
R13
CF1/4-303J
30K 5%
VREF
5
6
C11
0.1uF 100V
ECU-S2A104KBA
R43
CF1/4-103J
10K 5%
C4
1uF 100V
ECO-E1105KF
12934251
CR15
R2
28.7K
5043ED28K70F
U4
5962-8951103EX
C15
0.01uF 100V
ECU-S2A103KBA
BOOST_DRV
1
3
R3
CF1/4-222J
2.2K 5%
VOLT_CNT
6
6
CR17
12934251
U10
LM111J-8
R8
CF1/4-512J
5.1K 5%
C19
220pF
ECU-S2A221KBA
ECO-
2.2u
LM74

REVISIONS			
REV	DESCRIPTION	DATE	APPROVAL
X0	ORIGINAL RELEASE	6-14-95	

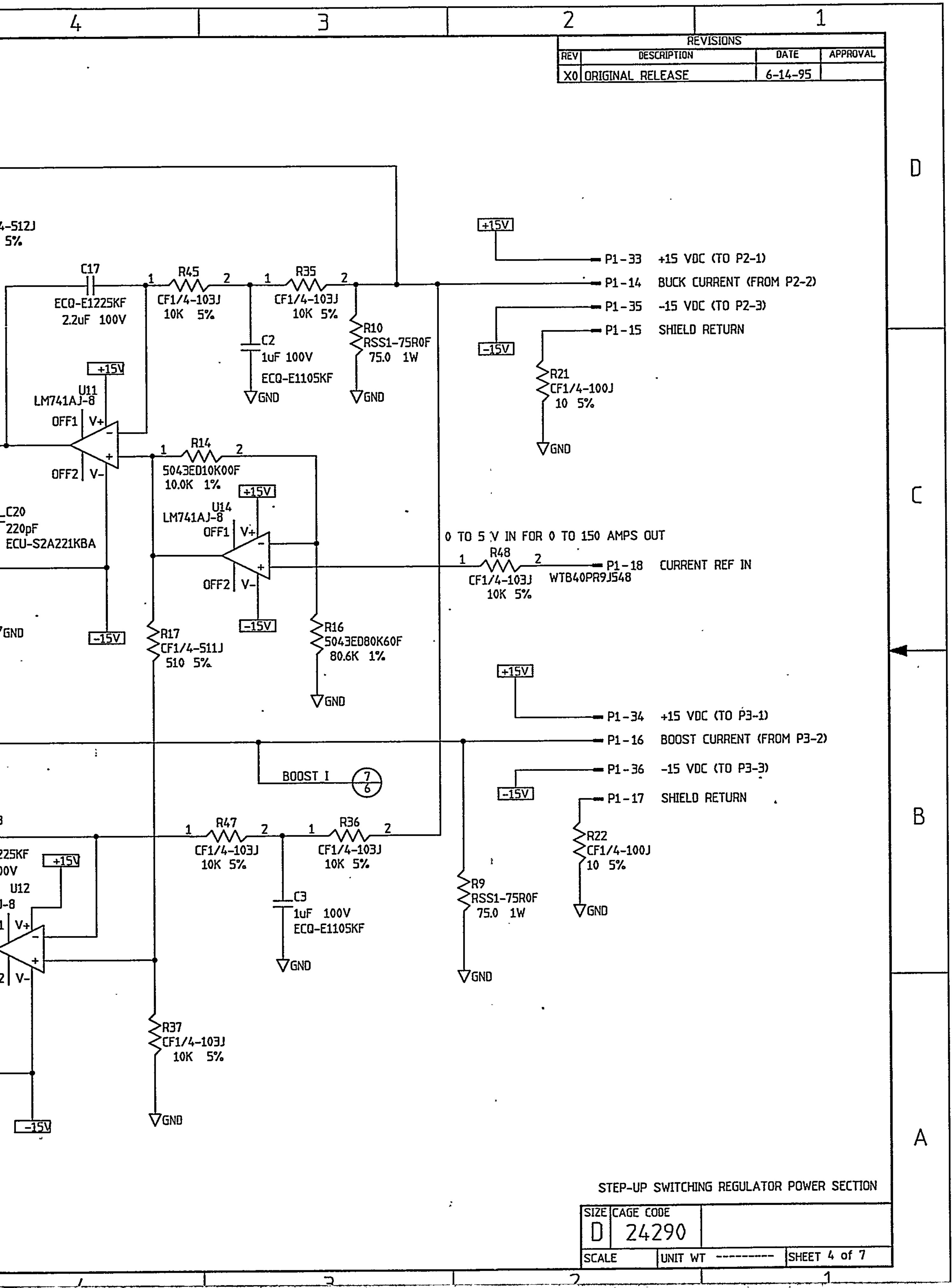
4
3
2
1
D
C
B
A
4-512J
5%
C17
ECQ-E1225KF
2.2uF 100V
R45
CF1/4-103J
10K 5%
R35
CF1/4-103J
10K 5%
C2
1uF 100V
ECQ-E1105KF
GND
R10
RSS1-75R0F
75.0 1W
GND
+15V
P1-33 +15 VDC (TO P2-1)
P1-14 BUCK CURRENT (FROM P2-2)
P1-35 -15 VDC (TO P2-3)
-15V
P1-15 SHIELD RETURN
R21
CF1/4-100J
10 5%
GND
+15V
U11
LM741AJ-8
OFF1
V+
OFF2
V-
R14
5043ED10K00F
10.0K 1%
C20
220pF
ECU-S2A221KBA
U14
LM741AJ-8
OFF1
V+
OFF2
V-
+15V
-15V
0 TO 5 V IN FOR 0 TO 150 AMPS OUT
R48
CF1/4-103J
10K 5%
P1-18 CURRENT REF IN
WTB40PR9J548
GND
-15V
R17
CF1/4-511J
510 5%
R16
5043ED80K60F
80.6K 1%
GND
+15V
P1-34 +15 VDC (TO P3-1)
P1-16 BOOST CURRENT (FROM P3-2)
BOOST I
7
6
P1-36 -15 VDC (TO P3-3)
-15V
P1-17 SHIELD RETURN
R22
CF1/4-100J
10 5%
GND
225KF
00V
U12
J-8
+15V
V+
V-
R47
CF1/4-103J
10K 5%
R36
CF1/4-103J
10K 5%
C3
1uF 100V
ECQ-E1105KF
GND
R9
RSS1-75R0F
75.0 1W
GND
R37
CF1/4-103J
10K 5%
GND
-15V

STEP-UP SWITCHING REGULATOR POWER SECTION

SIZE	CAGE CODE	
D	24290	
SCALE	UNIT WT ---------	SHEET 4 of 7

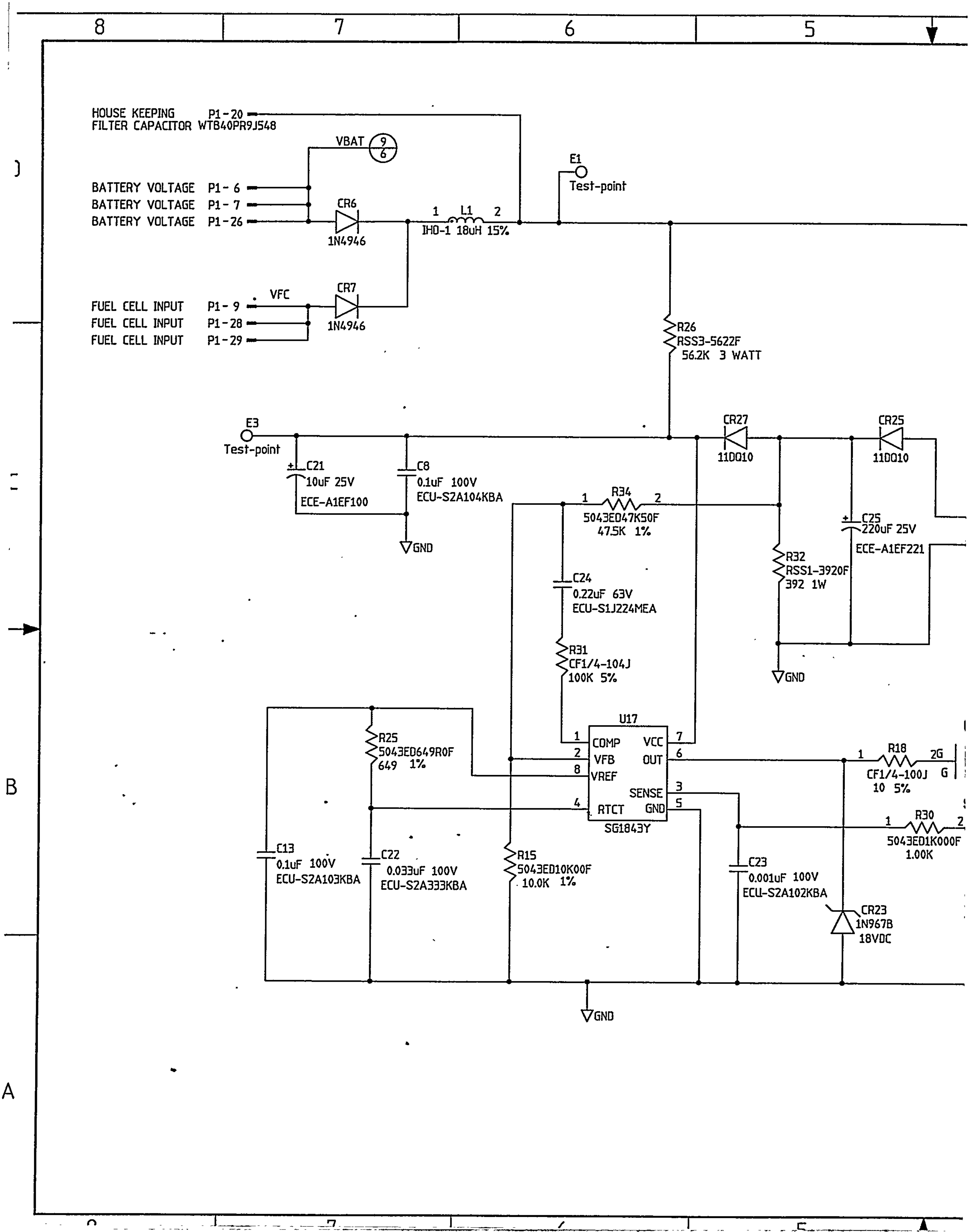
8
7
6
5
B
A
HOUSE KEEPING P1-20
FILTER CAPACITOR WTB40PR9J548
VBAT
9
6
E1
Test-point
BATTERY VOLTAGE P1-6
BATTERY VOLTAGE P1-7
BATTERY VOLTAGE P1-26
CR6
1N4946
1
L1
2
IHD-1 18uH 15%
FUEL CELL INPUT P1-9
FUEL CELL INPUT P1-28
FUEL CELL INPUT P1-29
VFC
CR7
1N4946
R26
RSS3-5622F
56.2K 3 WATT
E3
Test-point
C21
10uF 25V
ECE-A1EF100
C8
0.1uF 100V
ECU-S2A104KBA
GND
CR27
11DQ10
CR25
11DQ10
R34
1
2
5043ED47K50F
47.5K 1%
C25
220uF 25V
ECE-A1EF221
R32
RSS1-3920F
392 1W
GND
C24
0.22uF 63V
ECU-S1J224MEA
R31
CF1/4-104J
100K 5%
R25
5043ED649R0F
649 1%
U17
COMP
VCC
VFB
OUT
VREF
SENSE
RTCT
GND
1
2
8
4
7
6
3
5
SG1843Y
R18
1
2G
G
CF1/4-100J
10 5%
R30
1
2
5043ED1K000F
1.00K
C13
0.1uF 100V
ECU-S2A103KBA
C22
0.033uF 100V
ECU-S2A333KBA
R15
5043ED10K00F
10.0K 1%
C23
0.001uF 100V
ECU-S2A102KBA
CR23
1N967B
18VDC
GND

REVISIONS			
REV	DESCRIPTION	DATE	APPROVAL
X0	ORIGINAL RELEASE	6-14-95	

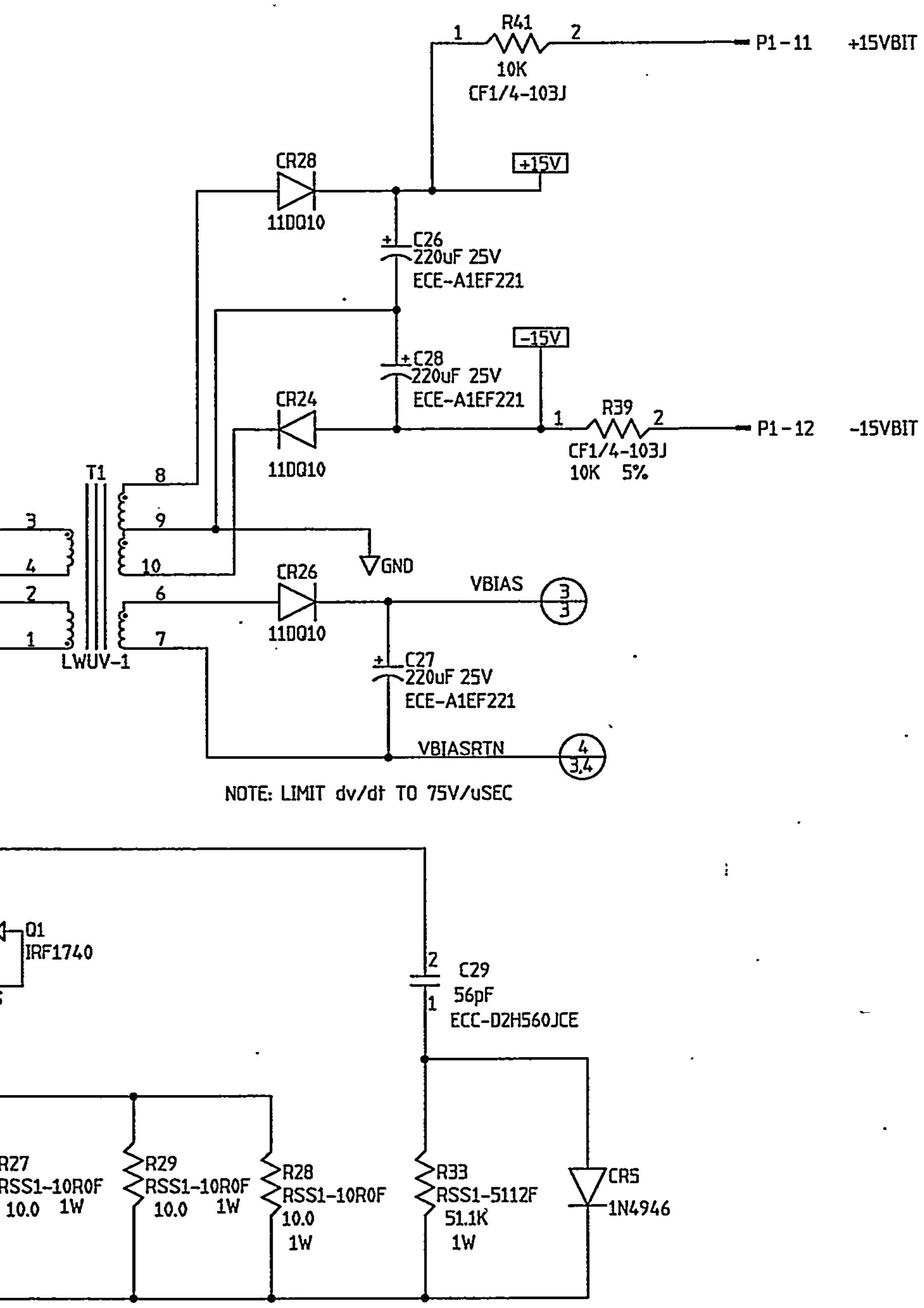

R41
1
2
10K
CF1/4-103J
P1-11
+15VBIT
CR28
11DQ10
+15V
C26
220uF 25V
ECE-A1EF221
-15V
C28
220uF 25V
ECE-A1EF221
CR24
11DQ10
R39
1
2
CF1/4-103J
10K 5%
P1-12
-15VBIT
T1
8
9
10
3
4
2
1
6
7
LWUV-1
GND
CR26
11DQ10
VBIAS
3
3
C27
220uF 25V
ECE-A1EF221
VBIASRTN
4
3,4
NOTE: LIMIT dv/dt TO 75V/uSEC
Q1
IRF1740
C29
2
1
56pF
ECC-D2H560JCE
R27
RSS1-10R0F
10.0 1W
R29
RSS1-10R0F
10.0 1W
R28
RSS1-10R0F
10.0
1W
R33
RSS1-5112F
51.1K
1W
CR5
1N4946

SIZE	CAGE CODE	
D	24290	
SCALE	UNIT WT -------	SHEET 5 of 7

VOLTAGE CONTROL LOOP

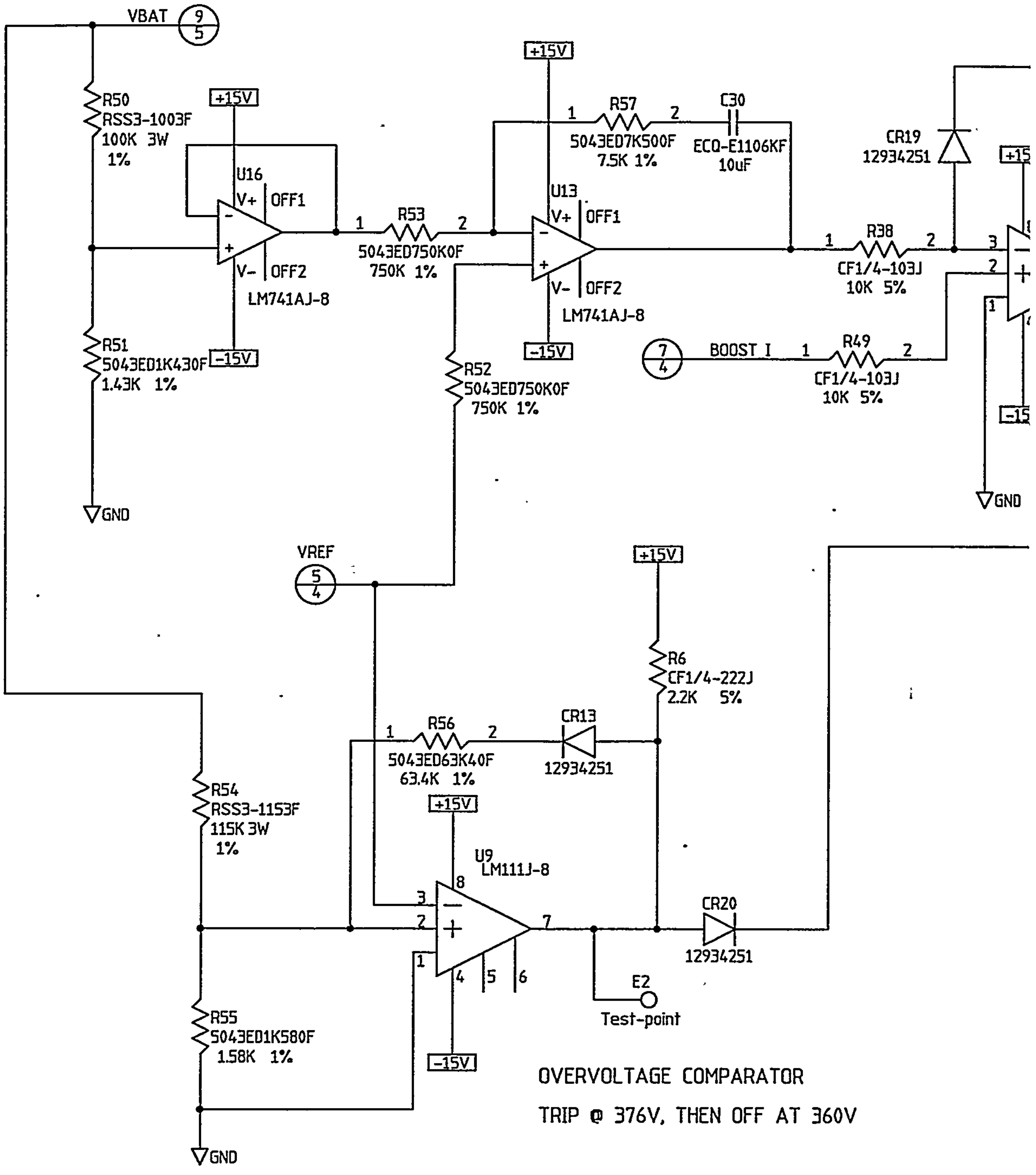

VBAT
9
5
R50
RSS3-1003F
100K 3W
1%
R51
5043ED1K430F
1.43K 1%
GND
+15V
U16
V+
OFF1
V-
OFF2
-15V
LM741AJ-8
1
R53
2
5043ED750K0F
750K 1%
+15V
U13
V+
OFF1
V-
OFF2
-15V
LM741AJ-8
1
R57
2
5043ED7K500F
7.5K 1%
C30
ECQ-E1106KF
10uF
R52
5043ED750K0F
750K 1%
CR19
12934251
+15
1
R38
2
CF1/4-103J
10K 5%
3
2
1
BOOST I
7
4
1
R49
2
CF1/4-103J
10K 5%
-15
GND
VREF
5
4
+15V
R6
CF1/4-222J
2.2K 5%
1
R56
2
5043ED63K40F
63.4K 1%
CR13
12934251
R54
RSS3-1153F
115K 3W
1%
+15V
U9
LM111J-8
8
3
2
1
7
4
5
6
CR20
12934251
E2
Test-point
R55
5043ED1K580F
1.58K 1%
-15V
GND

OVERVOLTAGE COMPARATOR

TRIP @ 376V, THEN OFF AT 360V

REVISIONS			
REV	DESCRIPTION	DATE	APPROVAL
X0	ORIGINAL RELEASE	6-14-95	

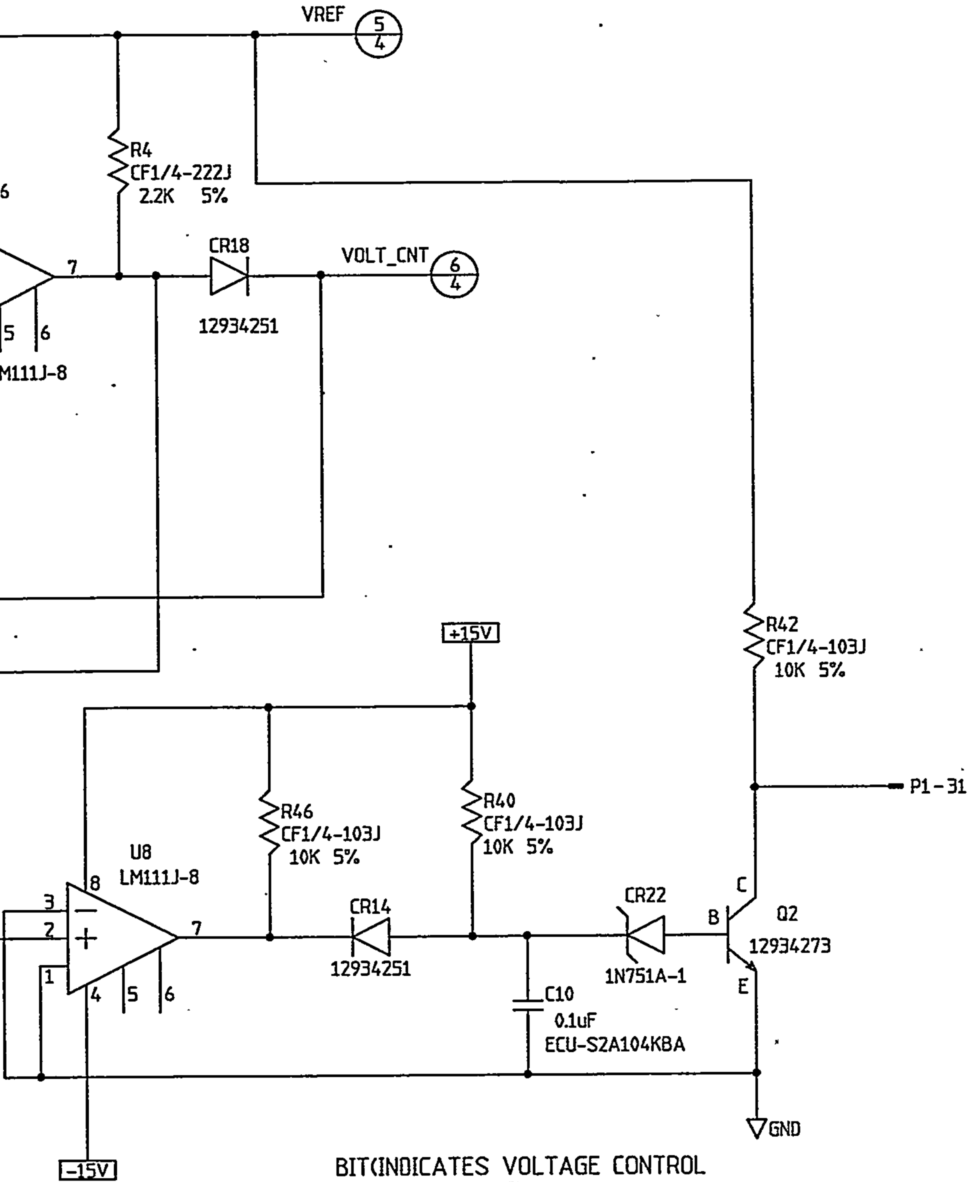

VREF
5/4
R4
CF1/4-222J
2.2K 5%
6
7
CR18
12934251
VOLT_CNT
6/4
5
6
M111J-8
+15V
R42
CF1/4-103J
10K 5%
P1-31 BIT
R46
CF1/4-103J
10K 5%
R40
CF1/4-103J
10K 5%
U8
LM111J-8
8
3
2
1
7
4
5
6
CR14
12934251
CR22
1N751A-1
C10
0.1uF
ECU-S2A104KBA
C
B
E
Q2
12934273
GND
-15V

BIT(INDICATES VOLTAGE CONTROL LOOP IS ACTIVE)

478 uSEC DELAY AT TURN OFF

HOUSEKEEPING SUPPLY

SIZE	CAGE CODE		
D	24290		
SCALE NONE	UNIT WT --------		SHEET 6 of 7

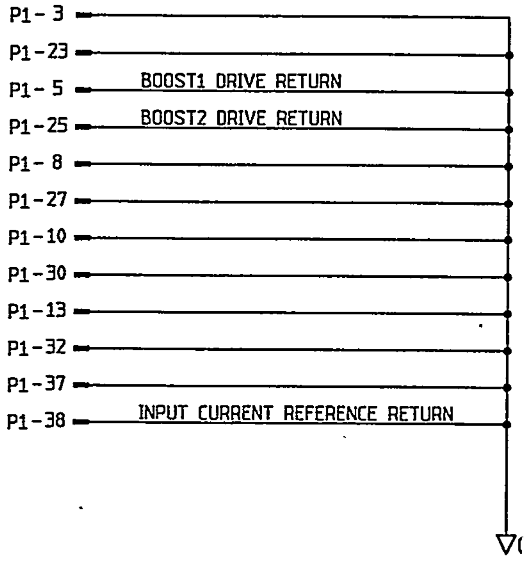
P1- 3
P1-23
P1- 5
BOOST1 DRIVE RETURN
P1-25
BOOST2 DRIVE RETURN
P1- 8
P1-27
P1-10
P1-30
P1-13
P1-32
P1-37
P1-38
INPUT CURRENT REFERENCE RETURN

NOTE: PIN NUMBERS 19, 39, 40 ARE SPARES.

4 3 2 1

REVISIONS

REV	DESCRIPTION	DATE	APPROVAL
X0	ORIGINAL RELEASE	6-14-95	

D

C

B

A

SIZE D	CAGE CODE 24290		
SCALE	UNIT WT	--------	SHEET 7 of 7

4 3 2 1

APPENDIX B
CONTROLLER DESIGN

The following tables define the Input/Output (I/O) interfaces to the Load Leveling Unit Controller (LLC) as they currently exist. The new DAC output address is not presently defined and will be required for completion of the LLC software

Table B-1. TPU I/O

Channel Number	Function	Description
0	DIO - Output	Maintenance Required Light
1	PWM - Output	SOC Meter
2	PWM - Output	Fan Speed Control
3	DIO - Output	FCS Self-Test
4	FQM - Input	Fan #1 RPM
5	FQM - Input	Fan # 2 RPM
6	DIO - Output	FCS ON/OFF
7	DIO - Output	Charge Lamp
8	Not Used	N/A
9	DIO - Output	Heater ON
10	D IO - Input	Ignition Switch ACCESSORY
11	DIO - Input	Ignition Switch ON
12	DIO - Input	Ignition Switch START
13	DIO - Output	Watchdog Timer RESET[1]
14	Not Used	N/A
15	Not Used	N/A

Notes:
1 Recommended that this output be moved to PE3.

Table B-2. Discrete Outputs, Non-CPU Resident (Address 10002H and any Even Address from 10000H to 107FFH)

Bit Number	Description
0	Module Select 0
1	Module Sel ect 1
2	Module Select 2
3	Module Select 3
4	Module Select 4
5	Module Select 5
6	Battery Voltage Select
7	Battery Voltage Read
8	Module Voltage Read Low
9	Module Voltage Read High
10	Battery Current Sensor Range High

Table B-2. Discrete Outputs, Non-CPU Resident (Address 10002H and any Even Address from 10000H to 107FFH) (Continued)

Bit Number	Description
11	LLC Power ON (Relay Latch)
12	Spare
13	Spare

Table B-3. CPU-Based Discrete I/O, Interrupts, and Serial Communications

Pin Name	Description
PQS6	DI, Pol arity of Battery Current
RXD	Serial Data Input
TXD	Serial Data Output
PF1	Interrupt, DI, Programmable, CCD Idle Detect
IRQ4	16C30 Serial Port B Interrupt Line
IRQ5	16C30 Serial Port A Interrupt Line
IRQ7	External Watchdog Timer Interrupt (NMI)
MOSI	Queued Serial Data Output
MISO	Queued Serial Data Input

Table B-4. Serial Analog Data Channels

Channel Number	Description
0	Multiplexed Module Voltages
1	Battery Pack Voltage
2	Battery Temperature Sensor #1
3	Battery Temperature Sensor #2
4	Battery Temperature Sensor #3
5	Battery Temperature Sensor #4
6	Battery Temperature Sensor #5
7	Battery Temperature Sensor #6
8	Not Used
9	Battery Current
10	Not Used

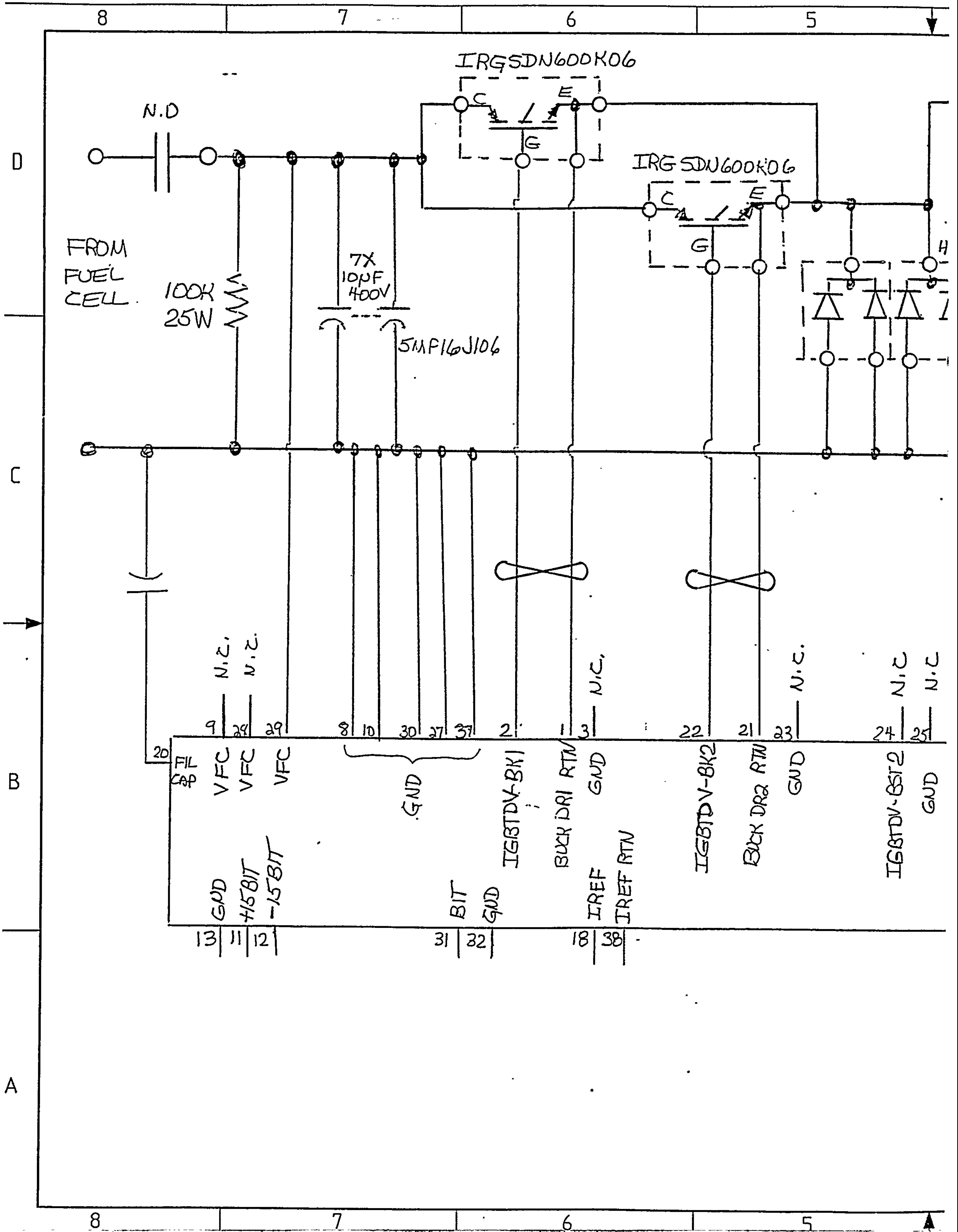
8
7
6
5
D
C
B
A
IRGSDN600K06
C
E
G
IRGSDN600K06
C
E
G
N.D
FROM FUEL CELL
100K 25W
7X 10µF 400V
5MP16J106
H
N.C.
N.C.
N.C.
N.C.
N.C.
N.C
9
28
29
8
10
30
27
37
2
1
3
22
21
23
24
25
20
FIL CAP
VFC
VFC
VFC
GND
IGBTDV-BK1
BUCK DR1 RTN
GND
IGBTDV-BK2
BUCK DR2 RTN
GND
IGBTDV-BST2
GND
GND
+15BIT
-15BIT
BIT
GND
IREF
IREF RTN
13
11
12
31
32
18
38

REVISIONS

REV	DESCRIPTION	DATE	APPROVAL

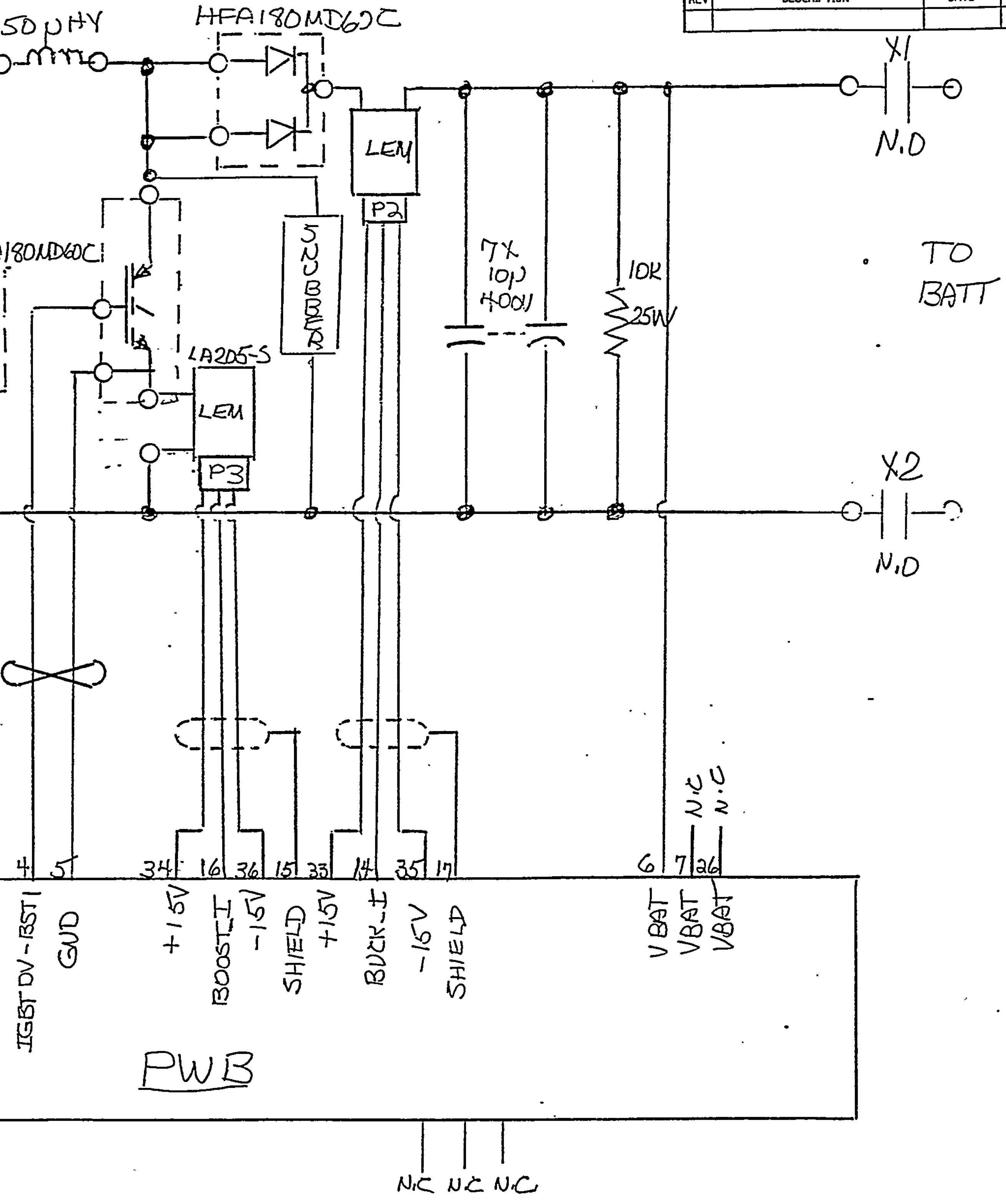

50 μHY
HFA180MD60C
LEM
P2
180MD60C
SNUBBER
7X
10μ
400V
10K
25W
X1
N.O
TO
BATT
LA205-S
LEM
P3
X2
N.O
N.C
N.C
4
5
34
16
36
15
33
14
35
17
6
7
26
IGBT DV-BST1
GND
+15V
BOOST_I
-15V
SHIELD
+15V
BUCK_I
-15V
SHIELD
VBAT
VBAT
VBAT
PWB
N.C N.C N.C

SIZE	CAGE CODE	
D	24290	
SCALE NONE	UNIT WT _________	SHEET 2 of 7

APPENDIX C
GAS MANAGEMENT CONTROLLER

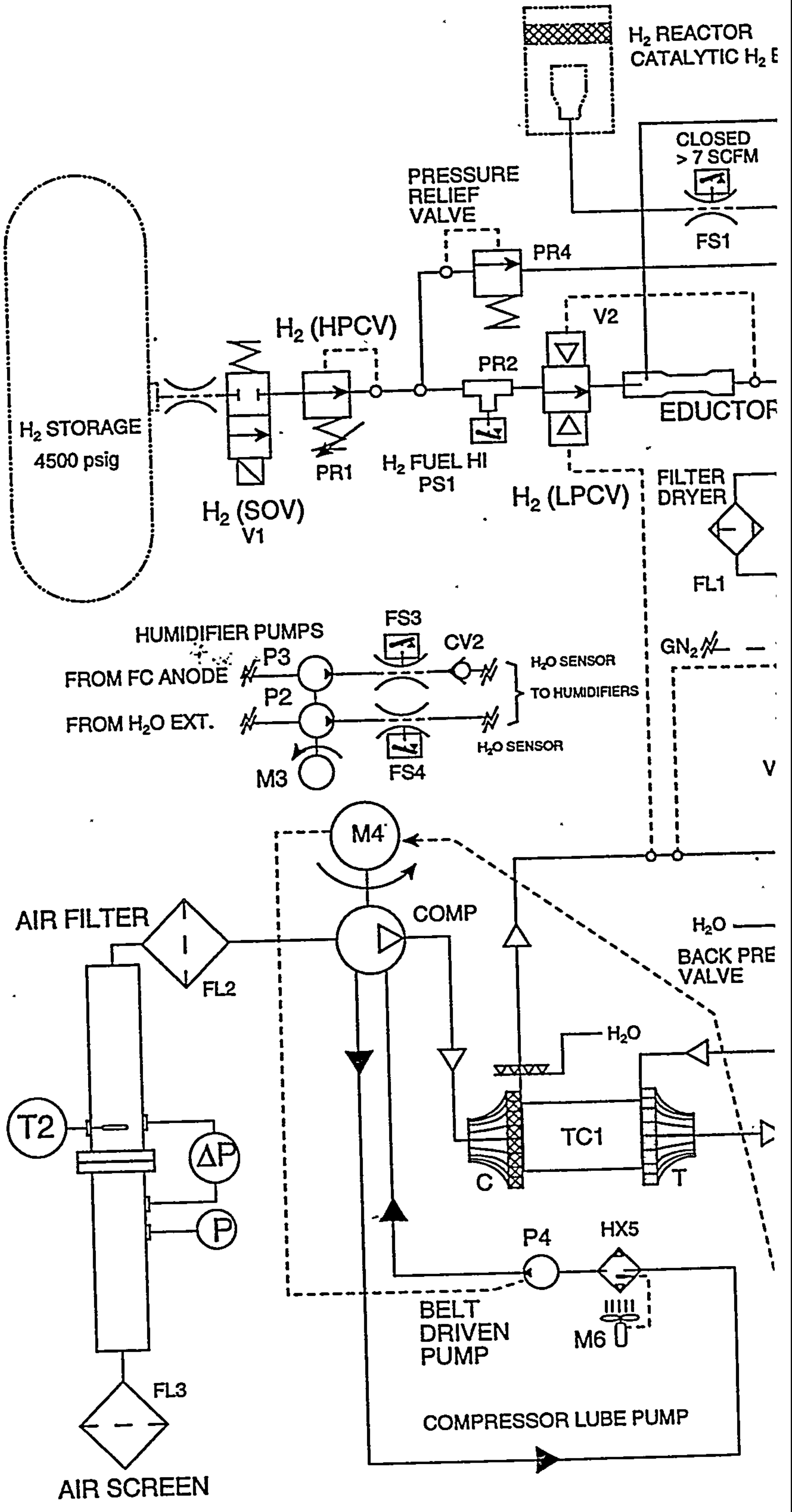

H_2 REACTOR
CATALYTIC H_2 E
CLOSED
> 7 SCFM
FS1
PRESSURE
RELIEF
VALVE
PR4
H_2 (HPCV)
V2
PR2
EDUCTOR
H_2 STORAGE
4500 psig
PR1
H_2 FUEL HI
PS1
H_2 (LPCV)
H_2 (SOV)
V1
FILTER
DRYER
FL1
HUMIDIFIER PUMPS
FS3
CV2
P3
FROM FC ANODE
H_2O SENSOR
TO HUMIDIFIERS
P2
FROM H_2O EXT.
H_2O SENSOR
M3
FS4
GN_2
V
M4
COMP
AIR FILTER
FL2
H_2O
BACK PRE
VALVE
H_2O
T2
ΔP
TC1
C
T
P
P4
HX5
BELT
DRIVEN
PUMP
M6
FL3
COMPRESSOR LUBE PUMP
AIR SCREEN

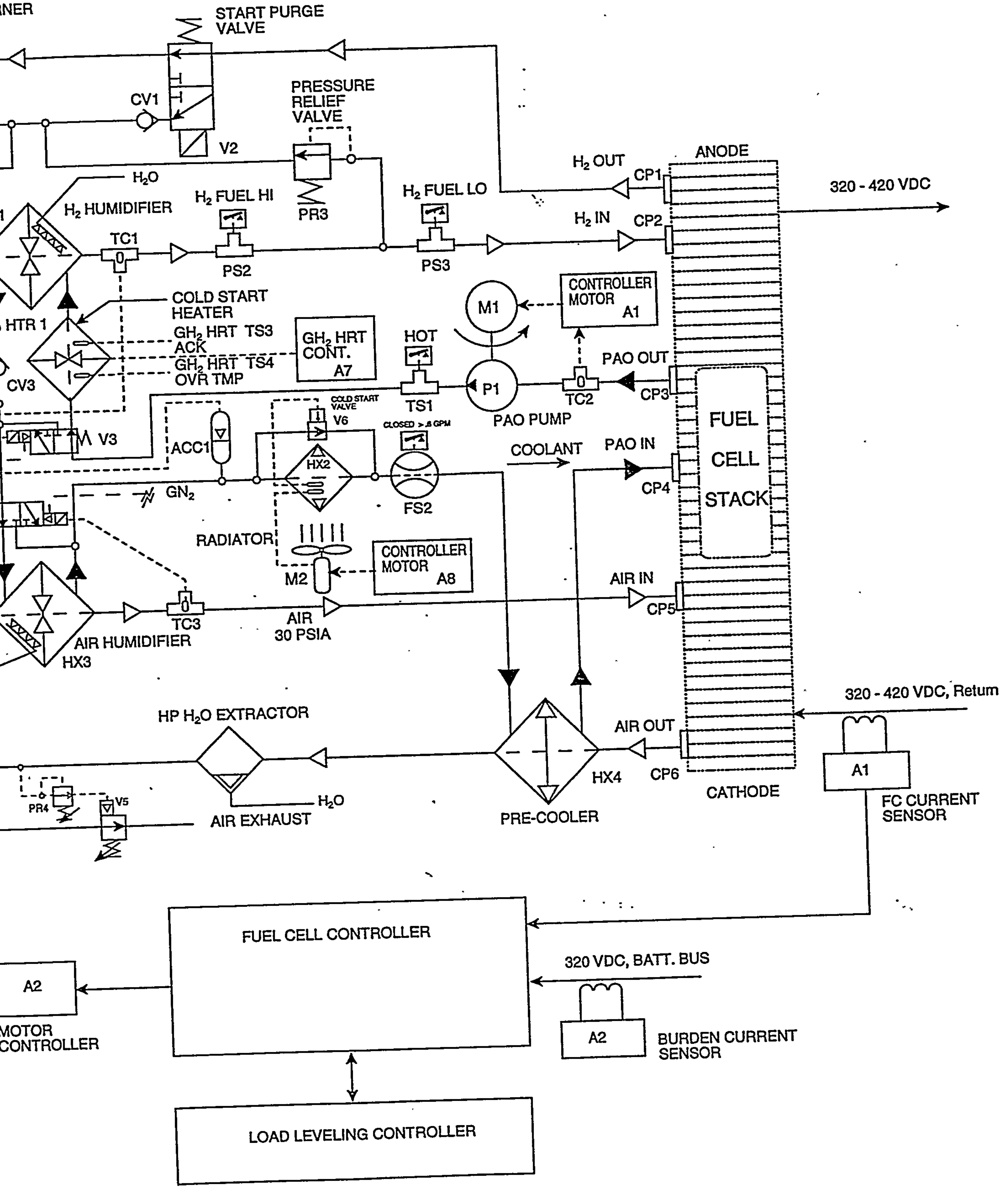

NER
START PURGE VALVE
CV1
PRESSURE RELIEF VALVE
V2
ANODE
H_2 OUT
CP1
320 - 420 VDC
H_2O
H_2 HUMIDIFIER
H_2 FUEL HI
PR3
H_2 FUEL LO
H_2 IN
CP2
TC1
PS2
PS3
COLD START HEATER
HTR 1
GH_2 HRT TS3 ACK
GH_2 HRT TS4 OVR TMP
GH_2 HRT CONT. A7
CONTROLLER MOTOR A1
M1
HOT
P1
TS1
TC2
PAO OUT
CP3
PAO PUMP
CV3
V3
ACC1
COLD START VALVE
V6
CLOSED > .8 GPM
HX2
FS2
COOLANT
PAO IN
CP4
FUEL CELL STACK
GN_2
RADIATOR
M2
CONTROLLER MOTOR A8
AIR IN
CP5
TC3
AIR 30 PSIA
AIR HUMIDIFIER
HX3
320 - 420 VDC, Return
HP H_2O EXTRACTOR
AIR OUT
A1
HX4
CP6
CATHODE
FC CURRENT SENSOR
PR4
V5
H_2O
AIR EXHAUST
PRE-COOLER
FUEL CELL CONTROLLER
320 VDC, BATT. BUS
A2
MOTOR CONTROLLER
A2
BURDEN CURRENT SENSOR
LOAD LEVELING CONTROLLER

APPENDIX D
LLU DESIGN TO COST SUMMARY

	2 - 1 - 95	5 - 3 - 95		PRODUCTION
	SMALL QTY.	SMALL QTY.	PROD. EST	GOAL
LLU ELECTRONICS				
LLC	$2,500	$1,350	$500	$150
CHOPPER/REGULATOR	$2,500	$1,850	$675	$150
PACKAGING/INTERCONNECTION	*	$900	$250	*
BATTERY PACK	$12,000	$11,000	$4,500	$500
LLU TOTAL	$17,0 00	$15,100	$5,925	$800

*PACKAGING ESTIMATES WERE INCLUDED AS A PART OF LLC.

APPENDIX E
SIMULATION MODELING DATA

This appendix provides the results which have been obtained from the DPHV simulations for each of the cycles described in section 2.1 of this document.

E.1 Baker Grade Simulations

Table E-1 shows the results of the simulation results for the Baker Grade. Steady state power is defined as the power required to maintain the vehicle speed at the 55 MPH limit after that speed has been obtained.

Table E-1. Simulation Code Result Comparison

Code	Peak Power (kW)	Steady State Power (kW)
SIMPLEV	57.69	39.31
CHYHV	57.63	38.53
Analytical	55.05	36.29

The results shown in the table indicate that there was good agreement between these simulation methods. The analytical solution did not include the rolling resistance force which is included in both the SIMPLEV and the CHYHV modeling codes. Regenerative braking also is not considered in these simulation results since no deceleration occurs in the Baker Grade cycle.

E.2 Acceleration Performance

The results for the AccelL and the Accel2 acceleration profiles are shown in Table E-2. There are no regenerative braking effects occurring during this cycle. The consistency of results between the analytical calculation and those from the CHYHV simulation gives further confidence in the results which have been obtained. All powers in this table are in kW.

Table E-2. Comparison of CHYHV and Analytical Peak Power Results

Cycle	CHYHV	Analytical
Accel2	101.6	103.3
AccelL	76.3	68.3

The acceleration curve for the AccelL cycle duplicates that which one would expect to occur for the Westinghouse motor performance in an acceleration phase. The results confirmed the finding that less power was required for the acceleration occurring in the early stages of the cycle than for the profile such as Accel2 in which a constant acceleration is maintained throughout the cycle.

E.3 Baker Grade Performance

The analysis for the Baker Grade cycle proceeded in the same manner as for the acceleration cycles. CHYHV was used to determine the vehicle peak and average power requirements. Table E-3 shows the comparison of the data obtained from CHYHV with that using analytical means.

Table E-3. Analytical versus CHYHV Baker Grade Data

Parameter Measured	CHYHV	Analytical
Peak Power (kW)	57.63	55.05
Steady State Power (kW)	39.31	36.29

E.4 FUDS/LA92 Cycle Performance Results

The FUDS and the LA92 Driving Cycle simulations were performed with the CHYHV simulation code using the same vehicle configurations as the acceleration and Baker Grade cycles. Results are shown in Table E-4. All system energies are representative of one cycle of operation.

Table E-4. DPHV System Response for FUDS/LA92 Cycles

Cycle	Peak Power (kW)	Average Power (kW)	System Energy (kWh)
FUDS	40.22	4.72	1.750
LA92	56.13	7.22	2.673

E.5 HIWAY Cycle Performance Results

The HIWAY Driving Cycle simulation was performed with the CHYHV simulation code using the same vehicle configurations as the acceleration and Baker Grade cycles. All system energies are representative of one cycle of operation. The system requirements were obtained with regenerative braking disabled. Thus the results shown in Table E-5 are conservative.

Table E-5. DPHV System Response for HIWAY Cycles

Cycle	Peak Power (kW)	Average Power (kW)	System Energy (kWh)
HIWAY	32.68	9.62	4.420

APPENDIX F
HYDROGEN STORAGE DESIGNS

This appendix contains the applicable codes and standards for hydrogen storage along with several configurations for the DPHV system with various storage designs.

Codes and Regulation	Site Setups	Mobil Systems	Cylinders	Refueling Devices/ Stations
NFPA 50A – Gaseous H2 at Consumer Sites	X			X
ASME (VIII) – Pressure Vessels	X	X	X	X
AGA/AGA – Various	X	X	X	X
ANSI – Various	X	X	X	X
USDOT – 3AL		X		
ISO – Various	X	X	X	X
CTC/Transport Canada		X		
ANSI/AGA NGV 1 – Refueling Devices				G
ANSI/AGA NGV 2 – NGV Containers		G	G	
DOT/NHTSA Motor Vehicle Safety Standards		G	G	
NFPA 52 – CNG Vehicular Fuel Storage		G	G	G
CAN1 b149 – NGV Containers and Refueling	G	G	G	G
CSA B51 (2) NGV Vehicle Cylinders			G	
Local Authority	X	X	X	X
Self Regulation	X	X	X	X

Figure F-1. Applicable Codes and Standards for Off- and On-Board Storage

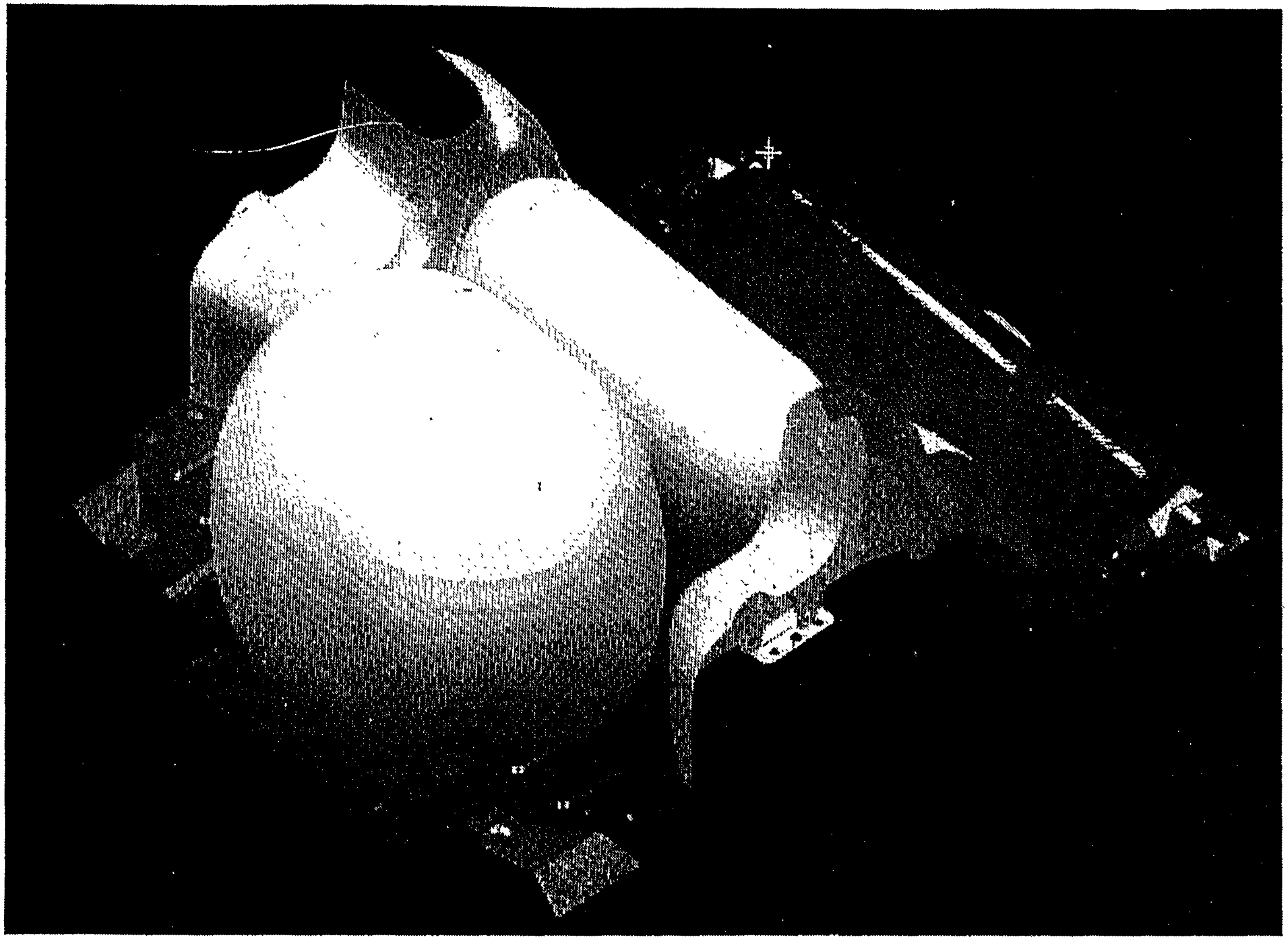

Figure F-2. Hydrogen Tank Installation Layout (2-Tank)

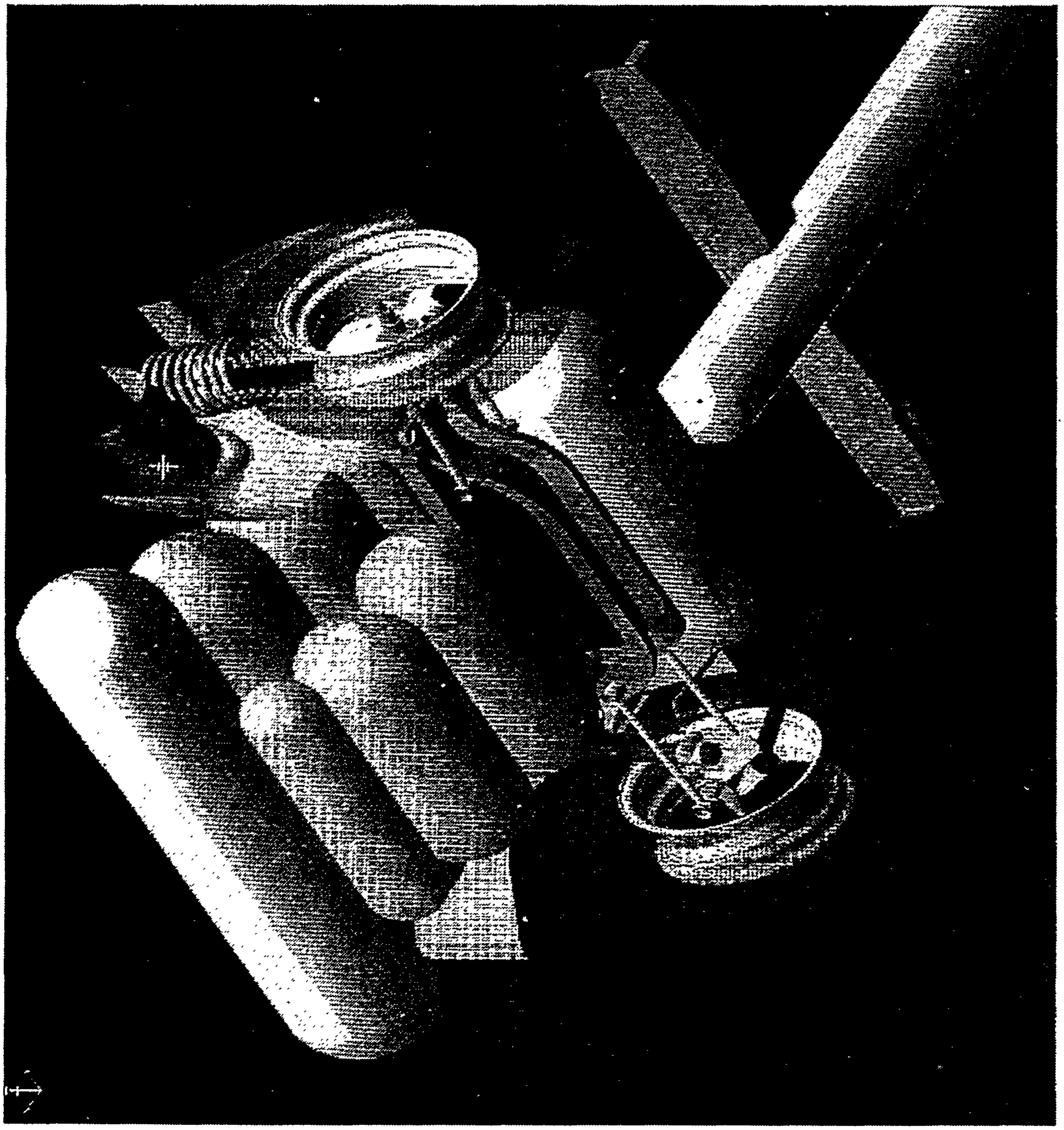

Figure F-3. Hydrogen Tank Installation Layout (9-Tank)

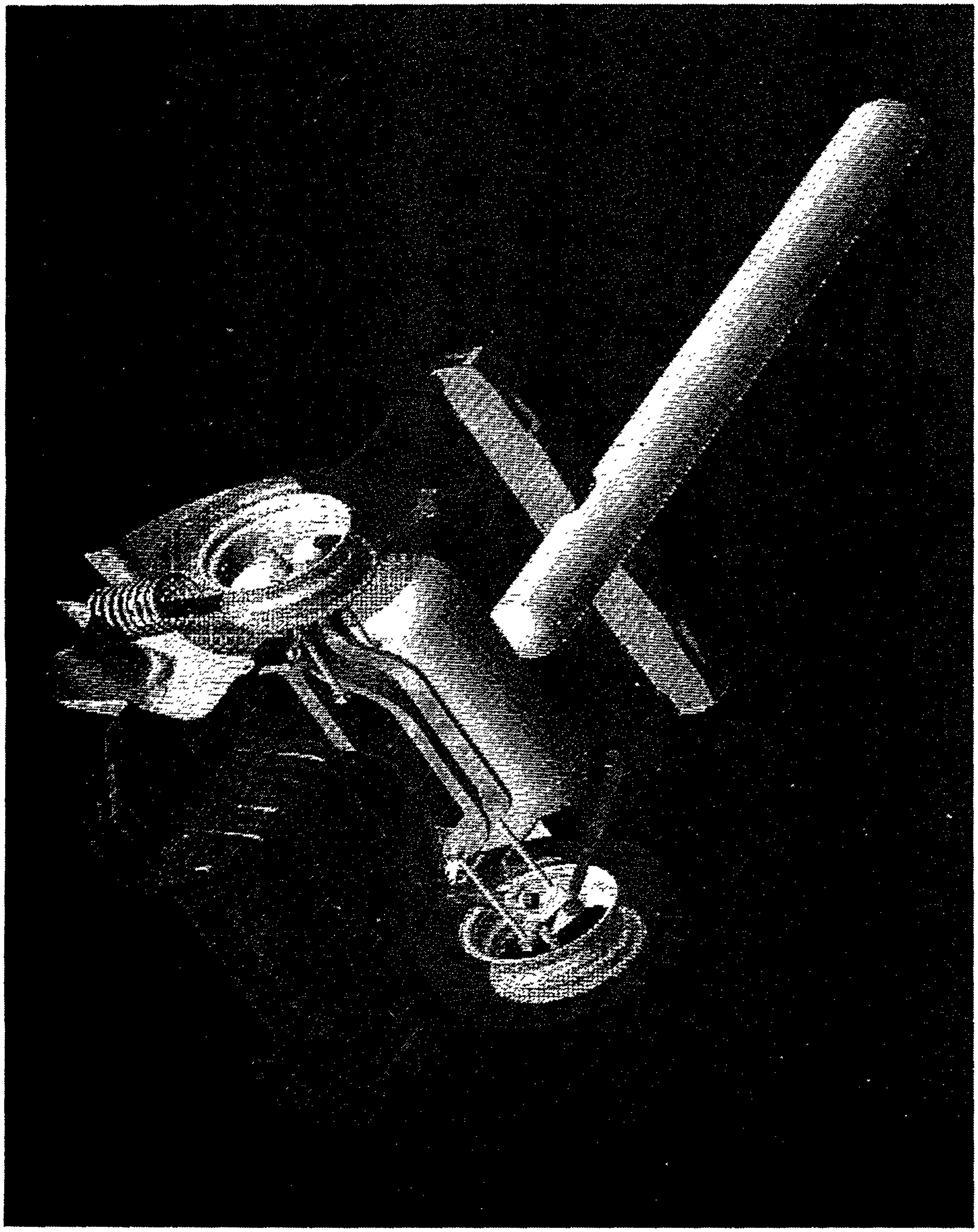

Figure F-4. Hydrogen Tank Installation Layout (5.4 ft^3)

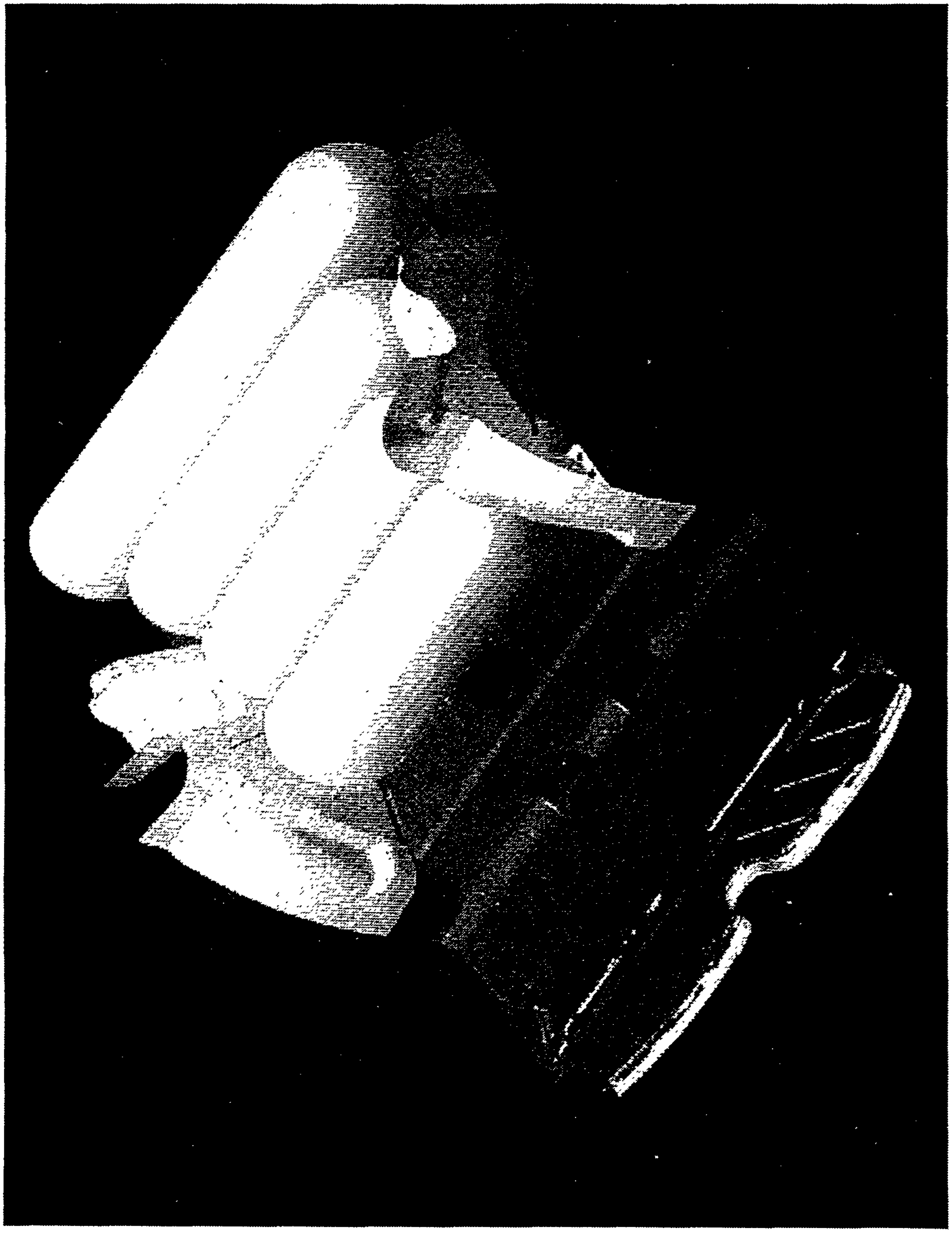

Figure F-5. Hydrogen Tank Installation Layout (4-Tank)

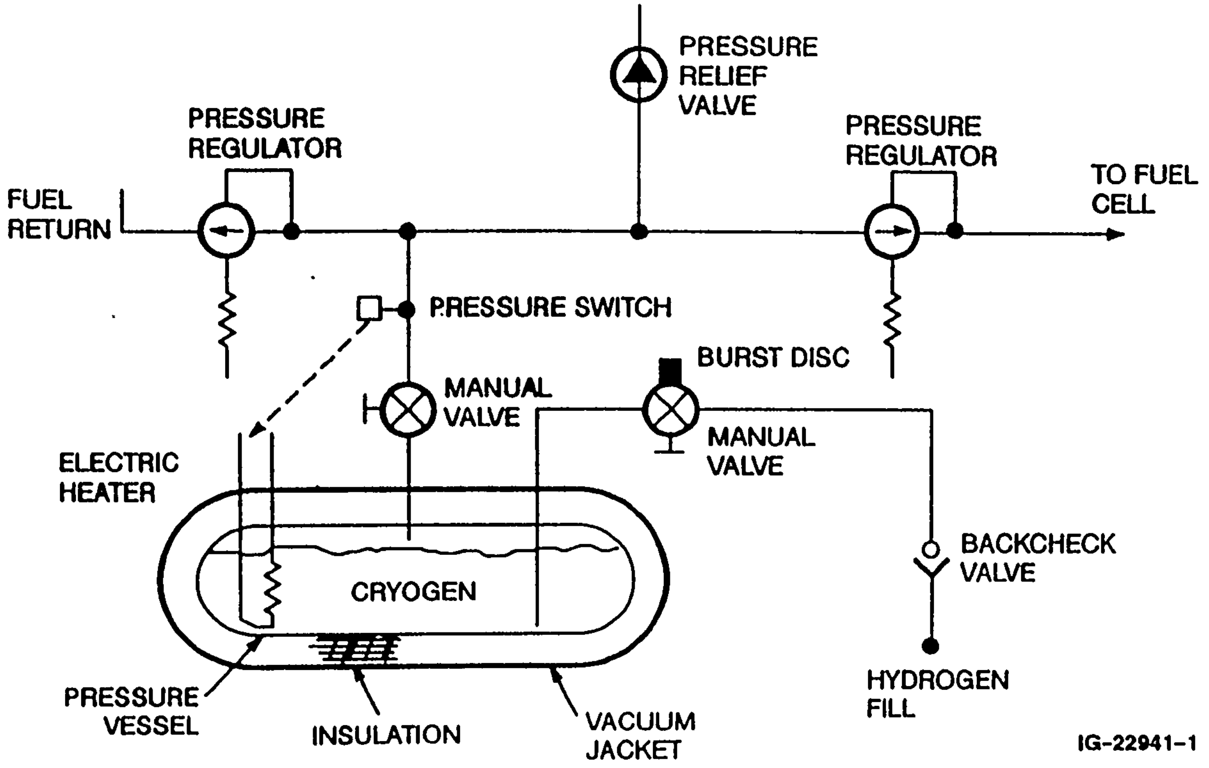
PRESSURE RELIEF VALVE
PRESSURE REGULATOR
FUEL RETURN
PRESSURE REGULATOR
TO FUEL CELL
PRESSURE SWITCH
BURST DISC
MANUAL VALVE
MANUAL VALVE
ELECTRIC HEATER
CRYOGEN
BACKCHECK VALVE
HYDROGEN FILL
PRESSURE VESSEL
INSULATION
VACUUM JACKET
IG-22941-1

Figure F-6. Liquid Hydrogen Storage System Schematic

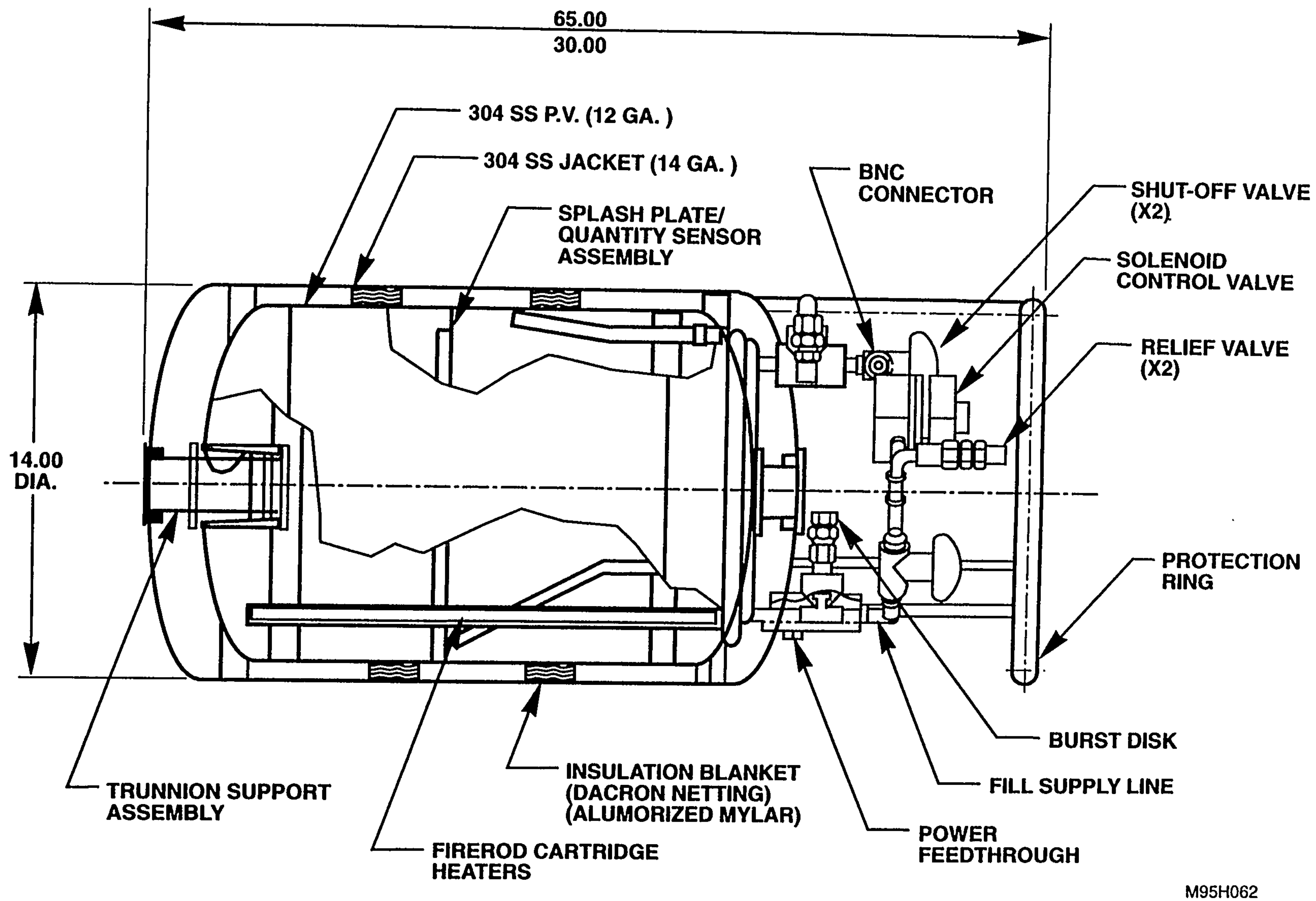
65.00
30.00
304 SS P.V. (12 GA.)
304 SS JACKET (14 GA.)
SPLASH PLATE/ QUANTITY SENSOR ASSEMBLY
BNC CONNECTOR
SHUT-OFF VALVE (X2)
SOLENOID CONTROL VALVE
RELIEF VALVE (X2)
14.00 DIA.
PROTECTION RING
BURST DISK
FILL SUPPLY LINE
POWER FEEDTHROUGH
TRUNNION SUPPORT ASSEMBLY
INSULATION BLANKET (DACRON NETTING) (ALUMORIZED MYLAR)
FIREROD CARTRIDGE HEATERS

M95H062
(5244)

Figure F-7. Current Liquid Methanol Tank Design